

MIT Open Access Articles

Measurement of the top quark charge in pp collisions at $\sqrt{s} = 7$ TeV with the ATLAS detector

The MIT Faculty has made this article openly available. **Please share** how this access benefits you. Your story matters.

Citation: Aad, G., T. Abajyan, B. Abbott, J. Abdallah, S. Abdel Khalek, A. A. Abdelalim, O. Abdinov, et al. "Measurement of the top quark charge in pp collisions at $\sqrt{s} = 7$ TeV with the ATLAS detector." *Journal of High Energy Physics* 2013, no. 11 (November 5, 2013). © CERN, for the benefit of the ATLAS collaboration.

As Published: [http://dx.doi.org/10.1007/jhep11\(2013\)031](http://dx.doi.org/10.1007/jhep11(2013)031)

Publisher: Springer-Verlag

Persistent URL: <http://hdl.handle.net/1721.1/84483>

Version: Final published version: final published article, as it appeared in a journal, conference proceedings, or other formally published context

Terms of use: Creative Commons Attribution



RECEIVED: July 17, 2013

REVISED: September 2, 2013

ACCEPTED: October 16, 2013

PUBLISHED: November 5, 2013

Measurement of the top quark charge in pp collisions at $\sqrt{s} = 7$ TeV with the ATLAS detector



The ATLAS collaboration

E-mail: atlas.publications@cern.ch

ABSTRACT: A measurement of the top quark electric charge is carried out in the ATLAS experiment at the Large Hadron Collider using 2.05 fb^{-1} of data at a centre-of-mass energy of 7 TeV. In units of the elementary electric charge, the top quark charge is determined to be 0.64 ± 0.02 (stat.) ± 0.08 (syst.) from the charges of the top quark decay products in single lepton $t\bar{t}$ candidate events. This excludes models that propose a heavy quark of electric charge $-4/3$, instead of the Standard Model top quark, with a significance of more than 8σ .

KEYWORDS: Hadron-Hadron Scattering, Top physics

ARXIV EPRINT: [1307.4568](https://arxiv.org/abs/1307.4568)

Contents

1	Introduction	1
2	The ATLAS detector	2
3	Data and simulation samples	3
4	Event selection	3
4.1	Object reconstruction	4
4.2	Selection of $t\bar{t}$ candidates	5
5	Top quark charge determination	5
5.1	Weighting procedure for b -jet charge calculation	6
5.2	Lepton and b -jet pairing algorithm	7
6	Signal and background expectations	8
6.1	Reconstructed signal distribution	8
6.2	Background	9
7	Results	11
7.1	Systematic uncertainties	17
8	Statistical comparison of the SM and exotic model	20
9	Conclusion	22
	The ATLAS collaboration	26

1 Introduction

It is generally accepted that the particle discovered at Fermilab in 1995 [1, 2] is the Standard Model (SM) top quark. However, a few years after the discovery a theoretical model appeared proposing an “exotic” quark of charge $-4/3$ and mass ≈ 170 GeV as an alternative to the SM top quark at this mass value [3]. Though this model has already been experimentally excluded a precise measurement of the top quark charge is important as it is one of the basic top quark properties. A strong preference for the SM top quark with electric charge of $+2/3$ (in units of the electron charge magnitude) was reported by the D0 and CDF collaborations [4, 5] but without the ultimate 5σ exclusion of a possible exotic quark with charge of $-4/3$. The CDF and D0 exclusion limits are 95%¹ and 92%,

¹The CDF collaboration has recently submitted an update of their analysis for publication, which results in a limit of 99% [6].

respectively. Therefore, it is still important to carry out a more precise measurement to definitively resolve this question with more than 5σ confidence level. Due to the excellent ATLAS detector performance, the analysis presented here not only demonstrates that the particle presently denoted by “top quark” is really the SM top quark decaying into a b -quark and a W^+ boson, but also allows for a direct measurement of its electric charge with a significantly improved precision. Moreover, from an experimental point of view it is interesting to demonstrate the high flavour tagging performance of the ATLAS experiment, i.e. its capability to distinguish between jets initiated by quarks and anti-quarks used in this study to find the correct Wb pairing in the $W^+W^-b\bar{b}$ system of the assumed $t\bar{t}$ final state.

The dominant decay channel of the top quark is to a b -quark through the charged weak current: $t \rightarrow W^+b$ ($\bar{t} \rightarrow W^-\bar{b}$). The measurement of the top quark charge requires the charges of both the W boson and the b -quark to be determined. While the former can be determined through W 's leptonic decay, the b -quark charge is not directly measurable due to quark confinement in hadrons. However, it is possible to establish a correlation between the charge of the b -quark and the charges of the collimated hadrons from the b -quark hadronization that form a b -jet. Within this approach, the charge can be determined using the lepton + jets ($t\bar{t} \rightarrow \ell^\pm \nu jj b\bar{b}$) or the dilepton ($t\bar{t} \rightarrow \ell^+ \nu \ell^- \bar{\nu} b\bar{b}$) channel. This paper presents the results of a top quark charge analysis based on the charges of the hadrons associated with the jet originating from a b -quark (b -jet) using the statistically more significant lepton + jets channel.

2 The ATLAS detector

The ATLAS detector is a multi-purpose particle physics apparatus operating at the beam interaction point IP1 of the Large Hadron Collider (LHC). A complete description is provided in ref. [7]. ATLAS uses a right-handed coordinate system with its origin at the centre of the detector (the nominal interaction point) and the z -axis along the beam pipe. The x -axis points to the centre of the LHC ring, and the y -axis points upward.

The innermost part is an inner tracking detector (ID) comprising a silicon pixel detector, a silicon microstrip detector, and a transition radiation tracker. The inner detector covers the pseudorapidity² range $|\eta| < 2.5$ and is surrounded by a thin superconducting solenoid providing a 2 T axial magnetic field, and by liquid-argon (LAr) electromagnetic sampling calorimeters with high granularity. An iron/scintillator tile calorimeter provides hadronic energy measurements in the central pseudorapidity range ($|\eta| < 1.7$). The end-cap and forward regions are instrumented with LAr sampling calorimeters for electromagnetic (EM) and hadronic energy measurements up to $|\eta| = 4.9$. The calorimeter system is surrounded by a muon spectrometer incorporating three superconducting toroid magnet assemblies, providing a toroidal magnetic field with bending power between 2.0 Tm and 7.5 Tm, and a pseudorapidity coverage of $|\eta| < 2.7$.

²The pseudorapidity is defined in terms of the polar angle with respect to the beam axis, θ , as $\eta = -\ln(\tan(\theta/2))$.

3 Data and simulation samples

This analysis uses the proton-proton collision data collected by the ATLAS experiment from March to August 2011 at a centre-of-mass energy of $\sqrt{s} = 7$ TeV corresponding to an integrated luminosity of $2.05 \pm 0.04 \text{ fb}^{-1}$ [8]. The data for the top quark charge study were collected using a single-muon and a single-electron trigger (see details in section 4). In this analysis we also use the dijet data sample collected using the combined muon-jet trigger which requires a reconstructed muon matched to a 10 GeV jet in the calorimeter.

Simulated event samples are used to estimate both the signal selection efficiency and some of the background contributions and also to calibrate the b -jet charge measurement. The response of the ATLAS detector is simulated using GEANT4 [9] and the resulting events are reconstructed by the same software [10] used for data.

The MC@NLO Monte Carlo (MC) generator v3.41, based on the next-to-leading-order (NLO) matrix elements [11, 12] with CTEQ6.6 [13] parton distribution functions (PDFs), is used for the parton-level hard scattering in $t\bar{t}$ production, and is interfaced to the HERWIG (v6.5) generator [14, 15] for simulation of the hadronization and fragmentation processes and to JIMMY [16] for simulation of the underlying event from multiple parton interactions. The POWHEG generator [17] in combination with the PYTHIA [18] or HERWIG generators is used for studying parton-shower systematic uncertainties. For the study of other systematic uncertainties (top quark mass dependence, initial and final state radiation (ISR/FSR)), $t\bar{t}$ samples produced with the ACERMC generator [19] interfaced with PYTHIA are used. The expected $t\bar{t}$ event yield is normalized to the cross-section of 164.6 pb, obtained with approximate next-to-next-to-leading-order (NNLO) QCD calculations [20]. Electroweak single-top-quark production is simulated using the MC@NLO generator and the event samples are normalized to approximate NNLO cross sections: 65 pb (t -channel) [21], 4.6 pb (s -channel) [22] and 15.7 pb (Wt channel) [23].

The background from W + jets and Z + jets production is simulated with the ALPGEN v2.13 generator [24] and CTEQ6L1 [25] PDFs in exclusive bins of parton multiplicity for multiplicities of less than five, and inclusively for five or more. The events are processed by HERWIG and JIMMY. The overall W + jets and Z + jets samples are normalized to the NNLO inclusive cross sections [26]. Diboson samples are produced using HERWIG and JIMMY with MRST2007LO [27] PDFs. Dijet samples used for crosscheck purposes (see section 8) are generated using the PYTHIA generator with the ATLAS AMBT2B PYTHIA tune [28] and with MRST2007LO PDFs.

4 Event selection

The reconstructed events are selected using criteria designed to identify the lepton + jets final states, i.e. $t\bar{t}$ events in which one of the W bosons decays leptonically and the other hadronically. This sample also contains a significant fraction of $t\bar{t}$ events where both W bosons decay leptonically, but one of the leptons is not reconstructed in the detector or fails the lepton identification requirements. In the simulated sample the events generated in both the single-lepton and dilepton channels are treated as signal if they satisfy the lepton + jets reconstruction criteria.

4.1 Object reconstruction

An electron candidate is defined as an energy cluster deposition in the EM calorimeter associated with a well-reconstructed charged particle track in the ID [29]. The candidate must have a shower shape consistent with expectations based on simulation, test-beam studies and $Z \rightarrow ee$ events in data. The associated ID track must satisfy quality criteria including the presence of high-threshold hits in the transition radiation tracker. All candidates are required to have transverse energy (E_T) above 25 GeV and $|\eta| < 2.47$, where η is the pseudorapidity of the EM calorimeter cluster associated with the electron. Candidates in the transition region between the barrel and end-cap calorimeters ($1.37 < |\eta| < 1.52$) are excluded.

Muon candidates are reconstructed by combining track segments from different layers of the muon chambers [30]. Such segments are assembled starting from the outermost layer, with a procedure that takes material effects into account, and are then matched with tracks found in the ID. The candidates are re-fitted exploiting the full track information from both the muon spectrometer and the ID. They are required to have transverse momenta (p_T) above 20 GeV and the candidate muon must be within $|\eta| < 2.5$.

Jet candidates are reconstructed using the anti- k_t algorithm [31] with jet radius parameter $R = 0.4$. These jets are calibrated to the hadronic energy scale, using a p_T - and $|\eta|$ -dependent correction factor obtained from simulation, test-beam and collision data [32].

The missing transverse momentum, E_T^{miss} , is calculated as the magnitude of the vector sum of the energy deposits in calorimeter cells associated with topological clusters [33], with the direction defined by the interaction vertex and position of the energy deposition in the calorimeter [34]. The calorimeter cells are associated with a parent physics object in a chosen order: electrons, jets and muons, such that a cell is uniquely associated with a single physics object. Cells belonging to electrons are calibrated at the EM energy scale whereas cells belonging to jets are corrected to the hadronic energy scale. Finally, the transverse momenta of muons passing the event selection are included, and the contributions from the calorimeter cells associated with the muons are subtracted. The remaining clusters not associated with electrons or jets are included at the EM energy scale.

Overlap between the different object categories is avoided by the following procedure. Jets within $\Delta R = 0.2$ of an electron passing the electron selection requirements are removed from the list of jet candidates.³ Muons within $\Delta R = 0.4$ of any jet with $p_T > 20$ GeV are rejected. In addition, if a selected electron is separated by less than $\Delta R = 0.4$ from any jet with $p_T > 20$ GeV, the event is rejected (for event selection see section 4.2).

Tracks used for the b -jet charge calculation (see section 5) are required to contain at least six hits in the silicon microstrip detector and at least one pixel hit. Only tracks with $p_T > 1$ GeV and $|\eta| < 2.5$ are considered. In addition, proximity to the pp collision primary vertex⁴ expressed in terms of impact parameter in the transverse plane, d_0 , and

³ ΔR is defined as a distance, $\Delta R = \sqrt{(\Delta\eta^2 + \Delta\phi^2)}$, in η - ϕ space, where η is the pseudorapidity and ϕ is the azimuthal angle around the beam pipe.

⁴The primary vertex is chosen as the reconstructed vertex with the highest $\sum p_T^2$ of associated tracks. At least five tracks with $p_T > 0.4$ GeV are required.

along the beam direction, z_0 , and good track fit quality are also required. The applied selection requirements on d_0 and z_0 are $|d_0| < 2$ mm and $|z_0 \cdot \sin(\theta)| < 10$ mm, and that on the quality of the track fit is $\chi^2/\text{ndf} < 2.5$.

For all reconstructed objects in the simulation, corrections are applied to compensate for the difference in reconstruction efficiencies and resolutions between data and simulation.

4.2 Selection of $t\bar{t}$ candidates

The $t\bar{t}$ candidates in the electron + jets or muon + jets final states are first selected with a single-electron or single-muon trigger with transverse energy or momentum thresholds at 20 GeV or 18 GeV, respectively. Events passing the trigger selection are required to contain exactly one reconstructed lepton, with $E_T > 25$ GeV for an electron or $p_T > 20$ GeV for a muon. At least four jets with transverse momenta $p_T > 25$ GeV and within the pseudorapidity range $|\eta| < 2.5$ are required. The missing transverse momentum, E_T^{miss} , has to exceed 35 GeV for the events with electrons, and 20 GeV for the events with muons. In addition, a primary vertex containing at least five charged particles with $p_T > 0.4$ GeV is required, and events containing jets with $p_T > 20$ GeV in poorly instrumented detector regions are removed.

The transverse mass of the leptonically decaying W boson in the event is reconstructed as $m_T(W) = \sqrt{2p_T^\ell p_T^\nu (1 - \cos(\phi^\ell - \phi^\nu))}$, where the measured E_T^{miss} magnitude and direction provide the transverse momentum, p_T^ν , and azimuthal angle, ϕ^ν , of the neutrino, and the superscript l stands for the e or μ . For events with electrons $m_T(W)$ has to exceed 25 GeV, while the sum of $m_T(W)$ and E_T^{miss} has to exceed 60 GeV for the events with muons.

Finally, at least one jet is required to be b -tagged using the b -tagging procedure described in ref. [35]. The procedure combines an algorithm based on jet track impact parameters with respect to the primary vertex with an algorithm exploiting the topology of b - and c -hadron weak decays inside the jet. The combination of the two algorithms is based on artificial neural network techniques with MC-simulated training samples and variables describing the topology of the decay chain used as the neural network input [36]. The chosen b -tagging operating point corresponds to a 70% tagging efficiency for b -jets in simulated $t\bar{t}$ events, while light-flavour jets are suppressed by approximately a factor of 100.

These selection requirements, common to most of the ATLAS $t\bar{t}$ analyses (see e.g. [37]), are further referred to as the basic $t\bar{t}$ requirements. They are followed by requirements specific for reconstruction of the b -quark charge. In order to use the track charge weighting method (see section 5.1), the presence of a second b -tagged jet is required. Each of the two b -tagged jets has to contain at least two well-reconstructed tracks with transverse momenta above 1 GeV within the pseudorapidity range $|\eta| < 2.5$. A pairing criterion between the lepton and a b -jet is also applied (see section 5).

5 Top quark charge determination

The correlation between the top or exotic quark charge and the charges of their decay products can be used for the quark charge determination. In the SM the top quark is

expected to decay according to

$$t^{(2/3)} \rightarrow b^{(-1/3)} + W^{(+1)}, \quad (5.1)$$

while the exotic quark (t_X) with charge $-4/3$ is assumed to decay according to

$$t_X^{(-4/3)} \rightarrow b^{(-1/3)} + W^{(-1)}, \quad (5.2)$$

where the electric charges of the particles are indicated in parentheses. Considering the subsequent leptonic decay of the W bosons, $W^\pm \rightarrow \ell^\pm + \nu_\ell(\bar{\nu}_\ell)$, the expectation for the SM case is that a positively charged lepton ℓ^+ is associated with the b -quark ($Q_b = -1/3$) from the same top quark, while for the exotic case it is just the opposite: ℓ^- is paired with the b -quark. In the SM case the product of charges of the top or anti-top quark decay products ($Q_{\ell^+} \times Q_b$ or $Q_{\ell^-} \times Q_{\bar{b}}$) always has a negative sign while in the exotic case the sign is positive.

The charge of the W boson is taken from the charge of the high- p_T lepton in the event. The charge of the quark initiating the b -jet is estimated from a weighted average of the charges of the tracks in the jet (see section 5.1). A lepton- b -jet pairing criterion (hereafter referred to as ℓb -pairing) is then applied to match the W boson to the b -jet from the same top quark (see section 5.2).

5.1 Weighting procedure for b -jet charge calculation

For the determination of the effective b -jet charge a weighting technique [38, 39] is applied in which the b -jet charge is defined as a weighted sum of the b -jet track charges,

$$Q_{b\text{-jet}} = \frac{\sum_i Q_i |\vec{j} \cdot \vec{p}_i|^\kappa}{\sum_i |\vec{j} \cdot \vec{p}_i|^\kappa}, \quad (5.3)$$

where Q_i and \vec{p}_i are the charge and momentum of the i -th track, \vec{j} defines the b -jet axis direction, and κ is a parameter which was set to be 0.5 for the best separation between b - and \bar{b} -jets mean charges using the standard MC@NLO $t\bar{t}$ simulated sample.

The calculation of the b -jet charge uses a maximum number of ten tracks with $p_T > 1$ GeV associated with the b -jet within a cone of $\Delta R < 0.25$. The b -jet tracks used in the calculation of the effective b -jet charge include not only the charged decay products of the b -hadron, but also b -fragmentation tracks, and can possibly also contain tracks from multiple interactions or pile-up. The mean number of charged tracks within the b -jet cone is six for $t\bar{t}$ b -jets. If there are more than ten associated tracks, the highest- p_T tracks are chosen. The maximum number of tracks, the minimum track p_T and the value of ΔR were optimized using the standard MC@NLO $t\bar{t}$ simulated sample. The optimization takes into account that the pile-up effect can be stronger for the high track multiplicity events and that low- p_T tracks, coming mainly from gluons, could dilute the jet charge.

The variable that is used to distinguish between the SM and exotic model scenarios is the combined lepton- b -jet charge (hereafter referred to as the combined charge) which is defined as

$$Q_{\text{comb}} = Q_{b\text{-jet}}^\ell \cdot Q_\ell, \quad (5.4)$$

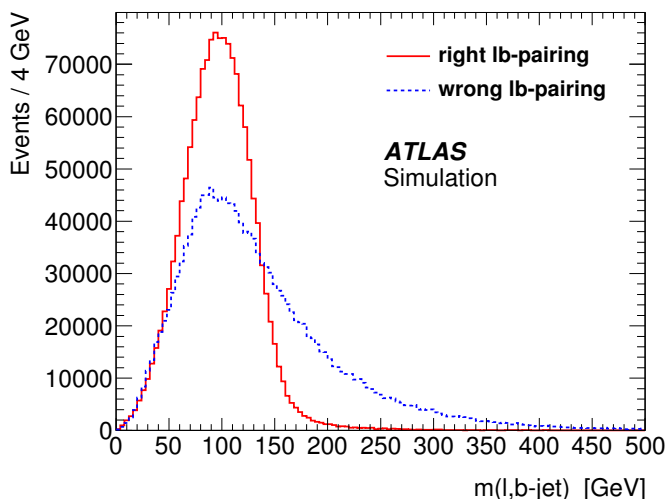


Figure 1. Lepton– b -jet invariant mass spectra for the lepton and b -jet pairs from the same top quark (right pairing, solid red line) and for those originating from two different top quarks (wrong pairing, dashed blue line).

where $Q_{b\text{-jet}}^\ell$ is the charge of the b -jet calculated with equation (5.3)⁵ and Q_ℓ the charge of the lepton, the two being associated via the lb -pairing described below.

5.2 Lepton and b -jet pairing algorithm

The lb -pairing is based on the invariant mass distribution of the lepton and the b -jet, $m(\ell, b\text{-jet})$. If the assignment is correct, assuming an ideal invariant mass resolution, $m(\ell, b\text{-jet})$ should not exceed the top quark mass provided that the decaying particle is the SM top quark. Otherwise, if the lepton and b -jet are not from the same decaying particle, there is no such restriction. This is shown in figure 1, where the invariant mass distribution of a lepton and a b -jet in the signal MC sample is plotted for the correct pairing and the wrong pairing, for events fulfilling the basic $t\bar{t}$ selection requirements. For MC events the reconstructed b -jet is paired with a parton-level b -quark if their separation ΔR is less than 0.2; similarly, $\Delta R < 0.2$ is required for the matching between parton-level and reconstructed leptons.

The lb -pairing requires events with two b -tags and only the events with b -jets that satisfy the conditions:

$$\begin{aligned}
 m(\ell, b\text{-jet}_1) < m_{\text{cut}} \quad \text{and} \quad m(\ell, b\text{-jet}_2) > m_{\text{cut}} \\
 \text{or} \\
 m(\ell, b\text{-jet}_2) < m_{\text{cut}} \quad \text{and} \quad m(\ell, b\text{-jet}_1) > m_{\text{cut}}
 \end{aligned}
 \tag{5.5}$$

are accepted. Here $b\text{-jet}_1$ and $b\text{-jet}_2$ denote the two b -tagged jets ordered in descending order of transverse momentum. The optimal value for the lb -pairing mass cut, m_{cut} , is

⁵The superscript ℓ is added to $Q_{b\text{-jet}}$ to stress that the b -jet is paired with a lepton.

a trade-off between the efficiency (ϵ) and purity (P) (see section 6.1) of the lb -pairing method. It was found by maximizing the quantity $\epsilon(2P - 1)^2$ which is largest and nearly constant in the region 140 GeV to 165 GeV. The value for the lb -pairing mass cut is chosen to be $m_{\text{cut}} = 155$ GeV. A similar interval for the optimal value of m_{cut} was obtained using the relative uncertainty of the mean combined charge as an alternative figure of merit in the optimization.

The efficiency of the lb -pairing procedure, defined as the ratio of the number of lb -pairs after and before the invariant mass cuts in equation 5.5, is small ($\epsilon=28\%$), but it gives a high purity ($P=87\%$). The efficiency of the full set of selections used in the analysis, with respect to the basic $t\bar{t}$ requirements, is reduced not only by the lb -pairing conditions but also by the requirement of the second b -tag (70% efficiency) and, to a lesser extent, by the b -jet track requirements (see section 4.1) with efficiency around 99%.

6 Signal and background expectations

The sensitivity for determining the SM top quark charge in the lepton+jets channel is investigated using MC and data control samples with the aim of finding the Q_{comb} expectations for the SM signal and background. Both single-lepton ($t\bar{t} \rightarrow \ell\nu jjb\bar{b}$) and dilepton ($t\bar{t} \rightarrow \ell\nu\ell\nu b\bar{b}$) samples are included for the signal.

6.1 Reconstructed signal distribution

In the MC analysis of the top quark charge the MC@NLO, POWHEG and ACERMC $t\bar{t}$ samples are used. MC@NLO is taken as the default generator. The b -jet charge spectra reconstructed for the $t\bar{t}$ electron + jets events from MC@NLO are presented in figure 2. The distributions of $Q_{b\text{-jet}}$ for b -jets paired with positive and negative leptons are shown after the lb -pairing. In addition, the Q_{comb} spectrum (see equation (5.4)) is also shown in the plot.

The peaks at ± 1 in figure 2 correspond to the cases where all the tracks within the b -jet cone of $\Delta R = 0.25$ have charges of the same sign. In these cases the weighting procedure (equation (5.3)) gives $Q_{b\text{-jet}} = \pm 1$.

The difference between the mean b -jet charges associated with ℓ^+ and ℓ^- is clearly seen in figure 2. The results of the MC b -jet charge analysis are summarized in table 1, where the mean combined charges and charge purities are shown for different MC generators and the individual lepton + jets channels. The uncertainties in the mean combined charges of all MC samples are downgraded to the integrated luminosity of 2.05 fb^{-1} corresponding to the size of the processed data sample. The charge purity, P_Q , is defined as

$$P_Q = \frac{N(Q_{\text{comb}} < 0)}{N(Q_{\text{comb}} < 0) + N(Q_{\text{comb}} \geq 0)}, \quad (6.1)$$

where $N(Q_{\text{comb}} < 0)$ and $N(Q_{\text{comb}} \geq 0)$ denote the number of events with $Q_{\text{comb}} < 0$ and $Q_{\text{comb}} \geq 0$, respectively. It is an important parameter which defines the quality of the b -jet charge weighting procedure. The higher P_Q is relative to 50%, the better the

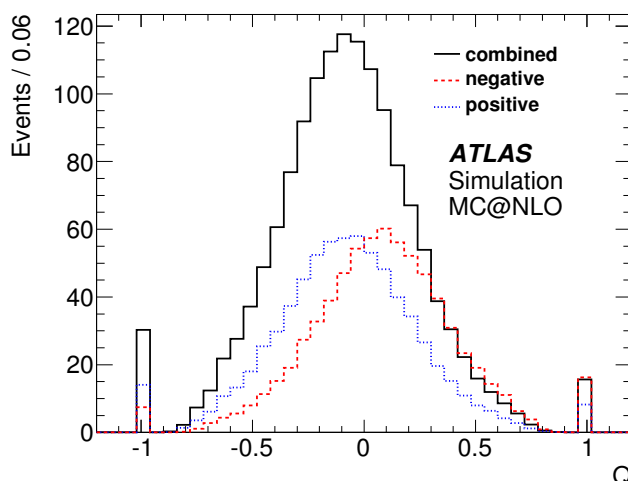


Figure 2. Distributions of the reconstructed b -jet charge in electron + jets $t\bar{t}$ events (MC@NLO) associated with positive (dotted blue line) and negative (dashed red line) leptons and the combined charge (solid black line) after the ℓb -pairing is applied. Here Q represents $Q_{b\text{-jet}}^\ell$ in the first two distributions and Q_{comb} in the third one.

flavour tagging identification is, i.e. the ability to distinguish between jets initiated by b - and \bar{b} -quarks. As shown in table 1, our procedure produces P_Q near 60%.

In general, as it follows from table 1, there is good agreement among the MC@NLO, POWHEG and ACERMC results on Q_{comb} . The combined (electron + muon channels) expectations agree to within 4%. Good agreement is also seen between the individual channels.

To evaluate the effect of the reconstruction on the combined charge, the mean associated b -jet charge reconstructed using the ℓb -pairing is compared with that based on the correct association of the lepton and b -jet using a MC generator-level matching. The comparison is carried out using the MC@NLO $t\bar{t}$ samples and the results are shown in table 2 for the electron + jets, muon + jets and combined electron+muon channels. The larger value of the average Q_{comb} for the MC matching can be explained by its 100% pairing purity. Table 2 shows that the expected mean combined charges obtained for the electron and muon channels are compatible within statistical errors for the MC matching. In the ℓb -pairing case a difference of 2.4σ between the electron and the muon channel is seen. The difference can be explained by the non-identical selection criteria used for these two channels and by the slight dependence of the ℓb -pairing efficiency and purity on lepton and b -jet transverse momentum. To illustrate that the analyzed sample of data does not have sufficient statistical power to be sensitive to such a difference, the statistical uncertainty quoted in table 1 has been scaled to the luminosity of the analyzed data sample (2.05 fb^{-1}).

6.2 Background

The main background processes for the top quark charge measurement in the lepton + jets channel are: W +jets production (the most significant background), Z +jets, multi-jet, diboson and single-top-quark production. The single-top-quark background gives the same

Generator	Channel	$\langle Q_{\text{comb}} \rangle$	P_Q
MC@NLO	e	-0.0802 ± 0.0065	0.610 ± 0.003
	μ	-0.0776 ± 0.0058	0.603 ± 0.003
	$e + \mu$	-0.0787 ± 0.0043	0.606 ± 0.002
POWHEG+HERWIG	e	-0.0739 ± 0.0070	0.595 ± 0.010
	μ	-0.0787 ± 0.0063	0.600 ± 0.008
	$e + \mu$	-0.0766 ± 0.0047	0.602 ± 0.006
POWHEG+PYTHIA	e	-0.0824 ± 0.0068	0.613 ± 0.010
	μ	-0.0703 ± 0.0063	0.594 ± 0.008
	$e + \mu$	-0.0756 ± 0.0046	0.602 ± 0.006
ACERMC+PYTHIA	e	-0.0728 ± 0.0065	0.598 ± 0.011
	μ	-0.0786 ± 0.0058	0.609 ± 0.008
	$e + \mu$	-0.0760 ± 0.0043	0.604 ± 0.007

Table 1. The expected mean combined charges ($\langle Q_{\text{comb}} \rangle$) and charge purities (P_Q) for the electron (e), muon (μ) and combined ($e + \mu$) channels compared for the $t\bar{t}$ MC@NLO, POWHEG+HERWIG, POWHEG+PYTHIA and ACERMC+PYTHIA simulated signal at 7 TeV in the lepton + jets channel obtained with the lb -pairing. The $\langle Q_{\text{comb}} \rangle$ values are shown with their statistical uncertainties scaled to the integrated luminosity of 2.05 fb^{-1} (see text). The uncertainty of P_Q is obtained from the full MC sample and is not downgraded to the integrated luminosity of the data as P_Q reflects the quality of the charge weighting procedure.

Pairing type	e	μ	$e + \mu$
MC matching	-0.1014 ± 0.0009	-0.1006 ± 0.0008	-0.1010 ± 0.0006
lb -pairing	-0.0802 ± 0.0008	-0.0776 ± 0.0007	-0.0787 ± 0.0005

Table 2. Comparison of the mean combined charge, $\langle Q_{\text{comb}} \rangle$, for the electron (e), muon (μ) and combined ($e + \mu$) channels obtained using the MC matching and lb -pairing. The charges are shown with their statistical uncertainties for the full $t\bar{t}$ MC@NLO sample.

sign of the mean b -jet charge as the signal. The MC simulation is expected to predict correctly all the processes with the exception of the multi-jet production and the normalization of the W +jets production. Though the probability for a multi-jet event to pass the event selection is very low, the production cross section is several orders of magnitude larger than that of top quark pair production, and due to fake leptons⁶ the multi-jet events can contribute to the background. This background is determined in a data-driven way employing the so-called Matrix Method [37]. This technique is based on the determination of the number of data events passing the full set of analysis selection criteria (tight selection) and that for a looser selection obtained by dropping the isolation requirement on the lepton. Using the number of events passing the tight and loose selections and the efficiencies for true and fake leptons, the number of fake-lepton events passing the tight $t\bar{t}$ selection criteria is found. The efficiencies are determined using appropriate control samples as is explained in detail in ref. [37].

⁶Fake lepton refers to both a non-prompt lepton and a jet misidentified as a lepton.

Process	Electron		Muon	
	$N_{\ell b}$	$\langle Q_{\text{comb}} \rangle$	$N_{\ell b}$	$\langle Q_{\text{comb}} \rangle$
$W + \text{jets}$	77 ± 15	-0.077 ± 0.050	132 ± 23	-0.047 ± 0.032
$Z + \text{jets}$	9 ± 3	0.078 ± 0.153	15 ± 4	-0.179 ± 0.086
Diboson	1 ± 1	-0.229 ± 0.573	2 ± 2	-0.071 ± 0.279
Multi-jet (DD)	18 ± 18	-0.018 ± 0.082	36 ± 36	-0.027 ± 0.028
Non-top-quark background	105 ± 24	-0.015 ± 0.041	185 ± 43	-0.052 ± 0.028
Single-top-quark	67 ± 11	-0.066 ± 0.042	80 ± 12	-0.051 ± 0.038
Signal	1420 ± 150	-0.080 ± 0.007	1830 ± 190	-0.078 ± 0.006
Signal + background	1600 ± 150	-0.075 ± 0.006	2100 ± 200	-0.074 ± 0.006

Table 3. Signal and background expectation after applying the ℓb -pairing separately for the electron and muon channels for 2.05 fb^{-1} integrated luminosity. Here, DD stands for “data driven”, $N_{\ell b}$ is the mean number of lepton- b -jet pairs and $\langle Q_{\text{comb}} \rangle$ is the reconstructed mean combined charge. The non-top-quark background is the total background not including single-top-quark events. The uncertainties include the statistical uncertainties and the uncertainties in the cross sections and integrated luminosity.

The estimation of the $W + \text{jets}$ background relies to a large extent on MC simulation, which is assumed to correctly describe the kinematics of the individual $W + \text{jets}$ channels, but the overall normalization and flavour fractions are determined from data. The $W + \text{jets}$ background is divided into four flavour groups: $W + b\bar{b} + \text{jets}$, $W + c\bar{c} + \text{jets}$, $W + c + \text{jets}$ and $W + \text{light-flavour-jets}$. The flavour composition of the jets is determined from data based on the fraction of $W + \text{jet(s)}$ events that have one or two tagged jets [40]. The MC predictions for the $W + b\bar{b} + \text{jets}$ and $W + c\bar{c} + \text{jets}$ components are scaled by a factor of 1.63 ± 0.76 , the $W + c + \text{jets}$ component by a factor of 1.11 ± 0.35 , and the light-flavour $W + \text{jets}$ component by a factor of 0.83 ± 0.18 (for details see ref. [41]).

The expected results for the electron and muon channels after all selections used in the analysis, including those used for the ℓb pairing, are shown in table 3. The uncertainties in the expected number of the signal and background events include not only the statistical uncertainties but also the cross-section uncertainties, which vary from 10% for signal and single-top-quark production to 100% for the multi-jet background, and the uncertainty in the integrated luminosity (1.8%).

7 Results

The distributions of the reconstructed quantities involved in the top quark charge determination, namely the distributions of b -jet and lepton p_T , E_T^{miss} and the number of tracks with $p_T > 1 \text{ GeV}$ in a b -jet, were compared to the expectations after applying the basic $t\bar{t}$ selection requirements and after the full set of the analysis requirements including two b -tags and ℓb -jet pairing. Fairly good agreement between data and MC distributions is observed. An example is seen in figure 3, which shows the b -jet p_T distribution after the basic $t\bar{t}$ requirements and after the full set of the analysis requirements.

To test the b -jet charge weighting procedure (see eq. (5.1)), the reconstructed distributions of the mean value of the absolute b -jet charge, shown as a function of b -jet p_T for the

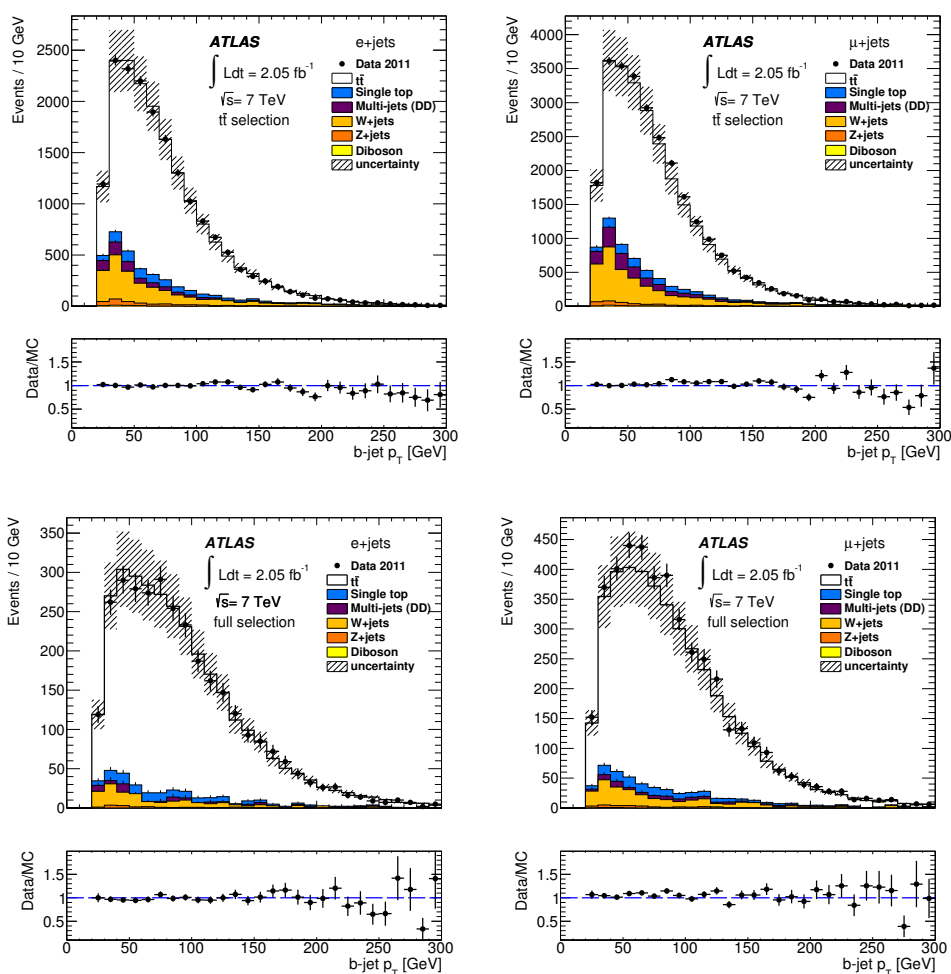


Figure 3. Data and MC comparison of the b -jet p_T distribution after the basic $t\bar{t}$ requirements (upper plots) and after the full set of requirements (bottom plots) for electron + jets (left) and muon + jets (right) events. The MC expectations for signal and background are normalized to 2.05 fb^{-1} using the expected cross sections. The shaded area belongs to the MC distribution and corresponds to a combination of the statistical uncertainties and the uncertainties in the cross sections and the integrated luminosity.

$t\bar{t}$ candidate events in data and MC simulation, are compared in figure 4 after the basic $t\bar{t}$ requirements and after the lb -pairing. The expected background is subtracted from the data distribution. The distributions in figure 4 are profile histograms containing in each bin the mean value with its uncertainty depicted as the corresponding error bar. Due to the high statistics of the MC samples, the error bars of the MC distributions are within the symbol size. Good agreement between the data and the MC simulation is observed. An advantage of using the absolute value of b -jet charge is that it can be used for comparison of data and MC in different stages of the candidate event selection while the combined charge is available only after the full set of selection criteria. The relation between the mean combined charge and the mean value of absolute b -jet charge was investigated in a dedicated

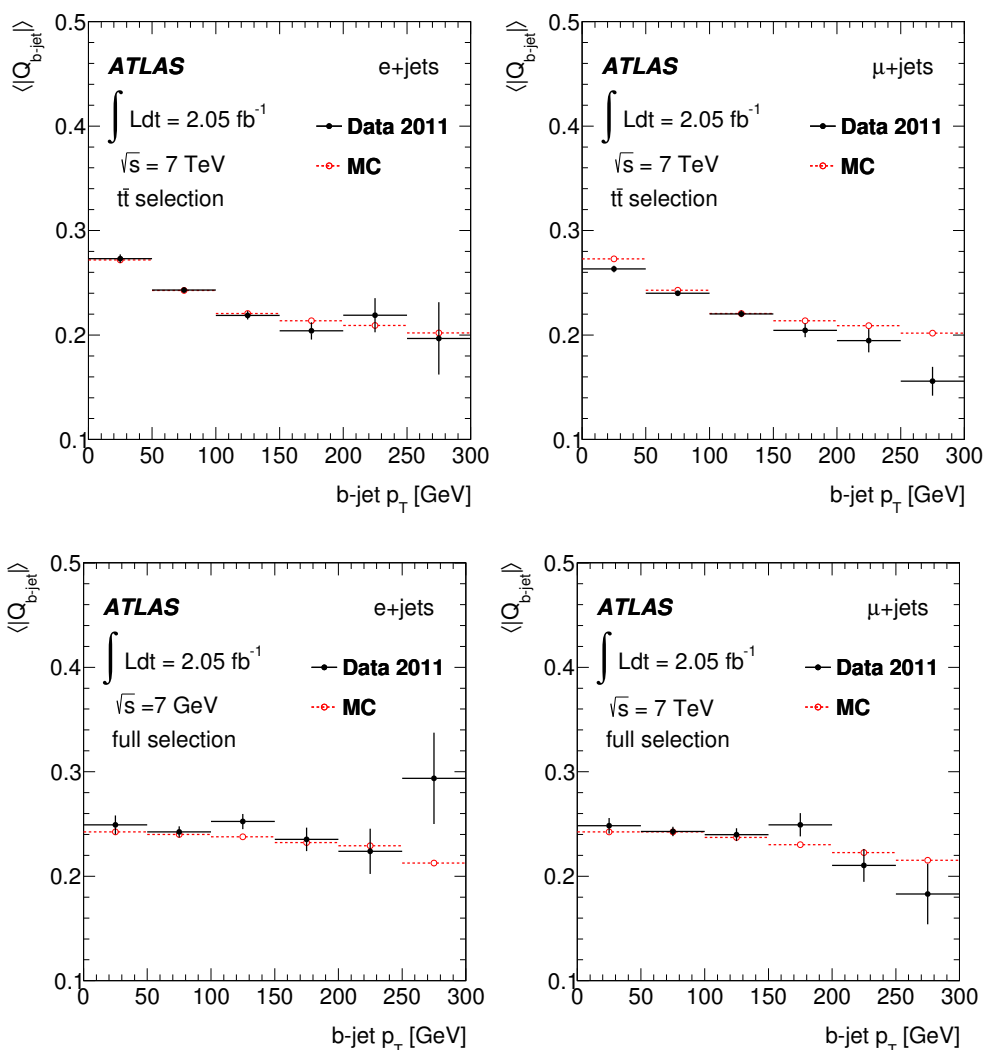


Figure 4. Data and MC comparison of the mean of the absolute value of the b -jet charge, $\langle |Q_{b\text{-jet}}| \rangle$, as a function of b -jet p_T after the basic $t\bar{t}$ requirements (upper plots) and after the full set of requirements (bottom plots) for electron + jets (left) and muon + jets (right) events. The data are shown after subtraction of the expected background and MC stands for MC@NLO $t\bar{t}$ events. Only statistical uncertainties are shown.

MC study, which showed a linear dependence. In addition, figure 4 demonstrates that the mean b -jet charge depends only weakly on the b -jet p_T , especially for the distributions after the lb -pairing, which makes the charge weighting procedure insensitive to uncertainties in the b -jet p_T distribution.

The increasing instantaneous LHC luminosity was accompanied by an increasing mean number of reconstructed pp interaction vertices per bunch crossing. This quantity, which is a measure of pile-up (presence of additional interactions in the event), increased from 6 to 17 during the analysed 2011 data-taking period. To assess the impact of pile-up, the mean of the absolute value of b -jet charge, $\langle |Q_{b\text{-jet}}| \rangle$, is reconstructed as a function of

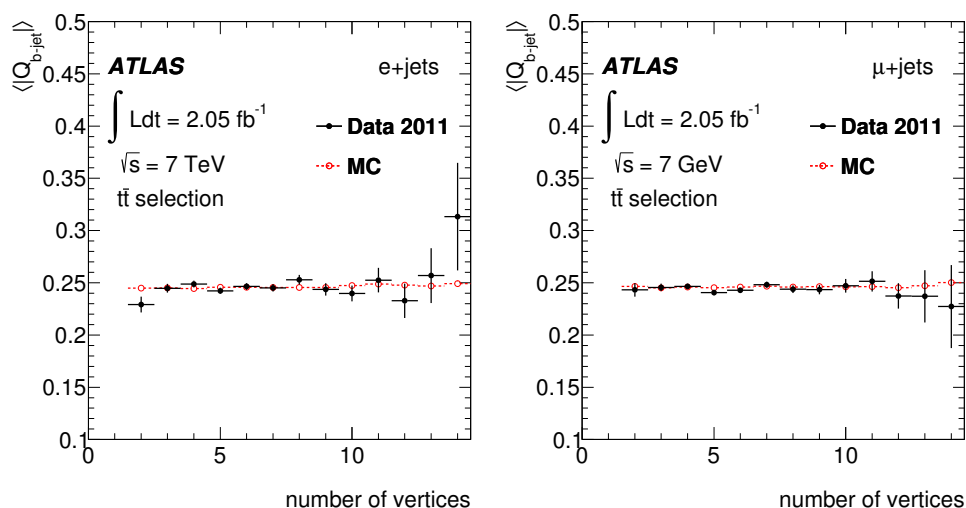


Figure 5. Data and MC (MC@NLO) comparison of the mean of the absolute value of the b -jet charge, $\langle |Q_{b\text{-jet}}| \rangle$, as a function of vertex multiplicity after all the $t\bar{t}$ requirements for electron + jets (left) and muon + jets (right) events.

Lepton channel	$N_{\ell b}^{\text{expect}}$	$N_{\ell b}^{\text{data}}$	$\langle Q_{\text{comb}} \rangle$		
			SM expected	XM expected	Data
e	1600 ± 150	1638	-0.075 ± 0.006	0.073 ± 0.006	-0.079 ± 0.008
μ	2100 ± 200	2276	-0.074 ± 0.006	0.065 ± 0.006	-0.075 ± 0.007
$e + \mu$	3700 ± 250	3914	-0.075 ± 0.004	0.069 ± 0.004	-0.077 ± 0.005

Table 4. Number of ℓb -pairs expected from MC simulation ($N_{\ell b}^{\text{expect}}$) and observed in data ($N_{\ell b}^{\text{data}}$), and reconstructed mean combined charge, $\langle Q_{\text{comb}} \rangle$, for the data in the different lepton + jets channels compared to those expected in the SM and the exotic model (XM). The uncertainties include the statistical uncertainties scaled to 2.05 fb^{-1} and the uncertainties in the cross sections and integrated luminosity.

the number of reconstructed pp interaction vertices for both the data and MC samples and with the full set of the $t\bar{t}$ requirements used in this analysis including two b -tags and ℓb -pairing. No dependence is observed for the level of pile-up present in the data sample, as shown by figure 5 for the absolute value of b -jet charge. The same level of stability is observed for the combined charge as a function of the primary vertex multiplicity.

Figure 6 compares the b -jet charge spectra after the basic $t\bar{t}$ cuts for the data and the expected sum of signal and background normalized to the integrated luminosity of 2.05 fb^{-1} . The charge spectra are symmetric around zero and show good agreement between data and MC.

The results for the combined charge are summarized in table 4. This table contains the number of reconstructed lepton- b -jet pairs along with the mean combined charge for the different channels. The uncertainties in the expected number of events in table 4 include the cross-section uncertainty and the 1.8% uncertainty in the integrated luminosity.

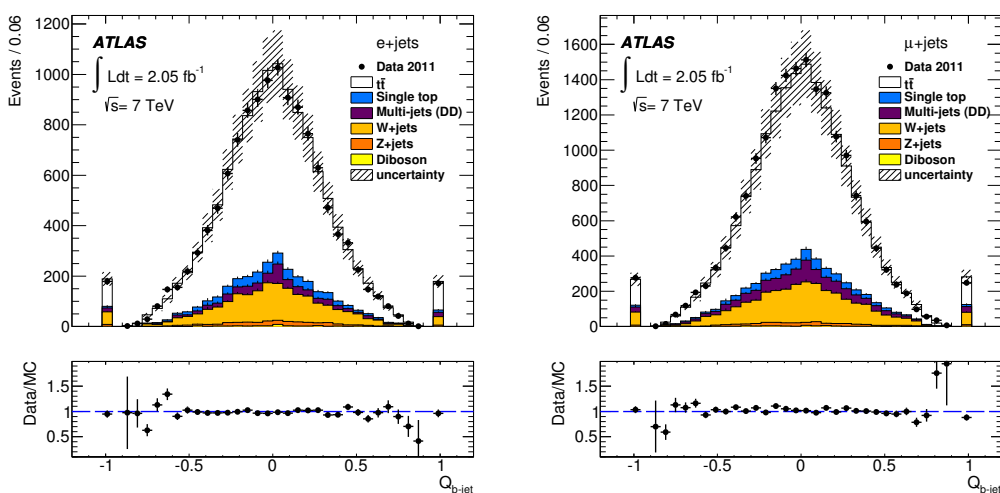


Figure 6. Data and MC comparison of the b -jet charge after the basic $t\bar{t}$ requirements for electron + jets (left) and muon + jets (right) events. The MC expectations for signal and background are normalized to 2.05 fb^{-1} using the expected cross sections. The shaded area corresponds to a combination of statistical uncertainties and uncertainties in the cross sections and integrated luminosity.

The combined charge for the exotic model in table 4 was obtained by inverting the signal $t\bar{t}$ and single-top-quark combined charges while the non-top-quark background charge was not changed. The inversion of the b -jet charge (or lepton charge) in a lepton- b -jet pair, provided that the lepton and b -jet come from a top quark decay, corresponds to a change of the decaying quark charge from $2/3$ to $-4/3$. Such an approximation of the process with the exotic quark should be appropriate since the exotic quark differs from the top quark only in the electric charge. Although this could result in higher photon radiation in the exotic quark case, and consequently in a slightly softer b -jet p_T spectrum, this should not influence the combined charge since the photon radiation in the top quark case is only a small effect and the b -jet charge depends only weakly on b -jet p_T . This was verified by studying the exotic quark combined charge directly using events generated by ACERMC. The ACERMC sample gives, within statistical uncertainties, a compatible result with that obtained using the inversion procedure applied to the SM MC@NLO sample.

From table 4 it can be concluded that the data agree with the SM top quark hypothesis within the uncertainties and that the observed and expected numbers of events are also consistent with each other. Figure 7 compares the reconstructed combined charge spectra for the data with MC expectations for signal and background after lb -pairing for the electron + jets (left) and muon + jets (right) final states, showing good agreement between the data and the SM expectations.

The top quark charge can be directly inferred from the background-subtracted Q_{comb} data distribution using a Q_{comb} to b -jet charge calibration coefficient obtained from MC. From the SM value of the b -quark charge ($Q_b = -1/3$) and the mean reconstructed value of the combined charge ($\langle Q_{\text{comb}} \rangle$) for signal events, the b -jet charge calibration coefficient

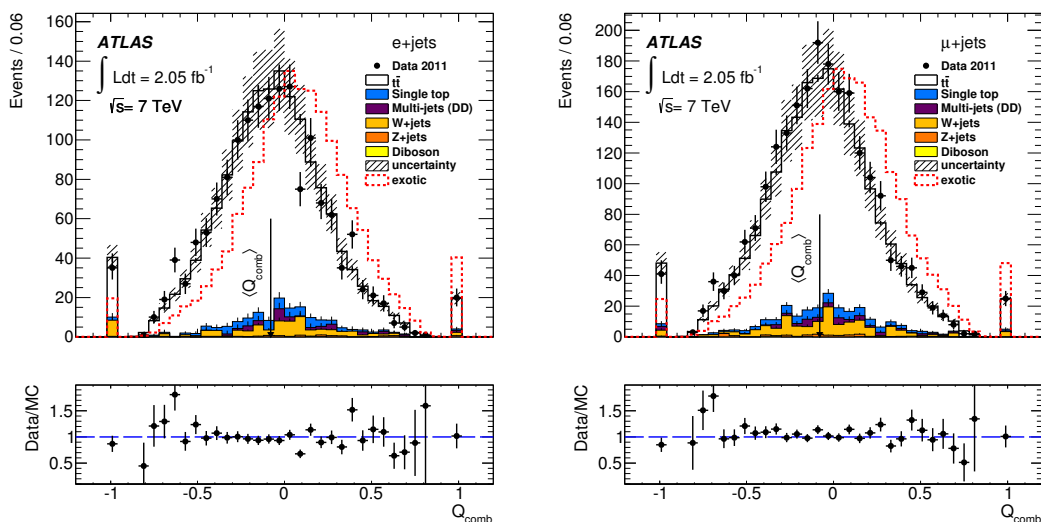


Figure 7. Distribution of the combined charge, Q_{comb} , in electron + jets (left) and muon + jets (right) final states. The full circles with error bars are data, the full black line corresponds to the SM scenario, and the dashed red line corresponds to the exotic model. The vertical line, labeled with $\langle Q_{\text{comb}} \rangle$, shows the mean value of the Q_{comb} distribution obtained from data. Only statistical uncertainties are shown.

$C_b = Q_b / \langle Q_{\text{comb}} \rangle$ is found to be 4.23 ± 0.03 (stat.) ± 0.07 (syst.) when evaluated using the full $t\bar{t}$ MC sample. The systematic uncertainty on C_b is taken as half the difference between the values of the calibration coefficient for the electron and muon channels. As mentioned in section 6.1 the small difference between the mean combined charges of the electron and muon channels arises as a consequence of different selection criteria used for these channels. The mean combined charge depends slightly on b -jet p_T and the $l\bar{b}$ -pairing purity and efficiency depend on lepton and b -jet p_T . Though these dependences are weak they should be taken into account if the common calibration coefficient is used. The top quark charge then can be calculated as

$$Q_{\text{top}} = 1 + Q_{\text{comb}}^{(\text{data})} \times C_b, \quad (7.1)$$

where $Q_{\text{comb}}^{(\text{data})}$ is the reconstructed b -jet charge obtained from the data after the subtraction of the expected background.

The mean value of the top quark charge for the electron + jets channel is $Q_{\text{top}} = 0.63 \pm 0.04$ (stat.) ± 0.11 (syst.) and that for the muon + jets channel is $Q_{\text{top}} = 0.65 \pm 0.03$ (stat.) ± 0.12 (syst.). The combined result using both channels is 0.64 ± 0.02 (stat.) ± 0.08 (syst.). This result is obtained from the mean of the combined histogram of Q_{comb} for the two channels. The quoted systematic uncertainty includes uncertainties on the calibration constant and all the uncertainties on the mean combined charge as described below.

7.1 Systematic uncertainties

The studies of systematic uncertainties connected with the combined charge follow methods similar to those used in other top quark studies (see e.g. ref. [37]). Each systematic effect is investigated by varying the corresponding quantity by $\pm 1\sigma$ with respect to the nominal value. If the direction of the variation is not defined (as in the case of the estimate resulting from the difference of two models, e.g. HERWIG and PYTHIA), the estimated variation is assumed to be the same size in the upward and the downward direction and the uncertainty on $\langle Q_{\text{comb}} \rangle$ is symmetrized. The following effects are taken into account.

Monte Carlo generators — the systematic uncertainties from MC generators are estimated by comparing the results obtained with the MC@NLO and POWHEG generators.

Showering and hadronization — the POWHEG samples with shower models from PYTHIA or HERWIG are compared and the difference is taken as the uncertainty due to the showering model.

Top quark mass — the uncertainty resulting from the assumed top quark mass is estimated using simulated $t\bar{t}$ samples with top quark mass in the range of 167.5–177.5 GeV in steps of 2.5 GeV. After fitting the mean values of Q_{comb} for different top quark mass samples the quoted systematic uncertainty is the largest of the differences between the fit function value at 172.5 GeV and at those at 172.5 ± 1.0 GeV.

Initial- and final-state radiation (ISR/FSR) — the ISR/FSR uncertainty is calculated using dedicated signal samples generated with ACERMC interfaced to PYTHIA. The parameters responsible for the level of ISR and FSR are varied in a range comparable to those used in the Perugia MC tunes [42]. Half of the difference between the minimum and maximum values of $\langle Q_{\text{comb}} \rangle$ is taken as the systematic uncertainty due to ISR/FSR.

Colour reconnection — the systematic uncertainty due to colour reconnection is determined using ACERMC interfaced to PYTHIA. Two different colour reconnection effects are simulated as described in refs. [42, 43] and for each effect the difference in the reconstructed combined charge between two levels of the colour reconnection is found. The larger difference is taken as the systematic uncertainty.

Missing transverse momentum — $E_{\text{T}}^{\text{miss}}$ is used in the event selection and can influence the reconstructed Q_{comb} . The impact of a possible mis-calibration is assessed by changing the measured $E_{\text{T}}^{\text{miss}}$ within its uncertainty. The systematic uncertainty of $E_{\text{T}}^{\text{miss}}$ includes the energy scale of clusters not associated with jets, electrons or muons and the accuracy of the pile-up simulations. The effect of a hardware failure in a part of the liquid-argon calorimeter is also taken into account. This uncertainty is assessed by varying the jet thresholds used for removing events with jets in the dead calorimeter region.

Multi-jet normalization — a 100% uncertainty on the number of multi-jet events due to the data-driven method is assumed in calculating the uncertainty of $\langle Q_{\text{comb}} \rangle$ connected with this normalization.

Single-top-quark normalization — the cross sections of individual single-top-quark channels are simultaneously varied within their theoretical uncertainty by $\pm 1\sigma$ and the largest difference in the combined signal and background $\langle Q_{\text{comb}} \rangle$ with respect to the nominal one is quoted as the systematic uncertainty due to the single-top-quark production cross section [44].

W + jets — the W +jets cross section is varied within its theoretical uncertainty (the uncertainty for inclusive W production of 4% and the additional uncertainty per each additional jet, of 24%, are added in quadrature). The uncertainties on the shapes of W +jets kinematic distributions are assessed by varying several parameters, such as the minimum transverse momentum of the partons and the functional form of the factorization scale in ALPGEN. The W +jets samples are reweighted according to each of these parameters and the quadratic sum of the uncertainties for the individual parameters is taken as the systematic uncertainty. Uncertainties connected with the scaling factors correcting the fractions of heavy flavour contributions in simulated W +jets samples are also taken into account.

Z + jets — the same prescription as for the normalization of W +jets events is also applied to Z +jets events.

b-tagging — the b -tagging efficiency and mistag probabilities in data and MC simulation are not identical. To reconcile the difference, b -tagging scale factors together with their uncertainties are derived per jet [35, 36]. They depend on the jet p_T and η and the underlying quark flavour. For the nominal result, the central values of the scale factors are applied, and the systematic uncertainty is estimated by changing their values within their uncertainties.

Lepton-related uncertainty — this item comprises the uncertainties due to MC modelling of the lepton identification, trigger efficiency, energy scale and energy resolution. Each simulated event is weighted with an appropriate scale factor (ratio of the measured efficiency to the simulated one) in order to reproduce the efficiencies seen in data. The uncertainties on the scale factors are included in the uncertainties on the acceptance values. Details can be found in ref. [37].

Jet energy scale — the jet energy scale (JES) and its uncertainty are derived by combining information from test-beam data, LHC collision data and MC simulations [45, 46]. The dependence of the JES uncertainty on the p_T and η of the reconstructed jet is used to scale the energy of each jet up or down by one standard deviation in the used MC sample. These variations are also propagated to the missing transverse energy. An uncertainty contribution to the JES due to pile-up events is also taken into account. An additional uncertainty is applied exclusively to b -jets. For each b -jet matched to a parton level b -quark a p_T -dependent uncertainty ranging from 2.5% for low- p_T jets to 0.76% for high- p_T jets is used.

The JES is the most significant source of systematic uncertainty. The reason is that changes in the JES have a large impact on the number of events with low- p_T b -jets and the purity of the ℓb -pairing degrades at low b -jet p_T . The number of events at high and low JES varies with respect to the nominal scale by 25% and 14%, respectively.

Jet energy resolution — the impact of the jet energy resolution is assessed by smearing the jet energy before performing the event selection. The energy of each reconstructed jet in the simulation is additionally smeared by a Gaussian function such that the width of the resulting Gaussian distribution includes the uncertainty on the jet energy resolution.

Jet reconstruction efficiency — the impact of the uncertainty in the jet reconstruction efficiency is evaluated by randomly dropping jets from events and determining the

Source	Systematic uncertainty (%)
MC statistics	0.7
MC generator	3.7
Parton shower	7.9
Colour reconnection	0.5
ISR/FSR	3.1
Top quark mass	0.3
Missing transverse energy	0.8
Jet energy scale	8.3
b -jet energy scale	3.3
Jet energy resolution	1.0
Jet reconstruction efficiency	0.7
b -tagging	0.3
Single top normalization	<0.1
W + jets	1.2
Z + jets	0.1
Multi-jet normalization	1.0
Electron-related uncertainty	1.3
Muon-related uncertainty	1.8
b -hadron fractions	0.7
Total uncertainty of $e + \mu$ -channel	13.2

Table 5. The systematic uncertainties for the combined charge. The total uncertainty is calculated by adding the individual ones in quadrature.

variation of $\langle Q_{\text{comb}} \rangle$ with respect to that of the nominal sample, following the prescription described in ref. [32].

Influence of b -hadron fractions — in the hadronization process that leads to a b -jet, different b -hadrons can be formed and the combined charge can depend on the b -hadron type. In addition, the mixing of B^0 and B_S^0 mesons needs to be taken into account. For the b -jets containing B^0 -mesons, it leads to a smaller mean combined charge in comparison with the jets containing charged B mesons. The effect for jets containing B_S^0 mesons, where the mixing probability is 50%, should lead to zero mean combined charge. The measured mixing probabilities ($\chi_d = 0.186$ (B^0) and $\chi_S = 0.5$ (B_S^0)) [47] are used to find the effective values of the mean combined charge for b -jets with B^0 and B_S^0 mesons. A study based on MC simulation shows that the mean combined charge for b -jets with b -baryons is about 74% of that for b -jets with B^\pm . The systematic uncertainty on the mean combined charge due to the uncertainties on the b -hadron production fractions, taken from ref. [45], has been evaluated by varying independently the production fractions for B^0 and B_S^0 mesons and b -baryons by 1 standard deviation up and down and adding the individual contributions in quadrature.

All other systematic uncertainties are small (less than 1%). A summary of all systematic uncertainties for the reconstruction of the combined charge in the electron and muon channels combined is shown in table 5.

Channel	Q_s	Q_b	Q_t	r_b	r_t
e	-0.080 ± 0.007	-0.015 ± 0.041	-0.066 ± 0.042	0.066 ± 0.018	0.042 ± 0.012
μ	-0.078 ± 0.006	-0.052 ± 0.028	-0.051 ± 0.038	0.088 ± 0.025	0.038 ± 0.011
$e + \mu$	-0.079 ± 0.004	-0.038 ± 0.023	-0.058 ± 0.028	0.079 ± 0.016	0.040 ± 0.008

Table 6. The nuisance parameters: the expected combined charge mean values and their standard deviations for the signal (Q_s), non-top-quark background (Q_b), single-top-quark background (Q_t) and the fractions of non-top-quark (r_b) and single-top-quark (r_t) backgrounds for an integrated luminosity of 2.05 fb^{-1} .

8 Statistical comparison of the SM and exotic model

The main result of this analysis — the compatibility of the data with the SM hypothesis of the top quark charge of $2/3$ — was evaluated using a statistical model. This model is based on the Cousins-Highland approach [48]. The test statistic used for this purpose is the mean value of the combined charge. Due to finite detector resolution and finite sample size, the mean value of the combined charge observed in the experiment can be treated as one realization of a random variable, \bar{Q} , the distribution of which characterizes all possible outcomes of the experiment. This variable can be expressed as

$$\bar{Q} = (1 - r_b - r_t) \cdot Q_s + r_b \cdot Q_b + r_t \cdot Q_t, \tag{8.1}$$

where Q_s , Q_b and Q_t are the combined charge mean values for the signal, background and single-top-quark processes, respectively, and r_b (r_t) is the fraction of the background (single-top-quark) events in the total sample of the candidate events.

The SM acceptance (critical) region [49, 50] is defined as $\bar{Q} < 0$ ($\bar{Q} > 0$). The decision boundary $\bar{Q} = 0$ unambiguously determines the confidence level α (probability to exclude the SM scenario if it is true) and the so-called false negative rate β (the probability of failing to reject the alternative hypothesis if it is true). The quantities Q_s , Q_b , Q_t , r_b and r_t are the nuisance parameters of the method and are assumed to be Gaussian random variables. The Gaussian nature of the combined charges was tested with 10 million MC experiments. In each experiment the mean combined charge was found by averaging 1000 combined charges generated from a MC-simulated combined charge spectrum for the muon channel. The obtained distribution of the mean combined charges was normally distributed and the Gaussian fit to the distribution showed a goodness-of-fit of $\chi^2/ndf = 86/103$. Their uncertainties scaled to the data integrated luminosity (2.05 fb^{-1}) are summarized in table 6. The two hypotheses are compared by calculating the p -value [49], the probability of obtaining a test statistic at least as extreme as the one that was actually observed provided that the null hypothesis is true. In order to obtain the p -value for the observed values of the test statistic $\langle Q_{\text{comb}} \rangle$ (see the data column of table 4), pseudo-experiments for both hypotheses, the SM as well as the exotic model, have been performed. To take into account a possible difference between MC and experimental data, a scale factor (SF) is defined as the ratio of experimental to MC mean combined charges for a QCD b -jet sample. The scale factor SF was found using double b -tagged dijet events containing a soft muon, where

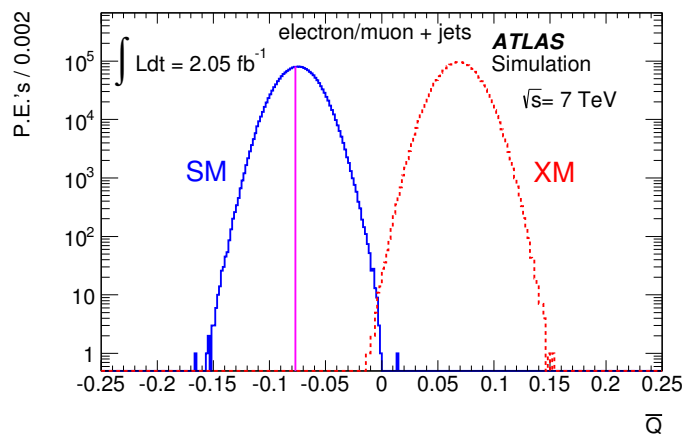


Figure 8. The expected distribution of the mean value of the combined charge, \bar{Q} , for the electron and muon channels resulting from pseudo-experiments for the SM (solid blue line) and the exotic (dashed red line) hypothesis for an integrated luminosity of 2.05 fb^{-1} . The magenta vertical line represents the value measured in the data.

the charge of the soft muon determines the flavour of the b -jet (i.e. if b or \bar{b} initiated the jet). This technique gives $\text{SF} = 1.00$ with a spread $\sigma = 0.19$. The technique based on the absolute value of the b -jet charge, i.e. based on the data-to-MC ratio from figure 4, leads to a scale factor compatible with unity with a spread $\sigma = 0.02$. To be conservative, the former value is used. The SF uncertainty is added in quadrature to the statistical and systematic uncertainties of the combined mean charge.

In figure 8 the distributions from the pseudo-experiments of the observed mean combined charge (\bar{Q}) are shown for both hypotheses, the SM (solid blue line) and the exotic model (dashed red line). The magenta line in this plot corresponds to the experimentally observed value Q_{obs} . The figure shows the results for the combined electron and muon channels. Each of these distributions is obtained from pseudo-experiments in which the nuisance parameters are sampled from Gaussian distributions with the mean values and standard deviations taken from table 6. In addition, the sampled charge \bar{Q} is Gaussian-smearred by the mean combined charge systematic uncertainty and by the SF uncertainty.

The p -values for the SM and the exotic model, the distance of Q_{obs} from the expected value of the exotic combined charge in standard deviations, and the quantities α and β , are summarized in table 7 for the combined electron and muon ($e + \mu$) channel as well as for the electrons (e) and muons (μ) channels separately.

From table 7 it can be seen that the data are fully compatible with the SM. The p -values for the SM scenario are high (the two-sided p -value is more than 80%) while those for the exotic hypothesis are very small (less than 10^{-7}). None of the 20 million exotic-hypothesis pseudo-experiments have \bar{Q} values below the observed value of the mean combined charge. Converting the p -value into the number of standard deviations for the exotic-scenario mean combined charge distribution, an exclusion at the level higher than 8σ is obtained for the combination of the electron and muon channels. This result assumes Gaussian-distributed

Channel	p_{SM}	p_{XM}	$\sigma_{\text{XM}}(\text{s.d.})$	α	β
e	0.813	$< 10^{-7}$	8.8	6.1×10^{-6}	1.1×10^{-5}
μ	0.960	$< 10^{-7}$	8.5	2.4×10^{-6}	4.0×10^{-5}
$e + \mu$	0.892	$< 10^{-7}$	8.9	2.4×10^{-6}	1.5×10^{-5}

Table 7. The p -values for the SM (p_{SM}) and exotic model (p_{XM}); the distance σ_{XM} of the observed value, Q_{obs} , from the expected value of the exotic combined charge in standard deviations (s.d.); the significance level (α) and the false negative rate (β) for the integrated luminosity of 2.05 fb^{-1} .

nuisance parameters, as supported by the performed MC experiments. Due to fact that most of the systematic uncertainties were combined and are common to the electron and muon channels, the differences in the nuisance parameters do not lead to large differences in the exclusion limits for the individual channels.

9 Conclusion

The top quark charge has been studied using 2.05 fb^{-1} of data accumulated by the ATLAS experiment at a centre-of-mass energy of 7 TeV . The measured top quark charge is 0.64 ± 0.02 (stat.) ± 0.08 (syst.). This result strongly favours the Standard Model and excludes models with an exotic quark with charge $-4/3$ instead of the top quark by more than 8σ .

Acknowledgments

We thank CERN for the very successful operation of the LHC, as well as the support staff from our institutions without whom ATLAS could not be operated efficiently.

We acknowledge the support of ANPCyT, Argentina; YerPhI, Armenia; ARC, Australia; BMWF and FWF, Austria; ANAS, Azerbaijan; SSTC, Belarus; CNPq and FAPESP, Brazil; NSERC, NRC and CFI, Canada; CERN; CONICYT, Chile; CAS, MOST and NSFC, China; COLCIENCIAS, Colombia; MSMT CR, MPO CR and VSC CR, Czech Republic; DNRF, DNSRC and Lundbeck Foundation, Denmark; EPLANET, ERC and NSRF, European Union; IN2P3-CNRS, CEA-DSM/IRFU, France; GNSF, Georgia; BMBF, DFG, HGF, MPG and AvH Foundation, Germany; GSRT and NSRF, Greece; ISF, MINERVA, GIF, DIP and Benoziyo Center, Israel; INFN, Italy; MEXT and JSPS, Japan; CNRST, Morocco; FOM and NWO, Netherlands; BRF and RCN, Norway; MNiSW, Poland; GRICES and FCT, Portugal; MERYS (MECTS), Romania; MES of Russia and ROSATOM, Russian Federation; JINR; MSTD, Serbia; MSSR, Slovakia; ARRS and MIZŠ, Slovenia; DST/NRF, South Africa; MICINN, Spain; SRC and Wallenberg Foundation, Sweden; SER, SNSF and Cantons of Bern and Geneva, Switzerland; NSC, Taiwan; TAEK, Turkey; STFC, the Royal Society and Leverhulme Trust, United Kingdom; DOE and NSF, U.S.A.

The crucial computing support from all WLCG partners is acknowledged gratefully, in particular from CERN and the ATLAS Tier-1 facilities at TRIUMF (Canada), NDGF (Denmark, Norway, Sweden), CC-IN2P3 (France), KIT/GridKA (Germany), INFN-CNAF (Italy), NL-T1 (Netherlands), PIC (Spain), ASGC (Taiwan), RAL (U.K.) and BNL (U.S.A.) and in the Tier-2 facilities worldwide.

Open Access. This article is distributed under the terms of the Creative Commons Attribution License which permits any use, distribution and reproduction in any medium, provided the original author(s) and source are credited.

References

- [1] CDF collaboration, *Observation of top quark production in $\bar{p}p$ collisions*, *Phys. Rev. Lett.* **74** (1995) 2626 [[hep-ex/9503002](#)] [[INSPIRE](#)].
- [2] D0 collaboration, S. Abachi et al., *Observation of the top quark*, *Phys. Rev. Lett.* **74** (1995) 2632 [[hep-ex/9503003](#)] [[INSPIRE](#)].
- [3] D. Chang, W.-F. Chang and E. Ma, *Alternative interpretation of the Tevatron top events*, *Phys. Rev. D* **59** (1999) 091503 [[hep-ph/9810531](#)] [[INSPIRE](#)].
- [4] D0 collaboration, V. Abazov et al., *Experimental discrimination between charge $2e/3$ top quark and charge $4e/3$ exotic quark production scenarios*, *Phys. Rev. Lett.* **98** (2007) 041801 [[hep-ex/0608044](#)] [[INSPIRE](#)].
- [5] CDF collaboration, *Exclusion of an Exotic Top Quark with $-4/3$ Electric Charge Using Soft Lepton Tagging*, *Phys. Rev. Lett.* **105** (2010) 101801 [[arXiv:1006.4597](#)] [[INSPIRE](#)].
- [6] CDF collaboration, *Exclusion of exotic top-like quarks with $-4/3$ electric charge using jet-charge tagging in single-lepton $t\bar{t}$ events at CDF*, *Phys. Rev. D* **88** (2013) 032003 [[arXiv:1304.4141](#)] [[INSPIRE](#)].
- [7] ATLAS collaboration, *The ATLAS Experiment at the CERN Large Hadron Collider*, 2008 *JINST* **3** S08003 [[INSPIRE](#)].
- [8] ATLAS collaboration, *Improved luminosity determination in pp collisions at $\sqrt{s} = 7$ TeV using the ATLAS detector at the LHC*, *Eur. Phys. J. C* **73** (2013) 2518 [[arXiv:1302.4393](#)] [[INSPIRE](#)].
- [9] GEANT4 collaboration, S. Agostinelli et al., *GEANT4: A Simulation toolkit*, *Nucl. Instrum. Meth. A* **506** (2003) 250 [[INSPIRE](#)].
- [10] ATLAS collaboration, *The ATLAS Simulation Infrastructure*, *Eur. Phys. J. C* **70** (2010) 823 [[arXiv:1005.4568](#)] [[INSPIRE](#)].
- [11] S. Frixione and B.R. Webber, *Matching NLO QCD computations and parton shower simulations*, *JHEP* **06** (2002) 029 [[hep-ph/0204244](#)] [[INSPIRE](#)].
- [12] S. Frixione, P. Nason and B.R. Webber, *Matching NLO QCD and parton showers in heavy flavor production*, *JHEP* **08** (2003) 007 [[hep-ph/0305252](#)] [[INSPIRE](#)].
- [13] P.M. Nadolsky et al., *Implications of CTEQ global analysis for collider observables*, *Phys. Rev. D* **78** (2008) 013004 [[arXiv:0802.0007](#)] [[INSPIRE](#)].
- [14] G. Corcella et al., *HERWIG 6: an event generator for hadron emission reactions with interfering gluons (including supersymmetric processes)*, *JHEP* **01** (2001) 010 [[hep-ph/0011363](#)] [[INSPIRE](#)].
- [15] S. Frixione, F. Stoeckli, P. Torrielli and B.R. Webber, *NLO QCD corrections in HERWIG++ with MC@NLO*, *JHEP* **01** (2011) 053 [[arXiv:1010.0568](#)] [[INSPIRE](#)].
- [16] J. Butterworth, J.R. Forshaw and M. Seymour, *Multiparton interactions in photoproduction at HERA*, *Z. Phys. C* **72** (1996) 637 [[hep-ph/9601371](#)] [[INSPIRE](#)].

- [17] P. Nason, *A new method for combining NLO QCD with shower Monte Carlo algorithms*, *JHEP* **11** (2004) 040 [[hep-ph/0409146](#)] [[INSPIRE](#)].
- [18] T. Sjöstrand, S. Mrenna and P.Z. Skands, *PYTHIA 6.4 Physics and Manual*, *JHEP* **05** (2006) 026 [[hep-ph/0603175](#)] [[INSPIRE](#)].
- [19] B.P. Kersevan and E. Richter-Was, *The Monte Carlo event generator AcerMC version 2.0 with interfaces to PYTHIA 6.2 and HERWIG 6.5*, [hep-ph/0405247](#) [[INSPIRE](#)].
- [20] M. Aliev et al., *HATHOR: HAdronic Top and Heavy quarks crOss section calculatoR*, *Comput. Phys. Commun.* **182** (2011) 1034 [[arXiv:1007.1327](#)] [[INSPIRE](#)].
- [21] N. Kidonakis, *Next-to-next-to-leading-order collinear and soft gluon corrections for t-channel single top quark production*, *Phys. Rev. D* **83** (2011) 091503 [[arXiv:1103.2792](#)] [[INSPIRE](#)].
- [22] N. Kidonakis, *NNLL resummation for s-channel single top quark production*, *Phys. Rev. D* **81** (2010) 054028 [[arXiv:1001.5034](#)] [[INSPIRE](#)].
- [23] N. Kidonakis, *Two-loop soft anomalous dimensions for single top quark associated production with a W^- or H^-* , *Phys. Rev. D* **82** (2010) 054018 [[arXiv:1005.4451](#)] [[INSPIRE](#)].
- [24] M. Mangano et al., *ALPGEN, a generator for hard multiparton processes in hadronic collisions*, *JHEP* **07** (2003) 001 [[hep-ex/0206293](#)].
- [25] J. Pumplin et al., *New generation of parton distributions with uncertainties from global QCD analysis*, *JHEP* **07** (2002) 012 [[hep-ph/0201195](#)] [[INSPIRE](#)].
- [26] K. Melnikov and F. Petriello, *Electroweak gauge boson production at hadron colliders through $O(\alpha_s^2)$* , *Phys. Rev. D* **74** (2006) 114017 [[hep-ph/0609070](#)] [[INSPIRE](#)].
- [27] A. Sherstnev and R. Thorne, *Parton Distributions for LO Generators*, *Eur. Phys. J. C* **55** (2008) 553 [[arXiv:0711.2473](#)] [[INSPIRE](#)].
- [28] ATLAS collaboration, *Further ATLAS tunes of PYTHIA6 and PYTHIA 8*, [ATL-PHYS-PUB-2011-014](#) (2011).
- [29] ATLAS collaboration, *Electron performance measurements with the ATLAS detector using the 2010 LHC proton-proton collision data*, *Eur. Phys. J. C* **72** (2012) 1909 [[arXiv:1110.3174](#)] [[INSPIRE](#)].
- [30] ATLAS collaboration, *Muon reconstruction efficiency in reprocessed 2010 LHC proton-proton collision data recorded with the ATLAS detector*, [ATLAS-CONF-2011-063](#) (2011).
- [31] M. Cacciari, G.P. Salam and G. Soyez, *The anti- k_t jet clustering algorithm*, *JHEP* **04** (2008) 063.
- [32] ATLAS collaboration, *Jet energy measurement with the ATLAS detector in proton-proton collisions at $\sqrt{s} = 7$ TeV*, *Eur. Phys. J. C* **73** (2013) 2304 [[arXiv:1112.6426](#)] [[INSPIRE](#)].
- [33] W. Lampl et al., *Calorimeter Clustering Algorithms: Description and Performance*, [ATL-LARG-PUB-2008-002](#) (2008).
- [34] ATLAS collaboration, *Performance of Missing Transverse Momentum Reconstruction in Proton-Proton Collisions at 7 TeV with ATLAS*, *Eur. Phys. J. C* **72** (2012) 1844 [[arXiv:1108.5602](#)] [[INSPIRE](#)].
- [35] ATLAS collaboration, *Measuring the b-tag efficiency in a top-pair sample with 4.7fb^{-1} of data from the ATLAS detector*, [ATLAS-CONF-2012-097](#) (2012).

- [36] ATLAS collaboration, *Commissioning of the ATLAS high-performance b-tagging algorithms in the 7 TeV collision data*, [ATLAS-CONF-2011-102](#) (2011).
- [37] ATLAS collaboration, *Measurement of the top quark-pair production cross section with ATLAS in pp collisions at $\sqrt{s} = 7$ TeV*, *Eur. Phys. J. C* **71** (2011) 1577 [[arXiv:1012.1792](#)] [[INSPIRE](#)].
- [38] R. Field and R. Feynman, *A Parametrization of the Properties of Quark Jets*, *Nucl. Phys. B* **136** (1978) 1 [[INSPIRE](#)].
- [39] ALEPH collaboration, *Determination of A-b(FB) using jet charge measurements in Z decays*, *Phys. Lett. B* **426** (1998) 217 [[INSPIRE](#)].
- [40] ATLAS collaboration, *Measurement of the cross section for the production of a W boson in association with b^- jets in pp collisions at $\sqrt{s} = 7$ TeV with the ATLAS detector*, *Phys. Lett. B* **707** (2012) 418 [[arXiv:1109.1470](#)] [[INSPIRE](#)].
- [41] ATLAS collaboration, *Measurements of top quark pair relative differential cross-sections with ATLAS in pp collisions at $\sqrt{s} = 7$ TeV*, *Eur. Phys. J. C* **73** (2013) 2261 [[arXiv:1207.5644](#)] [[INSPIRE](#)].
- [42] P.Z. Skands, *Tuning Monte Carlo Generators: The Perugia Tunes*, *Phys. Rev. D* **82** (2010) 074018 [[arXiv:1005.3457](#)] [[INSPIRE](#)].
- [43] TEV4LHC QCD WORKING GROUP collaboration, M.G. Albrow et al., *Tevatron-for-LHC Report of the QCD Working Group*, [hep-ph/0610012](#) [[INSPIRE](#)].
- [44] N. Kidonakis, *Single top quark production cross section at hadron colliders*, [PoS\(DIS 2010\)196](#) [[arXiv:1005.3330](#)] [[INSPIRE](#)].
- [45] ATLAS collaboration, *Measurement of inclusive jet and dijet cross sections in proton-proton collisions at 7 TeV centre-of-mass energy with the ATLAS detector*, *Eur. Phys. J. C* **71** (2011) 1512 [[arXiv:1009.5908](#)] [[INSPIRE](#)].
- [46] ATLAS collaboration, *Measurement of inclusive jet and dijet production in pp collisions at $\sqrt{s} = 7$ TeV using the ATLAS detector*, *Phys. Rev. D* **86** (2012) 014022 [[arXiv:1112.6297](#)] [[INSPIRE](#)].
- [47] PARTICLE DATA GROUP collaboration, J. Beringer et al., *Review of Particle Physics (RPP)*, *Phys. Rev. D* **86** (2012) 010001 [[INSPIRE](#)].
- [48] R.D. Cousins and V.L. Highland, *Incorporating systematic uncertainties into an upper limit*, *Nucl. Instrum. Meth. A* **320** (1992) 331 [[INSPIRE](#)].
- [49] F. James, *Statistical Methods in Experimental Physics*, North-Holland Publishing Co., Amsterdam The Netherlands (2006).
- [50] G. Cowan, *Statistical Data Analysis*, Clarendon Press, Oxford U.K. (1998).

The ATLAS collaboration

G. Aad⁴⁸, T. Abajyan²¹, B. Abbott¹¹², J. Abdallah¹², S. Abdel Khalek¹¹⁶, A.A. Abdelalim⁴⁹, O. Abidinov¹¹, R. Aben¹⁰⁶, B. Abi¹¹³, M. Abolins⁸⁹, O.S. AbouZeid¹⁵⁹, H. Abramowicz¹⁵⁴, H. Abreu¹³⁷, Y. Abulaiti^{147a,147b}, B.S. Acharya^{165a,165b,a}, L. Adamczyk^{38a}, D.L. Adams²⁵, T.N. Addy⁵⁶, J. Adelman¹⁷⁷, S. Adomeit⁹⁹, T. Adye¹³⁰, S. Aefsky²³, J.A. Aguilar-Saavedra^{125b,b}, M. Agustoni¹⁷, S.P. Ahlen²², F. Ahles⁴⁸, A. Ahmad¹⁴⁹, M. Ahsan⁴¹, G. Aielli^{134a,134b}, T.P.A. Åkesson⁸⁰, G. Akimoto¹⁵⁶, A.V. Akimov⁹⁵, M.A. Alam⁷⁶, J. Albert¹⁷⁰, S. Albrand⁵⁵, M. Aleksa³⁰, I.N. Aleksandrov⁶⁴, F. Alessandria^{90a}, C. Alexa^{26a}, G. Alexander¹⁵⁴, G. Alexandre⁴⁹, T. Alexopoulos¹⁰, M. Alhroob^{165a,165c}, M. Aliev¹⁶, G. Alimonti^{90a}, J. Alison³¹, B.M.M. Allbrooke¹⁸, L.J. Allison⁷¹, P.P. Allport⁷³, S.E. Allwood-Spiers⁵³, J. Almond⁸³, A. Aloisio^{103a,103b}, R. Alon¹⁷³, A. Alonso³⁶, F. Alonso⁷⁰, A. Altheimer³⁵, B. Alvarez Gonzalez⁸⁹, M.G. Alviggi^{103a,103b}, K. Amako⁶⁵, Y. Amaral Coutinho^{24a}, C. Amelung²³, V.V. Ammosov^{129,*}, S.P. Amor Dos Santos^{125a}, A. Amorim^{125a,c}, S. Amoroso⁴⁸, N. Amram¹⁵⁴, C. Anastopoulos³⁰, L.S. Ancu¹⁷, N. Andari³⁰, T. Andeen³⁵, C.F. Anders^{58b}, G. Anders^{58a}, K.J. Anderson³¹, A. Andreazza^{90a,90b}, V. Andrei^{58a}, X.S. Anduaga⁷⁰, S. Angelidakis⁹, P. Anger⁴⁴, A. Angerami³⁵, F. Anghinolfi³⁰, A. Anisenkov¹⁰⁸, N. Anjos^{125a}, A. Annovi⁴⁷, A. Antonaki⁹, M. Antonelli⁴⁷, A. Antonov⁹⁷, J. Antos^{145b}, F. Anulli^{133a}, M. Aoki¹⁰², L. Aperio Bella¹⁸, R. Apolle^{119,d}, G. Arabidze⁸⁹, I. Aracena¹⁴⁴, Y. Arai⁶⁵, A.T.H. Arce⁴⁵, S. Arfaoui¹⁴⁹, J-F. Arguin⁹⁴, S. Argyropoulos⁴², E. Arik^{19a,*}, M. Arik^{19a}, A.J. Armbruster⁸⁸, O. Arnaez⁸², V. Arnal⁸¹, A. Artamonov⁹⁶, G. Artoni^{133a,133b}, D. Arutinov²¹, S. Asai¹⁵⁶, N. Asbah⁹⁴, S. Ask²⁸, B. Åsman^{147a,147b}, L. Asquith⁶, K. Assamagan²⁵, R. Astalos^{145a}, A. Astbury¹⁷⁰, M. Atkinson¹⁶⁶, B. Auerbach⁶, E. Auge¹¹⁶, K. Augsten¹²⁷, M. Aourousseau^{146b}, G. Avolio³⁰, D. Axen¹⁶⁹, G. Azuelos^{94,e}, Y. Azuma¹⁵⁶, M.A. Baak³⁰, G. Baccaglioni^{90a}, C. Bacci^{135a,135b}, A.M. Bach¹⁵, H. Bachacou¹³⁷, K. Bachas¹⁵⁵, M. Backes⁴⁹, M. Backhaus²¹, J. Backus Mayes¹⁴⁴, E. Badescu^{26a}, P. Bagiacchi^{133a,133b}, P. Bagnaia^{133a,133b}, Y. Bai^{33a}, D.C. Bailey¹⁵⁹, T. Bain³⁵, J.T. Baines¹³⁰, O.K. Baker¹⁷⁷, S. Baker⁷⁷, P. Balek¹²⁸, F. Balli¹³⁷, E. Banas³⁹, P. Banerjee⁹⁴, Sw. Banerjee¹⁷⁴, D. Banfi³⁰, A. Bangert¹⁵¹, V. Bansal¹⁷⁰, H.S. Bansil¹⁸, L. Barak¹⁷³, S.P. Baranov⁹⁵, T. Barber⁴⁸, E.L. Barberio⁸⁷, D. Barberis^{50a,50b}, M. Barbero⁸⁴, D.Y. Bardin⁶⁴, T. Barillari¹⁰⁰, M. Barisonzi¹⁷⁶, T. Barklow¹⁴⁴, N. Barlow²⁸, B.M. Barnett¹³⁰, R.M. Barnett¹⁵, A. Baroncelli^{135a}, G. Barone⁴⁹, A.J. Barr¹¹⁹, F. Barreiro⁸¹, J. Barreiro Guimarães da Costa⁵⁷, R. Bartoldus¹⁴⁴, A.E. Barton⁷¹, V. Bartsch¹⁵⁰, A. Basye¹⁶⁶, R.L. Bates⁵³, L. Batkova^{145a}, J.R. Batley²⁸, A. Battaglia¹⁷, M. Battistin³⁰, F. Bauer¹³⁷, H.S. Bawa^{144,f}, S. Beale⁹⁹, T. Beau⁷⁹, P.H. Beauchemin¹⁶², R. Beccherle^{50a}, P. Bechtel²¹, H.P. Beck¹⁷, K. Becker¹⁷⁶, S. Becker⁹⁹, M. Beckingham¹³⁹, K.H. Becks¹⁷⁶, A.J. Beddall^{19c}, A. Beddall^{19c}, S. Bedikian¹⁷⁷, V.A. Bednyakov⁶⁴, C.P. Bee⁸⁴, L.J. Beamster¹⁰⁶, T.A. Beermann¹⁷⁶, M. Begel²⁵, C. Belanger-Champagne⁸⁶, P.J. Bell⁴⁹, W.H. Bell⁴⁹, G. Bella¹⁵⁴, L. Bellagamba^{20a}, A. Bellerive²⁹, M. Bellomo³⁰, A. Belloni⁵⁷, O. Beloborodova^{108,g}, K. Belotskiy⁹⁷, O. Beltramello³⁰, O. Benary¹⁵⁴, D. Benchekroun^{136a}, K. Bendtz^{147a,147b}, N. Benekos¹⁶⁶, Y. Benhammou¹⁵⁴, E. Benhar Nocchioli⁴⁹, J.A. Benitez Garcia^{160b}, D.P. Benjamin⁴⁵, J.R. Bensinger²³, K. Benslama¹³¹, S. Bentvelsen¹⁰⁶, D. Berge³⁰, E. Bergeaas Kuutmann¹⁶, N. Berger⁵, F. Berghaus¹⁷⁰, E. Berglund¹⁰⁶, J. Beringer¹⁵, P. Bernat⁷⁷, R. Bernhard⁴⁸, C. Bernius⁷⁸, F.U. Bernlochner¹⁷⁰, T. Berry⁷⁶, C. Bertella⁸⁴, F. Bertolucci^{123a,123b}, M.I. Besana^{90a,90b}, G.J. Besjes¹⁰⁵, N. Besson¹³⁷, S. Bethke¹⁰⁰, W. Bhimji⁴⁶, R.M. Bianchi³⁰, L. Bianchini²³, M. Bianco^{72a,72b}, O. Biebel⁹⁹, S.P. Bieniek⁷⁷, K. Bierwagen⁵⁴, J. Biesiada¹⁵, M. Biglietti^{135a}, H. Bilokon⁴⁷, M. Bindi^{20a,20b}, S. Binet¹¹⁶, A. Bingul^{19c}, C. Bini^{133a,133b}, B. Bittner¹⁰⁰, C.W. Black¹⁵¹, J.E. Black¹⁴⁴, K.M. Black²², R.E. Blair⁶, J.-B. Blanchard¹³⁷, T. Blazek^{145a}, I. Bloch⁴², C. Blocker²³, J. Blocki³⁹, W. Blum⁸², U. Blumenschein⁵⁴, G.J. Bobbink¹⁰⁶, V.S. Bobrovnikov¹⁰⁸, S.S. Bocchetta⁸⁰, A. Bocchi⁴⁵,

C.R. Boddy¹¹⁹, M. Boehler⁴⁸, J. Boek¹⁷⁶, T.T. Boek¹⁷⁶, N. Boelaert³⁶, J.A. Bogaerts³⁰,
A. Bogdanchikov¹⁰⁸, A. Bogouch^{91,*}, C. Bohm^{147a}, J. Bohm¹²⁶, V. Boisvert⁷⁶, T. Bold^{38a},
V. Boldea^{26a}, N.M. Bolnet¹³⁷, M. Bomben⁷⁹, M. Bona⁷⁵, M. Boonekamp¹³⁷, S. Bordini⁷⁹,
C. Borer¹⁷, A. Borisov¹²⁹, G. Borissov⁷¹, M. Borri⁸³, S. Borroni⁴², J. Bortfeldt⁹⁹,
V. Bortolotto^{135a,135b}, K. Bos¹⁰⁶, D. Boscherini^{20a}, M. Bosman¹², H. Boterenbrood¹⁰⁶,
J. Bouchami⁹⁴, J. Boudreau¹²⁴, E.V. Bouhova-Thacker⁷¹, D. Boumediene³⁴, C. Bourdarios¹¹⁶,
N. Bousson⁸⁴, S. Boutouil^{136d}, A. Boveia³¹, J. Boyd³⁰, I.R. Boyko⁶⁴, I. Bozovic-Jelisavcic^{13b},
J. Bracinik¹⁸, P. Branchini^{135a}, A. Brandt⁸, G. Brandt¹⁵, O. Brandt⁵⁴, U. Bratzler¹⁵⁷, B. Brau⁸⁵,
J.E. Brau¹¹⁵, H.M. Braun^{176,*}, S.F. Brazzale^{165a,165c}, B. Brelier¹⁵⁹, J. Bremer³⁰,
K. Brendlinger¹²¹, R. Brenner¹⁶⁷, S. Bressler¹⁷³, T.M. Bristow^{146c}, D. Britton⁵³, F.M. Brochu²⁸,
I. Brock²¹, R. Brock⁸⁹, F. Broggi^{90a}, C. Bromberg⁸⁹, J. Bronner¹⁰⁰, G. Brooijmans³⁵, T. Brooks⁷⁶,
W.K. Brooks^{32b}, G. Brown⁸³, P.A. Bruckman de Renstrom³⁹, D. Bruncko^{145b}, R. Bruneliere⁴⁸,
S. Brunet⁶⁰, A. Bruni^{20a}, G. Bruni^{20a}, M. Bruschi^{20a}, L. Bryngemark⁸⁰, T. Buanes¹⁴, Q. Buat⁵⁵,
F. Bucci⁴⁹, J. Buchanan¹¹⁹, P. Buchholz¹⁴², R.M. Buckingham¹¹⁹, A.G. Buckley⁴⁶, S.I. Buda^{26a},
I.A. Budagov⁶⁴, B. Budick¹⁰⁹, L. Bugge¹¹⁸, O. Bulekov⁹⁷, A.C. Bundock⁷³, M. Bunse⁴³,
T. Buran^{118,*}, H. Burckhart³⁰, S. Burdin⁷³, T. Burgess¹⁴, S. Burke¹³⁰, E. Busato³⁴, V. Büscher⁸²,
P. Bussey⁵³, C.P. Buszello¹⁶⁷, B. Butler⁵⁷, J.M. Butler²², C.M. Buttar⁵³, J.M. Butterworth⁷⁷,
W. Buttinger²⁸, M. Byszewski¹⁰, S. Cabrera Urbán¹⁶⁸, D. Caforio^{20a,20b}, O. Cakir^{4a},
P. Calafiura¹⁵, G. Calderini⁷⁹, P. Calfayan⁹⁹, R. Calkins¹⁰⁷, L.P. Caloba^{24a}, R. Caloi^{133a,133b},
D. Calvet³⁴, S. Calvet³⁴, R. Camacho Toro⁴⁹, P. Camarri^{134a,134b}, D. Cameron¹¹⁸,
L.M. Caminada¹⁵, R. Caminal Armadans¹², S. Campana³⁰, M. Campanelli⁷⁷, V. Canale^{103a,103b},
F. Canelli³¹, A. Canepa^{160a}, J. Cantero⁸¹, R. Cantrill⁷⁶, T. Cao⁴⁰, M.D.M. Capeans Garrido³⁰,
I. Caprini^{26a}, M. Caprini^{26a}, D. Capriotti¹⁰⁰, M. Capua^{37a,37b}, R. Caputo⁸², R. Cardarelli^{134a},
T. Carli³⁰, G. Carlino^{103a}, L. Carminati^{90a,90b}, S. Caron¹⁰⁵, E. Carquin^{32b},
G.D. Carrillo-Montoya^{146c}, A.A. Carter⁷⁵, J.R. Carter²⁸, J. Carvalho^{125a,h}, D. Casadei¹⁰⁹,
M.P. Casado¹², M. Cascella^{123a,123b}, C. Caso^{50a,50b,*}, E. Castaneda-Miranda¹⁷⁴, A. Castelli¹⁰⁶,
V. Castillo Gimenez¹⁶⁸, N.F. Castro^{125a}, G. Cataldi^{72a}, P. Catastini⁵⁷, A. Catinaccio³⁰,
J.R. Catmore³⁰, A. Cattai³⁰, G. Cattani^{134a,134b}, S. Caughron⁸⁹, V. Cavaliere¹⁶⁶, D. Cavalli^{90a},
M. Cavalli-Sforza¹², V. Cavasinni^{123a,123b}, F. Ceradini^{135a,135b}, B. Cerio⁴⁵, A.S. Cerqueira^{24b},
A. Cerri¹⁵, L. Cerrito⁷⁵, F. Cerutti¹⁵, A. Cervelli¹⁷, S.A. Cetin^{19b}, A. Chafaq^{136a},
D. Chakraborty¹⁰⁷, I. Chalupkova¹²⁸, K. Chan³, P. Chang¹⁶⁶, B. Chapleau⁸⁶, J.D. Chapman²⁸,
J.W. Chapman⁸⁸, D.G. Charlton¹⁸, V. Chavda⁸³, C.A. Chavez Barajas³⁰, S. Cheatham⁸⁶,
S. Chekanov⁶, S.V. Chekulaev^{160a}, G.A. Chelkov⁶⁴, M.A. Chelstowska¹⁰⁵, C. Chen⁶³, H. Chen²⁵,
S. Chen^{33c}, X. Chen¹⁷⁴, Y. Chen³⁵, Y. Cheng³¹, A. Cheplakov⁶⁴, R. Cherkaoui El Moursli^{136e},
V. Chernyatin²⁵, E. Cheu⁷, S.L. Cheung¹⁵⁹, L. Chevalier¹³⁷, V. Chiarella⁴⁷, G. Chiefari^{103a,103b},
J.T. Childers³⁰, A. Chilingarov⁷¹, G. Chiodini^{72a}, A.S. Chisholm¹⁸, R.T. Chislett⁷⁷, A. Chitan^{26a},
M.V. Chizhov⁶⁴, G. Choudalakis³¹, S. Chouridou⁹, B.K.B. Chow⁹⁹, I.A. Christidi⁷⁷,
A. Christov⁴⁸, D. Chromek-Burckhart³⁰, M.L. Chu¹⁵², J. Chudoba¹²⁶, G. Ciapetti^{133a,133b},
A.K. Ciftci^{4a}, R. Ciftci^{4a}, D. Cinca⁶², V. Cindro⁷⁴, A. Ciocio¹⁵, M. Cirilli⁸⁸, P. Cirkovic^{13b},
Z.H. Citron¹⁷³, M. Citterio^{90a}, M. Ciubancan^{26a}, A. Clark⁴⁹, P.J. Clark⁴⁶, R.N. Clarke¹⁵,
J.C. Clemens⁸⁴, B. Clement⁵⁵, C. Clement^{147a,147b}, Y. Coadou⁸⁴, M. Cokal^{165a,165c},
A. Coccaro¹³⁹, J. Cochran⁶³, S. Coelli^{90a}, L. Coffey²³, J.G. Cogan¹⁴⁴, J. Coggeshall¹⁶⁶, J. Colas⁵,
S. Cole¹⁰⁷, A.P. Colijn¹⁰⁶, N.J. Collins¹⁸, C. Collins-Tooth⁵³, J. Collot⁵⁵, T. Colombo^{120a,120b},
G. Colon⁸⁵, G. Compostella¹⁰⁰, P. Conde Muino^{125a}, E. Coniavitis¹⁶⁷, M.C. Conidi¹²,
S.M. Consonni^{90a,90b}, V. Consorti⁴⁸, S. Constantinescu^{26a}, C. Conta^{120a,120b}, G. Conti⁵⁷,
F. Conventi^{103a,i}, M. Cooke¹⁵, B.D. Cooper⁷⁷, A.M. Cooper-Sarkar¹¹⁹, N.J. Cooper-Smith⁷⁶,
K. Copic¹⁵, T. Cornelissen¹⁷⁶, M. Corradi^{20a}, F. Corriveau^{86,j}, A. Corso-Radu¹⁶⁴,
A. Cortes-Gonzalez¹⁶⁶, G. Cortiana¹⁰⁰, G. Costa^{90a}, M.J. Costa¹⁶⁸, D. Costanzo¹⁴⁰, D. Côté³⁰,

G. Cottin^{32a}, L. Courneyea¹⁷⁰, G. Cowan⁷⁶, B.E. Cox⁸³, K. Cranmer¹⁰⁹, S. Crépe-Renaudin⁵⁵, F. Crescioli⁷⁹, M. Cristinziani²¹, G. Crosetti^{37a,37b}, C.-M. Cuciuc^{26a}, C. Cuenca Almenar¹⁷⁷, T. Cuhadar Donszelmann¹⁴⁰, J. Cummings¹⁷⁷, M. Curatolo⁴⁷, C.J. Curtis¹⁸, C. Cuthbert¹⁵¹, H. Czirr¹⁴², P. Czodrowski⁴⁴, Z. Czyczula¹⁷⁷, S. D'Auria⁵³, M. D'Onofrio⁷³, A. D'Orazio^{133a,133b}, M.J. Da Cunha Sargedas De Sousa^{125a}, C. Da Via⁸³, W. Dabrowski^{38a}, A. Dafinca¹¹⁹, T. Dai⁸⁸, F. Dallaire⁹⁴, C. Dallapiccola⁸⁵, M. Dam³⁶, D.S. Damiani¹³⁸, A.C. Daniells¹⁸, H.O. Danielsson³⁰, V. Dao¹⁰⁵, G. Darbo^{50a}, G.L. Darlea^{26b}, S. Darmora⁸, J.A. Dassoulas⁴², W. Davey²¹, T. Davidek¹²⁸, N. Davidson⁸⁷, E. Davies^{119,d}, M. Davies⁹⁴, O. Davignon⁷⁹, A.R. Davison⁷⁷, Y. Davygora^{58a}, E. Dawe¹⁴³, I. Dawson¹⁴⁰, R.K. Daya-Ishmukhametova²³, K. De⁸, R. de Asmundis^{103a}, S. De Castro^{20a,20b}, S. De Cecco⁷⁹, J. de Graat⁹⁹, N. De Groot¹⁰⁵, P. de Jong¹⁰⁶, C. De La Taille¹¹⁶, H. De la Torre⁸¹, F. De Lorenzi⁶³, L. De Nooij¹⁰⁶, D. De Pedis^{133a}, A. De Salvo^{133a}, U. De Sanctis^{165a,165c}, A. De Santo¹⁵⁰, J.B. De Vivie De Regie¹¹⁶, G. De Zorzi^{133a,133b}, W.J. Dearnaley⁷¹, R. Debbes²⁵, C. Debenedetti⁴⁶, B. Dechenaux⁵⁵, D.V. Dedovich⁶⁴, J. Degenhardt¹²¹, J. Del Peso⁸¹, T. Del Prete^{123a,123b}, T. Delemontex⁵⁵, M. Deliyergiyev⁷⁴, A. Dell'Acqua³⁰, L. Dell'Asta²², M. Della Pietra^{103a,i}, D. della Volpe^{103a,103b}, M. Delmastro⁵, P.A. Delsart⁵⁵, C. Deluca¹⁰⁶, S. Demers¹⁷⁷, M. Demichev⁶⁴, A. Demilly⁷⁹, B. Demirkoz^{12,k}, S.P. Denisov¹²⁹, D. Derendarz³⁹, J.E. Derkaoui^{136d}, F. Derue⁷⁹, P. Dervan⁷³, K. Desch²¹, P.O. Deviveiros¹⁰⁶, A. Dewhurst¹³⁰, B. DeWilde¹⁴⁹, S. Dhaliwal¹⁰⁶, R. Dhullipudi^{78,l}, A. Di Ciaccio^{134a,134b}, L. Di Ciaccio⁵, C. Di Donato^{103a,103b}, A. Di Girolamo³⁰, B. Di Girolamo³⁰, S. Di Luise^{135a,135b}, A. Di Mattia¹⁵³, B. Di Micco^{135a,135b}, R. Di Nardo⁴⁷, A. Di Simone^{134a,134b}, R. Di Sipio^{20a,20b}, M.A. Diaz^{32a}, E.B. Diehl⁸⁸, J. Dietrich⁴², T.A. Dietzsch^{58a}, S. Diglio⁸⁷, K. Dindar Yagci⁴⁰, J. Dingfelder²¹, F. Dinut^{26a}, C. Dionisi^{133a,133b}, P. Dita^{26a}, S. Dita^{26a}, F. Dittus³⁰, F. Djama⁸⁴, T. Djobava^{51b}, M.A.B. do Vale^{24c}, A. Do Valle Wemans^{125a,m}, T.K.O. Doan⁵, D. Dobos³⁰, E. Dobson⁷⁷, J. Dodd³⁵, C. Doglioni⁴⁹, T. Doherty⁵³, T. Dohmae¹⁵⁶, Y. Doi^{65,*}, J. Dolejsi¹²⁸, Z. Dolezal¹²⁸, B.A. Dolgoshein^{97,*}, M. Donadelli^{24d}, J. Donini³⁴, J. Dopke³⁰, A. Doria^{103a}, A. Dos Anjos¹⁷⁴, A. Dotti^{123a,123b}, M.T. Dova⁷⁰, A.T. Doyle⁵³, M. Dris¹⁰, J. Dubbert⁸⁸, S. Dube¹⁵, E. Dubreuil³⁴, E. Duchovni¹⁷³, G. Duckeck⁹⁹, D. Duda¹⁷⁶, A. Dudarev³⁰, F. Dudziak⁶³, L. Dufflot¹¹⁶, M-A. Dufour⁸⁶, L. Duguid⁷⁶, M. Dührssen³⁰, M. Dunford^{58a}, H. Duran Yildiz^{4a}, M. Düren⁵², M. Dwuznik^{38a}, J. Ebke⁹⁹, S. Eckweiler⁸², W. Edson², C.A. Edwards⁷⁶, N.C. Edwards⁵³, W. Ehrenfeld²¹, T. Eifert¹⁴⁴, G. Eigen¹⁴, K. Einsweiler¹⁵, E. Eisenhandler⁷⁵, T. Ekelof¹⁶⁷, M. El Kacimi^{136c}, M. Ellert¹⁶⁷, S. Elles⁵, F. Ellinghaus⁸², K. Ellis⁷⁵, N. Ellis³⁰, J. Elmsheuser⁹⁹, M. Elsing³⁰, D. Emeliyanov¹³⁰, Y. Enari¹⁵⁶, O.C. Endner⁸², R. Engelmann¹⁴⁹, A. Engl⁹⁹, J. Erdmann¹⁷⁷, A. Ereditato¹⁷, D. Eriksson^{147a}, J. Ernst², M. Ernst²⁵, J. Ernwein¹³⁷, D. Errede¹⁶⁶, S. Errede¹⁶⁶, E. Ertel⁸², M. Escalier¹¹⁶, H. Esch⁴³, C. Escobar¹²⁴, X. Espinal Curull¹², B. Esposito⁴⁷, F. Etienne⁸⁴, A.I. Etienve¹³⁷, E. Etzion¹⁵⁴, D. Evangelakou⁵⁴, H. Evans⁶⁰, L. Fabbri^{20a,20b}, C. Fabre³⁰, G. Facini³⁰, R.M. Fakhruddinov¹²⁹, S. Falciano^{133a}, Y. Fang^{33a}, M. Fanti^{90a,90b}, A. Farbin⁸, A. Farilla^{135a}, T. Farooque¹⁵⁹, S. Farrell¹⁶⁴, S.M. Farrington¹⁷¹, P. Farthouat³⁰, F. Fassi¹⁶⁸, P. Fassnacht³⁰, D. Fassouliotis⁹, B. Fatholahzadeh¹⁵⁹, A. Favareto^{90a,90b}, L. Fayard¹¹⁶, P. Federic^{145a}, O.L. Fedin¹²², W. Fedorko¹⁶⁹, M. Fehling-Kaschek⁴⁸, L. Felgioni⁸⁴, C. Feng^{33d}, E.J. Feng⁶, H. Feng⁸⁸, A.B. Fenyuk¹²⁹, J. Ferencei^{145b}, W. Fernando⁶, S. Ferrag⁵³, J. Ferrando⁵³, V. Ferrara⁴², A. Ferrari¹⁶⁷, P. Ferrari¹⁰⁶, R. Ferrari^{120a}, D.E. Ferreira de Lima⁵³, A. Ferrer¹⁶⁸, D. Ferrere⁴⁹, C. Ferretti⁸⁸, A. Ferretto Parodi^{50a,50b}, M. Fiascaris³¹, F. Fiedler⁸², A. Filipčič⁷⁴, F. Filthaut¹⁰⁵, M. Fincke-Keeler¹⁷⁰, K.D. Finelli⁴⁵, M.C.N. Fiolhais^{125a,h}, L. Fiorini¹⁶⁸, A. Firan⁴⁰, J. Fischer¹⁷⁶, M.J. Fisher¹¹⁰, E.A. Fitzgerald²³, M. Flechl⁴⁸, I. Fleck¹⁴², P. Fleischmann¹⁷⁵, S. Fleischmann¹⁷⁶, G.T. Fletcher¹⁴⁰, G. Fletcher⁷⁵, T. Flick¹⁷⁶, A. Floderus⁸⁰, L.R. Flores Castillo¹⁷⁴, A.C. Florez Bustos^{160b}, M.J. Flowerdew¹⁰⁰, T. Fonseca Martin¹⁷, A. Formica¹³⁷, A. Forti⁸³,

D. Fortin^{160a}, D. Fournier¹¹⁶, H. Fox⁷¹, P. Francavilla¹², M. Franchini^{20a,20b}, S. Franchino³⁰,
 D. Francis³⁰, M. Franklin⁵⁷, S. Franz³⁰, M. Fraternali^{120a,120b}, S. Fratina¹²¹, S.T. French²⁸,
 C. Friedrich⁴², F. Friedrich⁴⁴, D. Froidevaux³⁰, J.A. Frost²⁸, C. Fukunaga¹⁵⁷,
 E. Fullana Torregrosa¹²⁸, B.G. Fulson¹⁴⁴, J. Fuster¹⁶⁸, C. Gabaldon³⁰, O. Gabizon¹⁷³,
 A. Gabrielli^{20a,20b}, A. Gabrielli^{133a,133b}, S. Gadatsch¹⁰⁶, T. Gadfort²⁵, S. Gadomski⁴⁹,
 G. Gagliardi^{50a,50b}, P. Gagnon⁶⁰, C. Galea⁹⁹, B. Galhardo^{125a}, E.J. Gallas¹¹⁹, V. Gallo¹⁷,
 B.J. Gallop¹³⁰, P. Gallus¹²⁷, K.K. Gan¹¹⁰, R.P. Gandrajula⁶², Y.S. Gao^{144,f}, A. Gaponenko¹⁵,
 F.M. Garay Walls⁴⁶, F. Garberson¹⁷⁷, C. García¹⁶⁸, J.E. García Navarro¹⁶⁸, M. Garcia-Sciveres¹⁵,
 R.W. Gardner³¹, N. Garelli¹⁴⁴, V. Garonne³⁰, C. Gatti⁴⁷, G. Gaudio^{120a}, B. Gaur¹⁴²,
 L. Gauthier⁹⁴, P. Gauzzi^{133a,133b}, I.L. Gavrilenko⁹⁵, C. Gay¹⁶⁹, G. Gaycken²¹, E.N. Gazis¹⁰,
 P. Ge^{33d,n}, Z. Gecse¹⁶⁹, C.N.P. Gee¹³⁰, D.A.A. Geerts¹⁰⁶, Ch. Geich-Gimbel²¹,
 K. Gellerstedt^{147a,147b}, C. Gemme^{50a}, A. Gemmell⁵³, M.H. Genest⁵⁵, S. Gentile^{133a,133b},
 M. George⁵⁴, S. George⁷⁶, D. Gerbaudo¹⁶⁴, A. Gershon¹⁵⁴, H. Ghazlane^{136b}, N. Ghodbane³⁴,
 B. Giacobbe^{20a}, S. Giagu^{133a,133b}, V. Giangiobbe¹², F. Gianotti³⁰, B. Gibbard²⁵, A. Gibson¹⁵⁹,
 S.M. Gibson³⁰, M. Gilchriese¹⁵, T.P.S. Gillam²⁸, D. Gillberg³⁰, A.R. Gillman¹³⁰,
 D.M. Gingrich^{3,e}, N. Giokaris⁹, M.P. Giordani^{165c}, R. Giordano^{103a,103b}, F.M. Giorgi¹⁶,
 P. Giovannini¹⁰⁰, P.F. Giraud¹³⁷, D. Giugni^{90a}, C. Giuliani⁴⁸, M. Giunta⁹⁴, B.K. Gjelsten¹¹⁸,
 I. Gkialas^{155,o}, L.K. Gladilin⁹⁸, C. Glasman⁸¹, J. Glatzer²¹, A. Glazov⁴², G.L. Glonti⁶⁴,
 J.R. Goddard⁷⁵, J. Godfrey¹⁴³, J. Godlewski³⁰, M. Goebel⁴², C. Goeringer⁸², S. Goldfarb⁸⁸,
 T. Golling¹⁷⁷, D. Golubkov¹²⁹, A. Gomes^{125a,c}, L.S. Gomez Fajardo⁴², R. Gonçalo⁷⁶,
 J. Goncalves Pinto Firmino Da Costa⁴², L. Gonella²¹, S. González de la Hoz¹⁶⁸,
 G. Gonzalez Parra¹², M.L. Gonzalez Silva²⁷, S. Gonzalez-Sevilla⁴⁹, J.J. Goodson¹⁴⁹,
 L. Goossens³⁰, P.A. Gorbounov⁹⁶, H.A. Gordon²⁵, I. Gorelov¹⁰⁴, G. Gorfine¹⁷⁶, B. Gorini³⁰,
 E. Gorini^{72a,72b}, A. Gorišek⁷⁴, E. Gornicki³⁹, A.T. Goshaw⁶, C. Gössling⁴³, M.I. Gostkin⁶⁴,
 I. Gough Eschrich¹⁶⁴, M. Gouighri^{136a}, D. Goujdami^{136c}, M.P. Goulette⁴⁹, A.G. Goussiou¹³⁹,
 C. Goy⁵, S. Gozpinar²³, L. Graber⁵⁴, I. Grabowska-Bold^{38a}, P. Grafström^{20a,20b}, K-J. Grahn⁴²,
 E. Gramstad¹¹⁸, F. Grancagnolo^{72a}, S. Grancagnolo¹⁶, V. Grassi¹⁴⁹, V. Gratchev¹²²,
 H.M. Gray³⁰, J.A. Gray¹⁴⁹, E. Graziani^{135a}, O.G. Grebenyuk¹²², T. Greenshaw⁷³,
 Z.D. Greenwood^{78,l}, K. Gregersen³⁶, I.M. Gregor⁴², P. Grenier¹⁴⁴, J. Griffiths⁸, N. Grigalashvili⁶⁴,
 A.A. Grillo¹³⁸, K. Grimm⁷¹, S. Grinstein¹², Ph. Gris³⁴, Y.V. Grishkevich⁹⁸, J.-F. Grivaz¹¹⁶,
 J.P. Grohs⁴⁴, A. Grohsjean⁴², E. Gross¹⁷³, J. Grosse-Knetter⁵⁴, J. Groth-Jensen¹⁷³, K. Grybel¹⁴²,
 F. Guescini⁴⁹, D. Guest¹⁷⁷, O. Gueta¹⁵⁴, C. Guicheney³⁴, E. Guido^{50a,50b}, T. Guillemin¹¹⁶,
 S. Guindon², U. Gul⁵³, J. Gunther¹²⁷, J. Guo³⁵, P. Gutierrez¹¹², N. Guttman¹⁵⁴, O. Gutzwiller¹⁷⁴,
 C. Guyot¹³⁷, C. Gwenlan¹¹⁹, C.B. Gwilliam⁷³, A. Haas¹⁰⁹, S. Haas³⁰, C. Haber¹⁵,
 H.K. Hadavand⁸, P. Haefner²¹, Z. Hajduk³⁹, H. Hakobyan¹⁷⁸, D. Hall¹¹⁹, G. Halladjian⁶²,
 K. Hamacher¹⁷⁶, P. Hamal¹¹⁴, K. Hamano⁸⁷, M. Hamer⁵⁴, A. Hamilton^{146a,p}, S. Hamilton¹⁶²,
 L. Han^{33b}, K. Hanagaki¹¹⁷, K. Hanawa¹⁶¹, M. Hance¹⁵, C. Handel⁸², P. Hanke^{58a}, J.R. Hansen³⁶,
 J.B. Hansen³⁶, J.D. Hansen³⁶, P.H. Hansen³⁶, P. Hansson¹⁴⁴, K. Hara¹⁶¹, A.S. Hard¹⁷⁴,
 T. Harenberg¹⁷⁶, S. Harkusha⁹¹, D. Harper⁸⁸, R.D. Harrington⁴⁶, O.M. Harris¹³⁹, J. Hartert⁴⁸,
 F. Hartjes¹⁰⁶, T. Haruyama⁶⁵, A. Harvey⁵⁶, S. Hasegawa¹⁰², Y. Hasegawa¹⁴¹, S. Hassani¹³⁷,
 S. Haug¹⁷, M. Hauschild³⁰, R. Hauser⁸⁹, M. Havranek²¹, C.M. Hawkes¹⁸, R.J. Hawkings³⁰,
 A.D. Hawkins⁸⁰, T. Hayakawa⁶⁶, T. Hayashi¹⁶¹, D. Hayden⁷⁶, C.P. Hays¹¹⁹, H.S. Hayward⁷³,
 S.J. Haywood¹³⁰, S.J. Head¹⁸, T. Heck⁸², V. Hedberg⁸⁰, L. Heelan⁸, S. Heim¹²¹, B. Heinemann¹⁵,
 S. Heisterkamp³⁶, J. Hejbal¹²⁶, L. Helary²², C. Heller⁹⁹, M. Heller³⁰, S. Hellman^{147a,147b},
 D. Hellmich²¹, C. Helsens³⁰, J. Henderson¹¹⁹, R.C.W. Henderson⁷¹, M. Henke^{58a}, A. Henrichs¹⁷⁷,
 A.M. Henriques Correia³⁰, S. Henrot-Versille¹¹⁶, C. Hensel⁵⁴, G.H. Herbert¹⁶, C.M. Hernandez⁸,
 Y. Hernández Jiménez¹⁶⁸, R. Herrberg-Schubert¹⁶, G. Herten⁴⁸, R. Hertenberger⁹⁹, L. Hervas³⁰,
 G.G. Hesketh⁷⁷, N.P. Hessey¹⁰⁶, R. Hickling⁷⁵, E. Higón-Rodríguez¹⁶⁸, J.C. Hill²⁸, K.H. Hiller⁴²,

S. Hillert²¹, S.J. Hillier¹⁸, I. Hinchliffe¹⁵, E. Hines¹²¹, M. Hirose¹¹⁷, D. Hirschbuehl¹⁷⁶,
 J. Hobbs¹⁴⁹, N. Hod¹⁰⁶, M.C. Hodgkinson¹⁴⁰, P. Hodgson¹⁴⁰, A. Hoecker³⁰, M.R. Hoferkamp¹⁰⁴,
 J. Hoffman⁴⁰, D. Hoffmann⁸⁴, J.I. Hofmann^{58a}, M. Hohlfield⁸², S.O. Holmgren^{147a},
 J.L. Holzbauer⁸⁹, T.M. Hong¹²¹, L. Hooft van Huysduynen¹⁰⁹, J-Y. Hostachy⁵⁵, S. Hou¹⁵²,
 A. Hoummada^{136a}, J. Howard¹¹⁹, J. Howarth⁸³, M. Hrabovsky¹¹⁴, I. Hristova¹⁶, J. Hrivnac¹¹⁶,
 T. Hryn'ova⁵, P.J. Hsu⁸², S.-C. Hsu¹³⁹, D. Hu³⁵, X. Hu²⁵, Z. Hubacek³⁰, F. Hubaut⁸⁴,
 F. Huegging²¹, A. Huettmann⁴², T.B. Huffman¹¹⁹, E.W. Hughes³⁵, G. Hughes⁷¹, M. Huhtinen³⁰,
 T.A. Hülsing⁸², M. Hurwitz¹⁵, N. Huseynov^{64,q}, J. Huston⁸⁹, J. Huth⁵⁷, G. Iacobucci⁴⁹,
 G. Iakovidis¹⁰, I. Ibragimov¹⁴², L. Iconomidou-Fayard¹¹⁶, J. Idarraga¹¹⁶, P. Iengo^{103a},
 O. Igonkina¹⁰⁶, Y. Ikegami⁶⁵, K. Ikematsu¹⁴², M. Ikeno⁶⁵, D. Iliadis¹⁵⁵, N. Ilic¹⁵⁹, T. Ince¹⁰⁰,
 P. Ioannou⁹, M. Iodice^{135a}, K. Iordanidou⁹, V. Ippolito^{133a,133b}, A. Irls Quiles¹⁶⁸, C. Isaksson¹⁶⁷,
 M. Ishino⁶⁷, M. Ishitsuka¹⁵⁸, R. Ishmukhametov¹¹⁰, C. Issever¹¹⁹, S. Istin^{19a}, A.V. Ivashin¹²⁹,
 W. Iwanski³⁹, H. Iwasaki⁶⁵, J.M. Izen⁴¹, V. Izzo^{103a}, B. Jackson¹²¹, J.N. Jackson⁷³, P. Jackson¹,
 M.R. Jaekel³⁰, V. Jain², K. Jakobs⁴⁸, S. Jakobsen³⁶, T. Jakoubek¹²⁶, J. Jakubek¹²⁷,
 D.O. Jamin¹⁵², D.K. Jana¹¹², E. Jansen⁷⁷, H. Jansen³⁰, J. Janssen²¹, A. Jantsch¹⁰⁰, M. Janus⁴⁸,
 R.C. Jared¹⁷⁴, G. Jarlskog⁸⁰, L. Jeanty⁵⁷, G.-Y. Jeng¹⁵¹, I. Jen-La Plante³¹, D. Jennens⁸⁷,
 P. Jenni³⁰, J. Jentzsch⁴³, C. Jeske¹⁷¹, P. Jež³⁶, S. Jézéquel⁵, M.K. Jha^{20a}, H. Ji¹⁷⁴, W. Ji⁸²,
 J. Jia¹⁴⁹, Y. Jiang^{33b}, M. Jimenez Belenguer⁴², S. Jin^{33a}, O. Jinnouchi¹⁵⁸, M.D. Joergensen³⁶,
 D. Joffe⁴⁰, M. Johansen^{147a,147b}, K.E. Johansson^{147a}, P. Johansson¹⁴⁰, S. Johnert⁴², K.A. Johns⁷,
 K. Jon-And^{147a,147b}, G. Jones¹⁷¹, R.W.L. Jones⁷¹, T.J. Jones⁷³, P.M. Jorge^{125a}, K.D. Joshi⁸³,
 J. Jovicevic¹⁴⁸, T. Jovin^{13b}, X. Ju¹⁷⁴, C.A. Jung⁴³, R.M. Jungst³⁰, P. Jussel⁶¹, A. Juste Rozas¹²,
 S. Kabana¹⁷, M. Kaci¹⁶⁸, A. Kaczmarska³⁹, P. Kadlecik³⁶, M. Kado¹¹⁶, H. Kagan¹¹⁰, M. Kagan⁵⁷,
 E. Kajomovitz¹⁵³, S. Kalinin¹⁷⁶, S. Kama⁴⁰, N. Kanaya¹⁵⁶, M. Kaneda³⁰, S. Kaneti²⁸,
 T. Kanno¹⁵⁸, V.A. Kantserov⁹⁷, J. Kanzaki⁶⁵, B. Kaplan¹⁰⁹, A. Kapliy³¹, D. Kar⁵³,
 K. Karakostas¹⁰, M. Karnevskiy⁸², V. Kartvelishvili⁷¹, A.N. Karyukhin¹²⁹, L. Kashif¹⁷⁴,
 G. Kasieczka^{58b}, R.D. Kass¹¹⁰, A. Kastanas¹⁴, Y. Kataoka¹⁵⁶, J. Katzy⁴², V. Kaushik⁷,
 K. Kawagoe⁶⁹, T. Kawamoto¹⁵⁶, G. Kawamura⁵⁴, S. Kazama¹⁵⁶, V.F. Kazanin¹⁰⁸,
 M.Y. Kazarinov⁶⁴, R. Keeler¹⁷⁰, P.T. Keener¹²¹, R. Kehoe⁴⁰, M. Keil⁵⁴, J.S. Keller¹³⁹,
 H. Keoshkerian⁵, O. Kepka¹²⁶, B.P. Kerševan⁷⁴, S. Kersten¹⁷⁶, K. Kessoku¹⁵⁶, J. Keung¹⁵⁹,
 F. Khalil-zada¹¹, H. Khandanyan^{147a,147b}, A. Khanov¹¹³, D. Kharchenko⁶⁴, A. Khodinov⁹⁷,
 A. Khomich^{58a}, T.J. Khoo²⁸, G. Khoraiuli²¹, A. Khoroshilov¹⁷⁶, V. Khovanskiy⁹⁶, E. Khramov⁶⁴,
 J. Khubua^{51b}, H. Kim^{147a,147b}, S.H. Kim¹⁶¹, N. Kimura¹⁷², O. Kind¹⁶, B.T. King⁷³, M. King⁶⁶,
 R.S.B. King¹¹⁹, S.B. King¹⁶⁹, J. Kirk¹³⁰, A.E. Kiryunin¹⁰⁰, T. Kishimoto⁶⁶, D. Kisielewska^{38a},
 T. Kitamura⁶⁶, T. Kittelmann¹²⁴, K. Kiuchi¹⁶¹, E. Kladiva^{145b}, M. Klein⁷³, U. Klein⁷³,
 K. Kleinknecht⁸², M. Klemetti⁸⁶, A. Klier¹⁷³, P. Klimek^{147a,147b}, A. Klimentov²⁵,
 R. Klingenberg⁴³, J.A. Klinger⁸³, E.B. Klinkby³⁶, T. Klioutchnikova³⁰, P.F. Klok¹⁰⁵,
 E.-E. Kluge^{58a}, P. Kluit¹⁰⁶, S. Kluth¹⁰⁰, E. Kneringer⁶¹, E.B.F.G. Knoops⁸⁴, A. Knue⁵⁴,
 B.R. Ko⁴⁵, T. Kobayashi¹⁵⁶, M. Kobel⁴⁴, M. Kocian¹⁴⁴, P. Kodys¹²⁸, S. Koenig⁸²,
 F. Koetsveld¹⁰⁵, P. Koesesarki²¹, T. Koffas²⁹, E. Koffeman¹⁰⁶, L.A. Kogan¹¹⁹, S. Kohlmann¹⁷⁶,
 F. Kohn⁵⁴, Z. Kohout¹²⁷, T. Kohriki⁶⁵, T. Koi¹⁴⁴, H. Kolanoski¹⁶, I. Koletsou^{90a}, J. Koll⁸⁹,
 A.A. Komar⁹⁵, Y. Komori¹⁵⁶, T. Kondo⁶⁵, K. Köneke³⁰, A.C. König¹⁰⁵, T. Kono^{42,r},
 A.I. Kononov⁴⁸, R. Konoplich^{109,s}, N. Konstantinidis⁷⁷, R. Kopeliansky¹⁵³, S. Koperny^{38a},
 L. Köpke⁸², A.K. Kopp⁴⁸, K. Korcyl³⁹, K. Kordas¹⁵⁵, A. Korn⁴⁶, A. Korol¹⁰⁸, I. Korolkov¹²,
 E.V. Korolkova¹⁴⁰, V.A. Korotkov¹²⁹, O. Kortner¹⁰⁰, S. Kortner¹⁰⁰, V.V. Kostyukhin²¹,
 S. Kotov¹⁰⁰, V.M. Kotov⁶⁴, A. Kotwal⁴⁵, C. Kourkoumelis⁹, V. Kouskoura¹⁵⁵, A. Koutsman^{160a},
 R. Kowalewski¹⁷⁰, T.Z. Kowalski^{38a}, W. Kozanecki¹³⁷, A.S. Kozhin¹²⁹, V. Kral¹²⁷,
 V.A. Kramarenko⁹⁸, G. Kramberger⁷⁴, M.W. Krasny⁷⁹, A. Krasznahorkay¹⁰⁹, J.K. Kraus²¹,
 A. Kravchenko²⁵, S. Kreiss¹⁰⁹, J. Kretzschmar⁷³, K. Kreutzfeldt⁵², N. Krieger⁵⁴, P. Krieger¹⁵⁹,

K. Kroeninger⁵⁴, H. Kroha¹⁰⁰, J. Kroll¹²¹, J. Kroseberg²¹, J. Krstic^{13a}, U. Kruchonak⁶⁴,
 H. Krüger²¹, T. Kruker¹⁷, N. Krumnack⁶³, Z.V. Krumshteyn⁶⁴, A. Kruse¹⁷⁴, M.K. Kruse⁴⁵,
 T. Kubota⁸⁷, S. Kudah^{4a}, S. Kuehn⁴⁸, A. Kugel^{58c}, T. Kuhl⁴², V. Kukhtin⁶⁴, Y. Kulchitsky⁹¹,
 S. Kuleshov^{32b}, M. Kuna⁷⁹, J. Kunkle¹²¹, A. Kupco¹²⁶, H. Kurashige⁶⁶, M. Kurata¹⁶¹,
 Y.A. Kurochkin⁹¹, V. Kus¹²⁶, E.S. Kuwertz¹⁴⁸, M. Kuze¹⁵⁸, J. Kvita¹⁴³, R. Kwee¹⁶, A. La Rosa⁴⁹,
 L. La Rotonda^{37a,37b}, L. Labarga⁸¹, S. Lablak^{136a}, C. Lacasta¹⁶⁸, F. Lacava^{133a,133b}, J. Lacey²⁹,
 H. Lacker¹⁶, D. Lacour⁷⁹, V.R. Lacuesta¹⁶⁸, E. Ladygin⁶⁴, R. Lafaye⁵, B. Laforge⁷⁹, T. Lagouri¹⁷⁷,
 S. Lai⁴⁸, H. Laier^{58a}, E. Laisne⁵⁵, L. Lambourne⁷⁷, C.L. Lampen⁷, W. Lampl⁷, E. Lançon¹³⁷,
 U. Landgraf⁴⁸, M.P.J. Landon⁷⁵, V.S. Lang^{58a}, C. Lange⁴², A.J. Lankford¹⁶⁴, F. Lanni²⁵,
 K. Lantzsich³⁰, A. Lanza^{120a}, S. Laplace⁷⁹, C. Lapoire²¹, J.F. Laporte¹³⁷, T. Lari^{90a}, A. Larner¹¹⁹,
 M. Lassnig³⁰, P. Laurelli⁴⁷, V. Lavorini^{37a,37b}, W. Lavrijsen¹⁵, P. Laycock⁷³, O. Le Dortz⁷⁹,
 E. Le Guirriec⁸⁴, E. Le Menedeu¹², T. LeCompte⁶, F. Ledroit-Guillon⁵⁵, H. Lee¹⁰⁶, J.S.H. Lee¹¹⁷,
 S.C. Lee¹⁵², L. Lee¹⁷⁷, G. Lefebvre⁷⁹, M. Lefebvre¹⁷⁰, M. Legendre¹³⁷, F. Legger⁹⁹, C. Leggett¹⁵,
 M. Lehmacher²¹, G. Lehmann Miotto³⁰, A.G. Leister¹⁷⁷, M.A.L. Leite^{24d}, R. Leitner¹²⁸,
 D. Lellouch¹⁷³, B. Lemmer⁵⁴, V. Lendermann^{58a}, K.J.C. Leney^{146c}, T. Lenz¹⁰⁶, G. Lenzen¹⁷⁶,
 B. Lenzi³⁰, K. Leonhardt⁴⁴, S. Leontsinis¹⁰, F. Lepold^{58a}, C. Leroy⁹⁴, J-R. Lessard¹⁷⁰,
 C.G. Lester²⁸, C.M. Lester¹²¹, J. Levêque⁵, D. Levin⁸⁸, L.J. Levinson¹⁷³, A. Lewis¹¹⁹,
 G.H. Lewis¹⁰⁹, A.M. Leyko²¹, M. Leyton¹⁶, B. Li^{33b}, B. Li⁸⁴, H. Li¹⁴⁹, H.L. Li³¹, S. Li^{33b,t},
 X. Li⁸⁸, Z. Liang^{119,u}, H. Liao³⁴, B. Liberti^{134a}, P. Lichard³⁰, K. Lie¹⁶⁶, J. Liebal²¹, W. Liebig¹⁴,
 C. Limbach²¹, A. Limosani⁸⁷, M. Limper⁶², S.C. Lin^{152,v}, F. Linde¹⁰⁶, B.E. Lindquist¹⁴⁹,
 J.T. Linnemann⁸⁹, E. Lipeles¹²¹, A. Lipniacka¹⁴, M. Lisovsky⁴², T.M. Liss¹⁶⁶, D. Lissauer²⁵,
 A. Lister¹⁶⁹, A.M. Litke¹³⁸, D. Liu¹⁵², J.B. Liu^{33b}, K. Liu^{33b,w}, L. Liu⁸⁸, M. Liu⁴⁵, M. Liu^{33b},
 Y. Liu^{33b}, M. Livan^{120a,120b}, S.S.A. Livermore¹¹⁹, A. Lleres⁵⁵, J. Llorente Merino⁸¹, S.L. Lloyd⁷⁵,
 F. Lo Sterzo^{133a,133b}, E. Lobodzinska⁴², P. Loch⁷, W.S. Lockman¹³⁸, T. Loddenkoetter²¹,
 F.K. Loebinger⁸³, A.E. Loevschall-Jensen³⁶, A. Loginov¹⁷⁷, C.W. Loh¹⁶⁹, T. Lohse¹⁶,
 K. Lohwasser⁴⁸, M. Lokajicek¹²⁶, V.P. Lombardo⁵, R.E. Long⁷¹, L. Lopes^{125a}, D. Lopez Mateos⁵⁷,
 J. Lorenz⁹⁹, N. Lorenzo Martinez¹¹⁶, M. Losada¹⁶³, P. Loscutoff¹⁵, M.J. Losty^{160a,*}, X. Lou⁴¹,
 A. Lounis¹¹⁶, K.F. Loureiro¹⁶³, J. Love⁶, P.A. Love⁷¹, A.J. Lowe^{144,f}, F. Lu^{33a}, H.J. Lubatti¹³⁹,
 C. Luci^{133a,133b}, A. Lucotte⁵⁵, D. Ludwig⁴², I. Ludwig⁴⁸, J. Ludwig⁴⁸, F. Luehring⁶⁰, W. Lukas⁶¹,
 L. Luminari^{133a}, E. Lund¹¹⁸, J. Lundberg^{147a,147b}, O. Lundberg^{147a,147b}, B. Lund-Jensen¹⁴⁸,
 J. Lundquist³⁶, M. Lungwitz⁸², D. Lynn²⁵, R. Lysak¹²⁶, E. Lytken⁸⁰, H. Ma²⁵, L.L. Ma¹⁷⁴,
 G. Maccarrone⁴⁷, A. Macchiolo¹⁰⁰, B. Maček⁷⁴, J. Machado Miguens^{125a}, D. Macina³⁰,
 R. Mackeprang³⁶, R. Madar⁴⁸, R.J. Madaras¹⁵, H.J. Maddocks⁷¹, W.F. Mader⁴⁴, A. Madsen¹⁶⁷,
 M. Maeno⁵, T. Maeno²⁵, L. Magnoni¹⁶⁴, E. Magradze⁵⁴, K. Mahboubi⁴⁸, J. Mahlstedt¹⁰⁶,
 S. Mahmoud⁷³, G. Mahout¹⁸, C. Maiani¹³⁷, C. Maidantchik^{24a}, A. Maio^{125a,c}, S. Majewski¹¹⁵,
 Y. Makida⁶⁵, N. Makovec¹¹⁶, P. Mal^{137,x}, B. Malaescu⁷⁹, Pa. Malecki³⁹, P. Malecki³⁹,
 V.P. Maleev¹²², F. Malek⁵⁵, U. Mallik⁶², D. Malon⁶, C. Malone¹⁴⁴, S. Maltezos¹⁰, V. Malyshev¹⁰⁸,
 S. Malyukov³⁰, J. Mamuzic^{13b}, L. Mandelli^{90a}, I. Mandić⁷⁴, R. Mandrysch⁶², J. Maneira^{125a},
 A. Manfredini¹⁰⁰, L. Manhaes de Andrade Filho^{24b}, J.A. Manjarres Ramos¹³⁷, A. Mann⁹⁹,
 P.M. Manning¹³⁸, A. Manousakis-Katsikakis⁹, B. Mansoulie¹³⁷, R. Mantifel⁸⁶, L. Mapelli³⁰,
 L. March¹⁶⁸, J.F. Marchand²⁹, F. Marchese^{134a,134b}, G. Marchiori⁷⁹, M. Marcisovsky¹²⁶,
 C.P. Marino¹⁷⁰, C.N. Marques^{125a}, F. Marroquim^{24a}, Z. Marshall¹²¹, L.F. Marti¹⁷,
 S. Marti-Garcia¹⁶⁸, B. Martin³⁰, B. Martin⁸⁹, J.P. Martin⁹⁴, T.A. Martin¹⁷¹, V.J. Martin⁴⁶,
 B. Martin dit Latour⁴⁹, H. Martinez¹³⁷, M. Martinez¹², S. Martin-Haugh¹⁵⁰, A.C. Martyniuk¹⁷⁰,
 M. Marx⁸³, F. Marzano^{133a}, A. Marzin¹¹², L. Masetti⁸², T. Mashimo¹⁵⁶, R. Mashinistov⁹⁵,
 J. Masik⁸³, A.L. Maslennikov¹⁰⁸, I. Massa^{20a,20b}, N. Massol⁵, P. Mastrandrea¹⁴⁹,
 A. Mastroberardino^{37a,37b}, T. Masubuchi¹⁵⁶, H. Matsunaga¹⁵⁶, T. Matsushita⁶⁶, P. Mättig¹⁷⁶,
 S. Mättig⁴², C. Mattravers^{119,d}, J. Maurer⁸⁴, S.J. Maxfield⁷³, D.A. Maximov^{108,g}, R. Mazini¹⁵²,

M. Mazur²¹, L. Mazzaferro^{134a,134b}, M. Mazzanti^{90a}, S.P. Mc Kee⁸⁸, A. McCarn¹⁶⁶,
 R.L. McCarthy¹⁴⁹, T.G. McCarthy²⁹, N.A. McCubbin¹³⁰, K.W. McFarlane^{56,*}, J.A. McFayden¹⁴⁰,
 G. Mchedlidze^{51b}, T. Mclaughlan¹⁸, S.J. McMahon¹³⁰, R.A. McPherson^{170,j}, A. Meade⁸⁵,
 J. Mechnich¹⁰⁶, M. Mechtel¹⁷⁶, M. Medinnis⁴², S. Meehan³¹, R. Meera-Lebbai¹¹², T. Meguro¹¹⁷,
 S. Mehlhase³⁶, A. Mehta⁷³, K. Meier^{58a}, C. Meineck⁹⁹, B. Meirose⁸⁰, C. Melachrinou³¹,
 B.R. Mellado Garcia^{146c}, F. Meloni^{90a,90b}, L. Mendoza Navas¹⁶³, A. Mengarelli^{20a,20b},
 S. Menke¹⁰⁰, E. Meoni¹⁶², K.M. Mercurio⁵⁷, N. Meric¹³⁷, P. Mermod⁴⁹, L. Merola^{103a,103b},
 C. Meroni^{90a}, F.S. Merritt³¹, H. Merritt¹¹⁰, A. Messina^{30,y}, J. Metcalfe²⁵, A.S. Mete¹⁶⁴,
 C. Meyer⁸², C. Meyer³¹, J-P. Meyer¹³⁷, J. Meyer³⁰, J. Meyer⁵⁴, S. Michal³⁰, R.P. Middleton¹³⁰,
 S. Migas⁷³, L. Mijović¹³⁷, G. Mikenberg¹⁷³, M. Mikestikova¹²⁶, M. Mikuž⁷⁴, D.W. Miller³¹,
 W.J. Mills¹⁶⁹, C. Mills⁵⁷, A. Milov¹⁷³, D.A. Milstead^{147a,147b}, D. Milstein¹⁷³, A.A. Minaenko¹²⁹,
 M. Miñano Moya¹⁶⁸, I.A. Minashvili⁶⁴, A.I. Mincer¹⁰⁹, B. Mindur^{38a}, M. Mineev⁶⁴, Y. Ming¹⁷⁴,
 L.M. Mir¹², G. Mirabelli^{133a}, J. Mitrevski¹³⁸, V.A. Mitsou¹⁶⁸, S. Mitsui⁶⁵, P.S. Miyagawa¹⁴⁰,
 J.U. Mjörnmark⁸⁰, T. Moe^{147a,147b}, V. Moeller²⁸, S. Mohapatra¹⁴⁹, W. Mohr⁴⁸, R. Moles-Valls¹⁶⁸,
 A. Molfetas³⁰, K. Mönig⁴², C. Monini⁵⁵, J. Monk³⁶, E. Monnier⁸⁴, J. Montejo Berlingen¹²,
 F. Monticelli⁷⁰, S. Monzani^{20a,20b}, R.W. Moore³, C. Mora Herrera⁴⁹, A. Moraes⁵³, N. Morange⁶²,
 J. Morel⁵⁴, D. Moreno⁸², M. Moreno Llácer¹⁶⁸, P. Morettini^{50a}, M. Morgenstern⁴⁴, M. Morii⁵⁷,
 S. Moritz⁸², A.K. Morley³⁰, G. Mornacchi³⁰, J.D. Morris⁷⁵, L. Morvaj¹⁰², N. Möser²¹,
 H.G. Moser¹⁰⁰, M. Mosidze^{51b}, J. Moss¹¹⁰, R. Mount¹⁴⁴, E. Mountricha^{10,z}, S.V. Mouraviev^{95,*},
 E.J.W. Moyse⁸⁵, R.D. Mudd¹⁸, F. Mueller^{58a}, J. Mueller¹²⁴, K. Mueller²¹, T. Mueller²⁸,
 T. Mueller⁸², D. Muenstermann³⁰, Y. Munwes¹⁵⁴, J.A. Murillo Quijada¹⁸, W.J. Murray¹³⁰,
 I. Mussche¹⁰⁶, E. Musto¹⁵³, A.G. Myagkov^{129,aa}, M. Myska¹²⁶, O. Nackenhorst⁵⁴, J. Nadal¹²,
 K. Nagai¹⁶¹, R. Nagai¹⁵⁸, Y. Nagai⁸⁴, K. Nagano⁶⁵, A. Nagarkar¹¹⁰, Y. Nagasaka⁵⁹, M. Nagel¹⁰⁰,
 A.M. Nairz³⁰, Y. Nakahama³⁰, K. Nakamura⁶⁵, T. Nakamura¹⁵⁶, I. Nakano¹¹¹,
 H. Namasivayam⁴¹, G. Nanava²¹, A. Napier¹⁶², R. Narayan^{58b}, M. Nash^{77,d}, T. Nattermann²¹,
 T. Naumann⁴², G. Navarro¹⁶³, H.A. Neal⁸⁸, P.Yu. Nechaeva⁹⁵, T.J. Neep⁸³, A. Negri^{120a,120b},
 G. Negri³⁰, M. Negrini^{20a}, S. Nektarijevic⁴⁹, A. Nelson¹⁶⁴, T.K. Nelson¹⁴⁴, S. Nemecek¹²⁶,
 P. Nemethy¹⁰⁹, A.A. Nepomuceno^{24a}, M. Nessi^{30,ab}, M.S. Neubauer¹⁶⁶, M. Neumann¹⁷⁶,
 A. Neusiedl⁸², R.M. Neves¹⁰⁹, P. Nevski²⁵, F.M. Newcomer¹²¹, P.R. Newman¹⁸, D.H. Nguyen⁶,
 V. Nguyen Thi Hong¹³⁷, R.B. Nickerson¹¹⁹, R. Nicolaidou¹³⁷, B. Nicquevert³⁰, F. Niedercorn¹¹⁶,
 J. Nielsen¹³⁸, N. Nikiforou³⁵, A. Nikiforov¹⁶, V. Nikolaenko^{129,aa}, I. Nikolic-Audit⁷⁹,
 K. Nikolics⁴⁹, K. Nikolopoulos¹⁸, P. Nilsson⁸, Y. Ninomiya¹⁵⁶, A. Nisati^{133a}, R. Nisius¹⁰⁰,
 T. Nobe¹⁵⁸, L. Nodulman⁶, M. Nomachi¹¹⁷, I. Nomidis¹⁵⁵, S. Norberg¹¹², M. Nordberg³⁰,
 J. Novakova¹²⁸, M. Nozaki⁶⁵, L. Nozka¹¹⁴, A.-E. Nuncio-Quiroz²¹, G. Nunes Hanninger⁸⁷,
 T. Nunnemann⁹⁹, E. Nurse⁷⁷, B.J. O'Brien⁴⁶, D.C. O'Neil¹⁴³, V. O'Shea⁵³, L.B. Oakes⁹⁹,
 F.G. Oakham^{29,e}, H. Oberlack¹⁰⁰, J. Ocariz⁷⁹, A. Ochi⁶⁶, M.I. Ochoa⁷⁷, S. Oda⁶⁹, S. Odaka⁶⁵,
 J. Odier⁸⁴, H. Ogren⁶⁰, A. Oh⁸³, S.H. Oh⁴⁵, C.C. Ohm³⁰, T. Ohshima¹⁰², W. Okamura¹¹⁷,
 H. Okawa²⁵, Y. Okumura³¹, T. Okuyama¹⁵⁶, A. Olariu^{26a}, A.G. Olchevski⁶⁴,
 S.A. Olivares Pino⁴⁶, M. Oliveira^{125a,h}, D. Oliveira Damazio²⁵, E. Oliver Garcia¹⁶⁸, D. Olivito¹²¹,
 A. Olszewski³⁹, J. Olszowska³⁹, A. Onofre^{125a,ac}, P.U.E. Onyisi^{31,ad}, C.J. Oram^{160a},
 M.J. Oreglia³¹, Y. Oren¹⁵⁴, D. Orestano^{135a,135b}, N. Orlando^{72a,72b}, C. Oropeza Barrera⁵³,
 R.S. Orr¹⁵⁹, B. Osculati^{50a,50b}, R. Ospanov¹²¹, G. Otero y Garzon²⁷, J.P. Ottersbach¹⁰⁶,
 M. Ouchrif^{136d}, E.A. Ouellette¹⁷⁰, F. Ould-Saada¹¹⁸, A. Ouraou¹³⁷, Q. Ouyang^{33a},
 A. Ovcharova¹⁵, M. Owen⁸³, S. Owen¹⁴⁰, V.E. Ozcan^{19a}, N. Ozturk⁸, A. Pacheco Pages¹²,
 C. Padilla Aranda¹², S. Pagan Griso¹⁵, E. Paganis¹⁴⁰, C. Pahl¹⁰⁰, F. Paige²⁵, P. Pais⁸⁵,
 K. Pajchel¹¹⁸, G. Palacino^{160b}, C.P. Palestini⁷, S. Palestini³⁰, D. Pallin³⁴, A. Palma^{125a},
 J.D. Palmer¹⁸, Y.B. Pan¹⁷⁴, E. Panagiotopoulou¹⁰, J.G. Panduro Vazquez⁷⁶, P. Pani¹⁰⁶,
 N. Panikashvili⁸⁸, S. Panitkin²⁵, D. Pantea^{26a}, A. Papadelis^{147a}, Th.D. Papadopoulou¹⁰,

K. Papageorgiou^{155,o}, A. Paramonov⁶, D. Paredes Hernandez³⁴, W. Park^{25,ae}, M.A. Parker²⁸,
 F. Parodi^{50a,50b}, J.A. Parsons³⁵, U. Parzefall⁴⁸, S. Pashapour⁵⁴, E. Pasqualucci^{133a},
 S. Passaggio^{50a}, A. Passeri^{135a}, F. Pastore^{135a,135b,*}, Fr. Pastore⁷⁶, G. Pásztor^{49,af},
 S. Patarai¹⁷⁶, N.D. Patel¹⁵¹, J.R. Pater⁸³, S. Patricelli^{103a,103b}, T. Pauly³⁰, J. Pearce¹⁷⁰,
 M. Pedersen¹¹⁸, S. Pedraza Lopez¹⁶⁸, M.I. Pedraza Morales¹⁷⁴, S.V. Peleganchuk¹⁰⁸,
 D. Pelikan¹⁶⁷, H. Peng^{33b}, B. Penning³¹, A. Penson³⁵, J. Penwell⁶⁰, T. Perez Cavalcanti⁴²,
 E. Perez Codina^{160a}, M.T. Pérez García-Estañ¹⁶⁸, V. Perez Reale³⁵, L. Perini^{90a,90b},
 H. Pernegger³⁰, R. Perrino^{72a}, P. Perrodo⁵, V.D. Peshekhonov⁶⁴, K. Peters³⁰, R.F.Y. Peters^{54,ag},
 B.A. Petersen³⁰, J. Petersen³⁰, T.C. Petersen³⁶, E. Petit⁵, A. Petridis^{147a,147b}, C. Petridou¹⁵⁵,
 E. Petrolo^{133a}, F. Petrucci^{135a,135b}, D. Petschull⁴², M. Petteni¹⁴³, R. Pezoa^{32b}, A. Phan⁸⁷,
 P.W. Phillips¹³⁰, G. Piacquadio¹⁴⁴, E. Pianori¹⁷¹, A. Picazio⁴⁹, E. Piccaro⁷⁵, M. Piccinini^{20a,20b},
 S.M. Piec⁴², R. Piegai²⁷, D.T. Pignotti¹¹⁰, J.E. Pilcher³¹, A.D. Pilkington⁷⁷, J. Pina^{125a,c},
 M. Pinamonti^{165a,165c,ah}, A. Pinder¹¹⁹, J.L. Pinfold³, A. Pingel³⁶, B. Pinto^{125a}, C. Pizio^{90a,90b},
 M.-A. Pleier²⁵, V. Pleskot¹²⁸, E. Plotnikova⁶⁴, P. Plucinski^{147a,147b}, A. Poblaguev²⁵, S. Poddar^{58a},
 F. Podlyski³⁴, R. Poettgen⁸², L. Poggioli¹¹⁶, D. Pohl²¹, M. Pohl⁴⁹, G. Polesello^{120a},
 A. Policicchio^{37a,37b}, R. Polifka¹⁵⁹, A. Polini^{20a}, V. Polychronakos²⁵, D. Pomeroy²³, K. Pommès³⁰,
 L. Pontecorvo^{133a}, B.G. Pope⁸⁹, G.A. Popeneciu^{26a}, D.S. Popovic^{13a}, A. Poppleton³⁰,
 X. Portell Bueso¹², G.E. Pospelov¹⁰⁰, S. Pospisil¹²⁷, I.N. Potrap⁶⁴, C.J. Potter¹⁵⁰, C.T. Potter¹¹⁵,
 G. Poulard³⁰, J. Poveda⁶⁰, V. Pozdnyakov⁶⁴, R. Prabhu⁷⁷, P. Pralavorio⁸⁴, A. Pranko¹⁵,
 S. Prasad³⁰, R. Pravahan²⁵, S. Prell⁶³, K. Pretzl¹⁷, D. Price⁶⁰, J. Price⁷³, L.E. Price⁶,
 D. Prieur¹²⁴, M. Primavera^{72a}, M. Proissl⁴⁶, K. Prokofiev¹⁰⁹, F. Prokoshin^{32b},
 E. Protopapadaki¹³⁷, S. Protopopescu²⁵, J. Proudfoot⁶, X. Prudent⁴⁴, M. Przybycien^{38a},
 H. Przysieszniak⁵, S. Psoroulas²¹, E. Ptacek¹¹⁵, E. Pueschel⁸⁵, D. Puldon¹⁴⁹, M. Purohit^{25,ae},
 P. Puzo¹¹⁶, Y. Pylypchenko⁶², J. Qian⁸⁸, A. Quadt⁵⁴, D.R. Quarrie¹⁵, W.B. Quayle¹⁷⁴,
 D. Quilty⁵³, M. Raas¹⁰⁵, V. Radeka²⁵, V. Radescu⁴², P. Radloff¹¹⁵, F. Ragusa^{90a,90b}, G. Rahal¹⁷⁹,
 S. Rajagopalan²⁵, M. Rammensee⁴⁸, M. Rammes¹⁴², A.S. Randle-Conde⁴⁰, K. Randrianarivony²⁹,
 C. Rangel-Smith⁷⁹, K. Rao¹⁶⁴, F. Rauscher⁹⁹, T.C. Rave⁴⁸, T. Ravenscroft⁵³, M. Raymond³⁰,
 A.L. Read¹¹⁸, D.M. Rebuffi^{120a,120b}, A. Redelbach¹⁷⁵, G. Redlinger²⁵, R. Reece¹²¹, K. Reeves⁴¹,
 A. Reinsch¹¹⁵, I. Reisinger⁴³, M. Relich¹⁶⁴, C. Rembser³⁰, Z.L. Ren¹⁵², A. Renaud¹¹⁶,
 M. Rescigno^{133a}, S. Resconi^{90a}, B. Resende¹³⁷, P. Reznicek⁹⁹, R. Rezvani⁹⁴, R. Richter¹⁰⁰,
 E. Richter-Was^{38b}, M. Ridel⁷⁹, P. Rieck¹⁶, M. Rijssenbeek¹⁴⁹, A. Rimoldi^{120a,120b}, L. Rinaldi^{20a},
 R.R. Rios⁴⁰, E. Ritsch⁶¹, I. Riu¹², G. Rivoltella^{90a,90b}, F. Rizatdinova¹¹³, E. Rizvi⁷⁵,
 S.H. Robertson^{86,j}, A. Robichaud-Veronneau¹¹⁹, D. Robinson²⁸, J.E.M. Robinson⁸³, A. Robson⁵³,
 J.G. Rocha de Lima¹⁰⁷, C. Roda^{123a,123b}, D. Roda Dos Santos³⁰, A. Roe⁵⁴, S. Roe³⁰,
 O. Röhne¹¹⁸, S. Rolli¹⁶², A. Romaniouk⁹⁷, M. Romano^{20a,20b}, G. Romeo²⁷, E. Romero Adam¹⁶⁸,
 N. Rompotis¹³⁹, L. Roos⁷⁹, E. Ros¹⁶⁸, S. Rosati^{133a}, K. Rosbach⁴⁹, A. Rose¹⁵⁰, M. Rose⁷⁶,
 G.A. Rosenbaum¹⁵⁹, P.L. Rosendahl¹⁴, O. Rosenthal¹⁴², V. Rossetti¹², E. Rossi^{133a,133b},
 L.P. Rossi^{50a}, M. Rotaru^{26a}, I. Roth¹⁷³, J. Rothberg¹³⁹, D. Rousseau¹¹⁶, C.R. Royon¹³⁷,
 A. Rozanov⁸⁴, Y. Rozen¹⁵³, X. Ruan^{33a,ai}, F. Rubbo¹², I. Rubinskiy⁴², N. Ruckstuhl¹⁰⁶,
 V.I. Rud⁹⁸, C. Rudolph⁴⁴, M.S. Rudolph¹⁵⁹, F. Rühr⁷, A. Ruiz-Martinez⁶³, L. Rumyantsev⁶⁴,
 Z. Rurikova⁴⁸, N.A. Rusakovich⁶⁴, A. Ruschke⁹⁹, J.P. Rutherford⁷, N. Ruthmann⁴⁸,
 P. Ruzicka¹²⁶, Y.F. Ryabov¹²², M. Rybar¹²⁸, G. Rybkin¹¹⁶, N.C. Ryder¹¹⁹, A.F. Saavedra¹⁵¹,
 A. Saddique³, I. Sadeh¹⁵⁴, H.F-W. Sadrozinski¹³⁸, R. Sadykov⁶⁴, F. Safai Tehrani^{133a},
 H. Sakamoto¹⁵⁶, G. Salamanna⁷⁵, A. Salamon^{134a}, M. Saleem¹¹², D. Salek³⁰, D. Salihagic¹⁰⁰,
 A. Salmikov¹⁴⁴, J. Salt¹⁶⁸, B.M. Salvachua Ferrando⁶, D. Salvatore^{37a,37b}, F. Salvatore¹⁵⁰,
 A. Salvucci¹⁰⁵, A. Salzburger³⁰, D. Sampsonidis¹⁵⁵, A. Sanchez^{103a,103b}, J. Sánchez¹⁶⁸,
 V. Sanchez Martinez¹⁶⁸, H. Sandaker¹⁴, H.G. Sander⁸², M.P. Sanders⁹⁹, M. Sandhoff¹⁷⁶,
 T. Sandoval²⁸, C. Sandoval¹⁶³, R. Sandstroem¹⁰⁰, D.P.C. Sankey¹³⁰, A. Sansoni⁴⁷, C. Santoni³⁴,

R. Santonico^{134a,134b}, H. Santos^{125a}, I. Santoyo Castillo¹⁵⁰, K. Sapp¹²⁴, J.G. Saraiva^{125a}, T. Sarangi¹⁷⁴, E. Sarkisyan-Grinbaum⁸, B. Sarrazin²¹, F. Sarri^{123a,123b}, G. Sartisohn¹⁷⁶, O. Sasaki⁶⁵, Y. Sasaki¹⁵⁶, N. Sasao⁶⁷, I. Satsounkevitch⁹¹, G. Sauvage^{5,*}, E. Sauvan⁵, J.B. Sauvan¹¹⁶, P. Savard^{159,e}, V. Savinov¹²⁴, D.O. Savu³⁰, C. Sawyer¹¹⁹, L. Sawyer^{78,l}, D.H. Saxon⁵³, J. Saxon¹²¹, C. Sbarra^{20a}, A. Sbrizzi³, D.A. Scannicchio¹⁶⁴, M. Scarcella¹⁵¹, J. Schaarschmidt¹¹⁶, P. Schacht¹⁰⁰, D. Schaefer¹²¹, A. Schaelicke⁴⁶, S. Schaepe²¹, S. Schaetzel^{58b}, U. Schäfer⁸², A.C. Schaffer¹¹⁶, D. Schaile⁹⁹, R.D. Schamberger¹⁴⁹, V. Scharf^{58a}, V.A. Schegelsky¹²², D. Scheirich⁸⁸, M. Schernau¹⁶⁴, M.I. Scherzer³⁵, C. Schiavi^{50a,50b}, J. Schieck⁹⁹, C. Schillo⁴⁸, M. Schioppa^{37a,37b}, S. Schlenker³⁰, E. Schmidt⁴⁸, K. Schmieden²¹, C. Schmitt⁸², C. Schmitt⁹⁹, S. Schmitt^{58b}, B. Schneider¹⁷, Y.J. Schnellbach⁷³, U. Schnoor⁴⁴, L. Schoeffel¹³⁷, A. Schoening^{58b}, A.L.S. Schorlemmer⁵⁴, M. Schott⁸², D. Schouten^{160a}, J. Schovancova¹²⁶, M. Schram⁸⁶, C. Schroeder⁸², N. Schroer^{58c}, M.J. Schultens²¹, H.-C. Schultz-Coulon^{58a}, H. Schulz¹⁶, M. Schumacher⁴⁸, B.A. Schumm¹³⁸, Ph. Schune¹³⁷, A. Schwartzman¹⁴⁴, Ph. Schwegler¹⁰⁰, Ph. Schwemling¹³⁷, R. Schwienhorst⁸⁹, J. Schwindling¹³⁷, T. Schwindt²¹, M. Schwoerer⁵, F.G. Sciacca¹⁷, E. Scifo¹¹⁶, G. Sciolla²³, W.G. Scott¹³⁰, F. Scutti²¹, J. Searcy⁸⁸, G. Sedov⁴², E. Sedykh¹²², S.C. Seidel¹⁰⁴, A. Seiden¹³⁸, F. Seifert⁴⁴, J.M. Seixas^{24a}, G. Sekhniaidze^{103a}, S.J. Sekula⁴⁰, K.E. Selbach⁴⁶, D.M. Seliverstov¹²², G. Sellers⁷³, M. Seman^{145b}, N. Semprini-Cesari^{20a,20b}, C. Serfon³⁰, L. Serin¹¹⁶, L. Serkin⁵⁴, T. Serre⁸⁴, R. Seuster^{160a}, H. Severini¹¹², A. Sfyrila³⁰, E. Shabalina⁵⁴, M. Shamim¹¹⁵, L.Y. Shan^{33a}, J.T. Shank²², Q.T. Shao⁸⁷, M. Shapiro¹⁵, P.B. Shatalov⁹⁶, K. Shaw^{165a,165c}, P. Sherwood⁷⁷, S. Shimizu¹⁰², M. Shimojima¹⁰¹, T. Shin⁵⁶, M. Shiyakova⁶⁴, A. Shmeleva⁹⁵, M.J. Shochet³¹, D. Short¹¹⁹, S. Shrestha⁶³, E. Shulga⁹⁷, M.A. Shupe⁷, P. Sicho¹²⁶, A. Sidoti^{133a}, F. Siegert⁴⁸, Dj. Sijacki^{13a}, O. Silbert¹⁷³, J. Silva^{125a}, Y. Silver¹⁵⁴, D. Silverstein¹⁴⁴, S.B. Silverstein^{147a}, V. Simak¹²⁷, O. Simard⁵, Lj. Simic^{13a}, S. Simion¹¹⁶, E. Simioni⁸², B. Simmons⁷⁷, R. Simoniello^{90a,90b}, M. Simonyan³⁶, P. Sinervo¹⁵⁹, N.B. Sinev¹¹⁵, V. Sipica¹⁴², G. Siragusa¹⁷⁵, A. Sircar⁷⁸, A.N. Sisakyan^{64,*}, S.Yu. Sivoklokov⁹⁸, J. Sjölin^{147a,147b}, T.B. Sjurson¹⁴, L.A. Skinnari¹⁵, H.P. Skottowe⁵⁷, K. Skovpen¹⁰⁸, P. Skubic¹¹², M. Slater¹⁸, T. Slavicek¹²⁷, K. Sliwa¹⁶², V. Smakhtin¹⁷³, B.H. Smart⁴⁶, L. Smestad¹¹⁸, S.Yu. Smirnov⁹⁷, Y. Smirnov⁹⁷, L.N. Smirnova^{98,aj}, O. Smirnova⁸⁰, K.M. Smith⁵³, M. Smizanska⁷¹, K. Smolek¹²⁷, A.A. Snesarev⁹⁵, G. Snidero⁷⁵, J. Snow¹¹², S. Snyder²⁵, R. Sobie^{170,j}, J. Sodomka¹²⁷, A. Soffer¹⁵⁴, D.A. Soh^{152,u}, C.A. Solans³⁰, M. Solar¹²⁷, J. Solc¹²⁷, E.Yu. Soldatov⁹⁷, U. Soldevila¹⁶⁸, E. Solfaroli Camillocci^{133a,133b}, A.A. Solodkov¹²⁹, O.V. Solovyanov¹²⁹, V. Solovyev¹²², N. Soni¹, A. Sood¹⁵, V. Sopko¹²⁷, B. Sopko¹²⁷, M. Sosebee⁸, R. Soualah^{165a,165c}, P. Soueid⁹⁴, A. Soukharev¹⁰⁸, D. South⁴², S. Spagnolo^{72a,72b}, F. Spanò⁷⁶, R. Spighi^{20a}, G. Spigo³⁰, R. Spiwoks³⁰, M. Spousta^{128,ak}, T. Spreitzer¹⁵⁹, B. Spurlock⁸, R.D. St. Denis⁵³, J. Stahlman¹²¹, R. Stamen^{58a}, E. Stanecka³⁹, R.W. Stanek⁶, C. Stanescu^{135a}, M. Stanescu-Bellu⁴², M.M. Stanitzki⁴², S. Stapnes¹¹⁸, E.A. Starchenko¹²⁹, J. Stark⁵⁵, P. Staroba¹²⁶, P. Starovoitov⁴², R. Staszewski³⁹, A. Staude⁹⁹, P. Stavina^{145a,*}, G. Steele⁵³, P. Steinbach⁴⁴, P. Steinberg²⁵, I. Stekl¹²⁷, B. Stelzer¹⁴³, H.J. Stelzer⁸⁹, O. Stelzer-Chilton^{160a}, H. Stenzel⁵², S. Stern¹⁰⁰, G.A. Stewart³⁰, J.A. Stillings²¹, M.C. Stockton⁸⁶, M. Stoebe⁸⁶, K. Stoerig⁴⁸, G. Stoicea^{26a}, S. Stonjek¹⁰⁰, A.R. Stradling⁸, A. Straessner⁴⁴, J. Strandberg¹⁴⁸, S. Strandberg^{147a,147b}, A. Strandlie¹¹⁸, M. Strang¹¹⁰, E. Strauss¹⁴⁴, M. Strauss¹¹², P. Strizenc^{145b}, R. Ströhmer¹⁷⁵, D.M. Strom¹¹⁵, J.A. Strong^{76,*}, R. Stroynowski⁴⁰, B. Stugu¹⁴, I. Stumer^{25,*}, J. Stupak¹⁴⁹, P. Sturm¹⁷⁶, N.A. Styles⁴², D. Su¹⁴⁴, HS. Subramania³, R. Subramaniam⁷⁸, A. Succurro¹², Y. Sugaya¹¹⁷, C. Suhr¹⁰⁷, M. Suk¹²⁷, V.V. Sulin⁹⁵, S. Sultansoy^{4c}, T. Sumida⁶⁷, X. Sun⁵⁵, J.E. Sundermann⁴⁸, K. Suruliz¹⁴⁰, G. Susinno^{37a,37b}, M.R. Sutton¹⁵⁰, Y. Suzuki⁶⁵, Y. Suzuki⁶⁶, M. Svatos¹²⁶, S. Swedish¹⁶⁹, M. Swiatlowski¹⁴⁴, I. Sykora^{145a}, T. Sykora¹²⁸, D. Ta¹⁰⁶, K. Tackmann⁴², A. Taffard¹⁶⁴, R. Tafirout^{160a}, N. Taiblum¹⁵⁴, Y. Takahashi¹⁰², H. Takai²⁵,

R. Takashima⁶⁸, H. Takeda⁶⁶, T. Takeshita¹⁴¹, Y. Takubo⁶⁵, M. Talby⁸⁴, A. Talyshev^{108,g}, J.Y.C. Tam¹⁷⁵, M.C. Tamsett^{78,al}, K.G. Tan⁸⁷, J. Tanaka¹⁵⁶, R. Tanaka¹¹⁶, S. Tanaka¹³², S. Tanaka⁶⁵, A.J. Tanasijczuk¹⁴³, K. Tani⁶⁶, N. Tannoury⁸⁴, S. Tapprogge⁸², D. Tardif¹⁵⁹, S. Tarem¹⁵³, F. Tarrade²⁹, G.F. Tartarelli^{90a}, P. Tas¹²⁸, M. Tasevsky¹²⁶, T. Tashiro⁶⁷, E. Tassi^{37a,37b}, Y. Tayalati^{136d}, C. Taylor⁷⁷, F.E. Taylor⁹³, G.N. Taylor⁸⁷, W. Taylor^{160b}, M. Teinturier¹¹⁶, F.A. Teischinger³⁰, M. Teixeira Dias Castanheira⁷⁵, P. Teixeira-Dias⁷⁶, K.K. Temming⁴⁸, H. Ten Kate³⁰, P.K. Teng¹⁵², S. Terada⁶⁵, K. Terashi¹⁵⁶, J. Terron⁸¹, M. Testa⁴⁷, R.J. Teuscher^{159,j}, J. Therhaag²¹, T. Theveneaux-Pelzer³⁴, S. Thoma⁴⁸, J.P. Thomas¹⁸, E.N. Thompson³⁵, P.D. Thompson¹⁸, P.D. Thompson¹⁵⁹, A.S. Thompson⁵³, L.A. Thomsen³⁶, E. Thomson¹²¹, M. Thomson²⁸, W.M. Thong⁸⁷, R.P. Thun^{88,*}, F. Tian³⁵, M.J. Tibbetts¹⁵, T. Tic¹²⁶, V.O. Tikhomirov⁹⁵, Y.A. Tikhonov^{108,g}, S. Timoshenko⁹⁷, E. Tiouchichine⁸⁴, P. Tipton¹⁷⁷, S. Tisserant⁸⁴, T. Todorov⁵, S. Todorova-Nova¹⁶², B. Toggerson¹⁶⁴, J. Tojo⁶⁹, S. Tokár^{145a}, K. Tokushuku⁶⁵, K. Tollefson⁸⁹, L. Tomlinson⁸³, M. Tomoto¹⁰², L. Tompkins³¹, K. Toms¹⁰⁴, A. Tonoyan¹⁴, C. Topfel¹⁷, N.D. Topilin⁶⁴, E. Torrence¹¹⁵, H. Torres⁷⁹, E. Torró Pastor¹⁶⁸, J. Toth^{84,af}, F. Touchard⁸⁴, D.R. Tovey¹⁴⁰, H.L. Tran¹¹⁶, T. Trefzger¹⁷⁵, L. Tremblet³⁰, A. Tricoli³⁰, I.M. Trigger^{160a}, S. Trincaz-Duvoid⁷⁹, M.F. Tripiana⁷⁰, N. Triplett²⁵, W. Trischuk¹⁵⁹, B. Trocmé⁵⁵, C. Troncon^{90a}, M. Trottier-McDonald¹⁴³, M. Trovatelli^{135a,135b}, P. True⁸⁹, M. Trzebinski³⁹, A. Trzupek³⁹, C. Tsarouchas³⁰, J.C-L. Tseng¹¹⁹, M. Tsiakiris¹⁰⁶, P.V. Tsiarehsha⁹¹, D. Tsionou¹³⁷, G. Tsipolitis¹⁰, S. Tsiskaridze¹², V. Tsiskaridze⁴⁸, E.G. Tskhadadze^{51a}, I.I. Tsukerman⁹⁶, V. Tsulaia¹⁵, J.-W. Tsung²¹, S. Tsuno⁶⁵, D. Tsybychev¹⁴⁹, A. Tua¹⁴⁰, A. Tudorache^{26a}, V. Tudorache^{26a}, J.M. Tuggle³¹, A.N. Tuna¹²¹, M. Turala³⁹, D. Turecek¹²⁷, I. Turk Cakir^{4d}, R. Turra^{90a,90b}, P.M. Tuts³⁵, A. Tykhonov⁷⁴, M. Tylmad^{147a,147b}, M. Tyndel¹³⁰, K. Uchida²¹, I. Ueda¹⁵⁶, R. Ueno²⁹, M. Ughetto⁸⁴, M. Uglund¹⁴, M. Uhlenbrock²¹, F. Ukegawa¹⁶¹, G. Unal³⁰, A. Undrus²⁵, G. Unel¹⁶⁴, F.C. Ungaro⁴⁸, Y. Unno⁶⁵, D. Urbaniec³⁵, P. Urquijo²¹, G. Usai⁸, L. Vacavant⁸⁴, V. Vacek¹²⁷, B. Vachon⁸⁶, S. Vahsen¹⁵, N. Valencic¹⁰⁶, S. Valentineti^{20a,20b}, A. Valero¹⁶⁸, L. Valery³⁴, S. Valkar¹²⁸, E. Valladolid Gallego¹⁶⁸, S. Vallecorsa¹⁵³, J.A. Valls Ferrer¹⁶⁸, R. Van Berg¹²¹, P.C. Van Der Deijl¹⁰⁶, R. van der Geer¹⁰⁶, H. van der Graaf¹⁰⁶, R. Van Der Leeuw¹⁰⁶, D. van der Ster³⁰, N. van Eldik³⁰, P. van Gemmeren⁶, J. Van Nieuwkoop¹⁴³, I. van Vulpen¹⁰⁶, M. Vanadia¹⁰⁰, W. Vandelli³⁰, A. Vaniachine⁶, P. Vankov⁴², F. Vannucci⁷⁹, R. Vari^{133a}, E.W. Varnes⁷, T. Varol⁸⁵, D. Varouchas¹⁵, A. Vartapetian⁸, K.E. Varvell¹⁵¹, V.I. Vassilakopoulos⁵⁶, F. Vazeille³⁴, T. Vazquez Schroeder⁵⁴, F. Veloso^{125a}, S. Veneziano^{133a}, A. Ventura^{72a,72b}, D. Ventura⁸⁵, M. Venturi⁴⁸, N. Venturi¹⁵⁹, V. Vercesi^{120a}, M. Verducci¹³⁹, W. Verkerke¹⁰⁶, J.C. Vermeulen¹⁰⁶, A. Vest⁴⁴, M.C. Vetterli^{143,e}, I. Vichou¹⁶⁶, T. Vickey^{146c,am}, O.E. Vickey Boeriu^{146c}, G.H.A. Viehhauser¹¹⁹, S. Viel¹⁶⁹, M. Villa^{20a,20b}, M. Villaplana Perez¹⁶⁸, E. Vilucchi⁴⁷, M.G. Vincter²⁹, V.B. Vinogradov⁶⁴, J. Virzi¹⁵, O. Vitells¹⁷³, M. Viti⁴², I. Vivarelli⁴⁸, F. Vives Vaque³, S. Vlachos¹⁰, D. Vladoiu⁹⁹, M. Vlasak¹²⁷, A. Vogel²¹, P. Vokac¹²⁷, G. Volpi⁴⁷, M. Volpi⁸⁷, G. Volpini^{90a}, H. von der Schmitt¹⁰⁰, H. von Radziewski⁴⁸, E. von Toerne²¹, V. Vorobel¹²⁸, M. Vos¹⁶⁸, R. Voss³⁰, J.H. Vossebeld⁷³, N. Vranjes¹³⁷, M. Vranjes Milosavljevic¹⁰⁶, V. Vrba¹²⁶, M. Vreeswijk¹⁰⁶, T. Vu Anh⁴⁸, R. Vuillermet³⁰, I. Vukotic³¹, Z. Vykydal¹²⁷, W. Wagner¹⁷⁶, P. Wagner²¹, S. Wahrmund⁴⁴, J. Wakabayashi¹⁰², S. Walch⁸⁸, J. Walder⁷¹, R. Walker⁹⁹, W. Walkowiak¹⁴², R. Wall¹⁷⁷, P. Waller⁷³, B. Walsh¹⁷⁷, C. Wang⁴⁵, H. Wang¹⁷⁴, H. Wang⁴⁰, J. Wang¹⁵², J. Wang^{33a}, K. Wang⁸⁶, R. Wang¹⁰⁴, S.M. Wang¹⁵², T. Wang²¹, X. Wang¹⁷⁷, A. Warburton⁸⁶, C.P. Ward²⁸, D.R. Wardrop⁷⁷, M. Warsinsky⁴⁸, A. Washbrook⁴⁶, C. Wasicki⁴², I. Watanabe⁶⁶, P.M. Watkins¹⁸, A.T. Watson¹⁸, I.J. Watson¹⁵¹, M.F. Watson¹⁸, G. Watts¹³⁹, S. Watts⁸³, A.T. Waugh¹⁵¹, B.M. Waugh⁷⁷, M.S. Weber¹⁷, J.S. Webster³¹, A.R. Weidberg¹¹⁹, P. Weigell¹⁰⁰, J. Weingarten⁵⁴, C. Weiser⁴⁸, P.S. Wells³⁰, T. Wenaus²⁵, D. Wendland¹⁶, Z. Weng^{152,u},

T. Wengler³⁰, S. Wenig³⁰, N. Wermes²¹, M. Werner⁴⁸, P. Werner³⁰, M. Werth¹⁶⁴, M. Wessels^{58a}, J. Wetter¹⁶², K. Whalen²⁹, A. White⁸, M.J. White⁸⁷, R. White^{32b}, S. White^{123a,123b}, S.R. Whitehead¹¹⁹, D. Whiteson¹⁶⁴, D. Whittington⁶⁰, D. Wicke¹⁷⁶, F.J. Wickens¹³⁰, W. Wiedenmann¹⁷⁴, M. Wielers^{80,d}, P. Wienemann²¹, C. Wiglesworth³⁶, L.A.M. Wiik-Fuchs²¹, P.A. Wijeratne⁷⁷, A. Wildauer¹⁰⁰, M.A. Wildt^{42,r}, I. Wilhelm¹²⁸, H.G. Wilkens³⁰, J.Z. Will⁹⁹, E. Williams³⁵, H.H. Williams¹²¹, S. Williams²⁸, W. Willis^{35,*}, S. Willocq⁸⁵, J.A. Wilson¹⁸, A. Wilson⁸⁸, I. Wingerter-Seez⁵, S. Winkelmann⁴⁸, F. Winklmeier³⁰, M. Wittgen¹⁴⁴, T. Wittig⁴³, J. Wittkowski⁹⁹, S.J. Wollstadt⁸², M.W. Wolter³⁹, H. Wolters^{125a,h}, W.C. Wong⁴¹, G. Wooden⁸⁸, B.K. Wosiek³⁹, J. Wotschack³⁰, M.J. Woudstra⁸³, K.W. Wozniak³⁹, K. Wraight⁵³, M. Wright⁵³, B. Wrona⁷³, S.L. Wu¹⁷⁴, X. Wu⁴⁹, Y. Wu⁸⁸, E. Wulf³⁵, B.M. Wynne⁴⁶, S. Xella³⁶, M. Xiao¹³⁷, S. Xie⁴⁸, C. Xu^{33b,z}, D. Xu^{33a}, L. Xu^{33b}, B. Yabsley¹⁵¹, S. Yacoob^{146b,an}, M. Yamada⁶⁵, H. Yamaguchi¹⁵⁶, Y. Yamaguchi¹⁵⁶, A. Yamamoto⁶⁵, K. Yamamoto⁶³, S. Yamamoto¹⁵⁶, T. Yamamura¹⁵⁶, T. Yamanaka¹⁵⁶, K. Yamauchi¹⁰², T. Yamazaki¹⁵⁶, Y. Yamazaki⁶⁶, Z. Yan²², H. Yang^{33e}, H. Yang¹⁷⁴, U.K. Yang⁸³, Y. Yang¹¹⁰, Z. Yang^{147a,147b}, S. Yanush⁹², L. Yao^{33a}, Y. Yasu⁶⁵, E. Yatsenko⁴², K.H. Yau Wong²¹, J. Ye⁴⁰, S. Ye²⁵, A.L. Yen⁵⁷, E. Yildirim⁴², M. Yilmaz^{4b}, R. Yoosoofmiya¹²⁴, K. Yorita¹⁷², R. Yoshida⁶, K. Yoshihara¹⁵⁶, C. Young¹⁴⁴, C.J.S. Young¹¹⁹, S. Youssef²², D. Yu²⁵, D.R. Yu¹⁵, J. Yu⁸, J. Yu¹¹³, L. Yuan⁶⁶, A. Yurkewicz¹⁰⁷, B. Zabinski³⁹, R. Zaidan⁶², A.M. Zaitsev^{129,aa}, S. Zambito²³, L. Zanello^{133a,133b}, D. Zanzi¹⁰⁰, A. Zaytsev²⁵, C. Zeitnitz¹⁷⁶, M. Zeman¹²⁷, A. Zemla³⁹, O. Zenin¹²⁹, T. Ženiš^{145a}, D. Zerwas¹¹⁶, G. Zevi della Porta⁵⁷, D. Zhang⁸⁸, H. Zhang⁸⁹, J. Zhang⁶, L. Zhang¹⁵², X. Zhang^{33d}, Z. Zhang¹¹⁶, Z. Zhao^{33b}, A. Zhemchugov⁶⁴, J. Zhong¹¹⁹, B. Zhou⁸⁸, N. Zhou¹⁶⁴, Y. Zhou¹⁵², C.G. Zhu^{33d}, H. Zhu⁴², J. Zhu⁸⁸, Y. Zhu^{33b}, X. Zhuang^{33a}, A. Zibell⁹⁹, D. Zieminska⁶⁰, N.I. Zimin⁶⁴, C. Zimmermann⁸², R. Zimmermann²¹, S. Zimmermann²¹, S. Zimmermann⁴⁸, Z. Zinonos^{123a,123b}, M. Ziolkowski¹⁴², R. Zitoun⁵, L. Živković³⁵, V.V. Zmouchko^{129,*}, G. Zobernig¹⁷⁴, A. Zoccoli^{20a,20b}, M. zur Nedden¹⁶, V. Zutshi¹⁰⁷, L. Zwalinski³⁰.

¹ School of Chemistry and Physics, University of Adelaide, Adelaide, Australia

² Physics Department, SUNY Albany, Albany NY, U.S.A.

³ Department of Physics, University of Alberta, Edmonton AB, Canada

⁴ (a) Department of Physics, Ankara University, Ankara; (b) Department of Physics, Gazi University, Ankara; (c) Division of Physics, TOBB University of Economics and Technology, Ankara; (d) Turkish Atomic Energy Authority, Ankara, Turkey

⁵ LAPP, CNRS/IN2P3 and Université de Savoie, Annecy-le-Vieux, France

⁶ High Energy Physics Division, Argonne National Laboratory, Argonne IL, U.S.A.

⁷ Department of Physics, University of Arizona, Tucson AZ, U.S.A.

⁸ Department of Physics, The University of Texas at Arlington, Arlington TX, U.S.A.

⁹ Physics Department, University of Athens, Athens, Greece

¹⁰ Physics Department, National Technical University of Athens, Zografou, Greece

¹¹ Institute of Physics, Azerbaijan Academy of Sciences, Baku, Azerbaijan

¹² Institut de Física d'Altes Energies and Departament de Física de la Universitat Autònoma de Barcelona and ICREA, Barcelona, Spain

¹³ (a) Institute of Physics, University of Belgrade, Belgrade; (b) Vinca Institute of Nuclear Sciences, University of Belgrade, Belgrade, Serbia

¹⁴ Department for Physics and Technology, University of Bergen, Bergen, Norway

¹⁵ Physics Division, Lawrence Berkeley National Laboratory and University of California, Berkeley CA, U.S.A.

¹⁶ Department of Physics, Humboldt University, Berlin, Germany

¹⁷ Albert Einstein Center for Fundamental Physics and Laboratory for High Energy Physics, University of Bern, Bern, Switzerland

¹⁸ School of Physics and Astronomy, University of Birmingham, Birmingham, United Kingdom

- 19 (a) *Department of Physics, Bogazici University, Istanbul;* (b) *Department of Physics, Dogus University, Istanbul;* (c) *Department of Physics Engineering, Gaziantep University, Gaziantep, Turkey*
- 20 (a) *INFN Sezione di Bologna;* (b) *Dipartimento di Fisica e Astronomia, Università di Bologna, Bologna, Italy*
- 21 *Physikalisches Institut, University of Bonn, Bonn, Germany*
- 22 *Department of Physics, Boston University, Boston MA, U.S.A.*
- 23 *Department of Physics, Brandeis University, Waltham MA, U.S.A.*
- 24 (a) *Universidade Federal do Rio De Janeiro COPPE/EE/IF, Rio de Janeiro;* (b) *Federal University of Juiz de Fora (UFJF), Juiz de Fora;* (c) *Federal University of Sao Joao del Rei (UFSJ), Sao Joao del Rei;* (d) *Instituto de Fisica, Universidade de Sao Paulo, Sao Paulo, Brazil*
- 25 *Physics Department, Brookhaven National Laboratory, Upton NY, U.S.A.*
- 26 (a) *National Institute of Physics and Nuclear Engineering, Bucharest;* (b) *University Politehnica Bucharest, Bucharest;* (c) *West University in Timisoara, Timisoara, Romania*
- 27 *Departamento de Física, Universidad de Buenos Aires, Buenos Aires, Argentina*
- 28 *Cavendish Laboratory, University of Cambridge, Cambridge, United Kingdom*
- 29 *Department of Physics, Carleton University, Ottawa ON, Canada*
- 30 *CERN, Geneva, Switzerland*
- 31 *Enrico Fermi Institute, University of Chicago, Chicago IL, U.S.A.*
- 32 (a) *Departamento de Física, Pontificia Universidad Católica de Chile, Santiago;* (b) *Departamento de Física, Universidad Técnica Federico Santa María, Valparaíso, Chile*
- 33 (a) *Institute of High Energy Physics, Chinese Academy of Sciences, Beijing;* (b) *Department of Modern Physics, University of Science and Technology of China, Anhui;* (c) *Department of Physics, Nanjing University, Jiangsu;* (d) *School of Physics, Shandong University, Shandong;* (e) *Physics Department, Shanghai Jiao Tong University, Shanghai, China*
- 34 *Laboratoire de Physique Corpusculaire, Clermont Université and Université Blaise Pascal and CNRS/IN2P3, Clermont-Ferrand, France*
- 35 *Nevis Laboratory, Columbia University, Irvington NY, U.S.A.*
- 36 *Niels Bohr Institute, University of Copenhagen, Kobenhavn, Denmark*
- 37 (a) *INFN Gruppo Collegato di Cosenza;* (b) *Dipartimento di Fisica, Università della Calabria, Rende, Italy*
- 38 (a) *AGH University of Science and Technology, Faculty of Physics and Applied Computer Science, Krakow;* (b) *Marian Smoluchowski Institute of Physics, Jagiellonian University, Krakow, Poland*
- 39 *The Henryk Niewodniczanski Institute of Nuclear Physics, Polish Academy of Sciences, Krakow, Poland*
- 40 *Physics Department, Southern Methodist University, Dallas TX, U.S.A.*
- 41 *Physics Department, University of Texas at Dallas, Richardson TX, U.S.A.*
- 42 *DESY, Hamburg and Zeuthen, Germany*
- 43 *Institut für Experimentelle Physik IV, Technische Universität Dortmund, Dortmund, Germany*
- 44 *Institut für Kern- und Teilchenphysik, Technical University Dresden, Dresden, Germany*
- 45 *Department of Physics, Duke University, Durham NC, U.S.A.*
- 46 *SUPA - School of Physics and Astronomy, University of Edinburgh, Edinburgh, United Kingdom*
- 47 *INFN Laboratori Nazionali di Frascati, Frascati, Italy*
- 48 *Fakultät für Mathematik und Physik, Albert-Ludwigs-Universität, Freiburg, Germany*
- 49 *Section de Physique, Université de Genève, Geneva, Switzerland*
- 50 (a) *INFN Sezione di Genova;* (b) *Dipartimento di Fisica, Università di Genova, Genova, Italy*
- 51 (a) *E. Andronikashvili Institute of Physics, Iv. Javakishvili Tbilisi State University, Tbilisi;* (b) *High Energy Physics Institute, Tbilisi State University, Tbilisi, Georgia*
- 52 *II Physikalisches Institut, Justus-Liebig-Universität Giessen, Giessen, Germany*
- 53 *SUPA - School of Physics and Astronomy, University of Glasgow, Glasgow, United Kingdom*
- 54 *II Physikalisches Institut, Georg-August-Universität, Göttingen, Germany*

- 55 *Laboratoire de Physique Subatomique et de Cosmologie, Université Joseph Fourier and CNRS/IN2P3 and Institut National Polytechnique de Grenoble, Grenoble, France*
- 56 *Department of Physics, Hampton University, Hampton VA, U.S.A.*
- 57 *Laboratory for Particle Physics and Cosmology, Harvard University, Cambridge MA, U.S.A.*
- 58 ^(a) *Kirchhoff-Institut für Physik, Ruprecht-Karls-Universität Heidelberg, Heidelberg;* ^(b) *Physikalisches Institut, Ruprecht-Karls-Universität Heidelberg, Heidelberg;* ^(c) *ZITI Institut für technische Informatik, Ruprecht-Karls-Universität Heidelberg, Mannheim, Germany*
- 59 *Faculty of Applied Information Science, Hiroshima Institute of Technology, Hiroshima, Japan*
- 60 *Department of Physics, Indiana University, Bloomington IN, U.S.A.*
- 61 *Institut für Astro- und Teilchenphysik, Leopold-Franzens-Universität, Innsbruck, Austria*
- 62 *University of Iowa, Iowa City IA, U.S.A.*
- 63 *Department of Physics and Astronomy, Iowa State University, Ames IA, U.S.A.*
- 64 *Joint Institute for Nuclear Research, JINR Dubna, Dubna, Russia*
- 65 *KEK, High Energy Accelerator Research Organization, Tsukuba, Japan*
- 66 *Graduate School of Science, Kobe University, Kobe, Japan*
- 67 *Faculty of Science, Kyoto University, Kyoto, Japan*
- 68 *Kyoto University of Education, Kyoto, Japan*
- 69 *Department of Physics, Kyushu University, Fukuoka, Japan*
- 70 *Instituto de Física La Plata, Universidad Nacional de La Plata and CONICET, La Plata, Argentina*
- 71 *Physics Department, Lancaster University, Lancaster, United Kingdom*
- 72 ^(a) *INFN Sezione di Lecce;* ^(b) *Dipartimento di Matematica e Fisica, Università del Salento, Lecce, Italy*
- 73 *Oliver Lodge Laboratory, University of Liverpool, Liverpool, United Kingdom*
- 74 *Department of Physics, Jožef Stefan Institute and University of Ljubljana, Ljubljana, Slovenia*
- 75 *School of Physics and Astronomy, Queen Mary University of London, London, United Kingdom*
- 76 *Department of Physics, Royal Holloway University of London, Surrey, United Kingdom*
- 77 *Department of Physics and Astronomy, University College London, London, United Kingdom*
- 78 *Louisiana Tech University, Ruston LA, U.S.A.*
- 79 *Laboratoire de Physique Nucléaire et de Hautes Energies, UPMC and Université Paris-Diderot and CNRS/IN2P3, Paris, France*
- 80 *Fysiska institutionen, Lunds universitet, Lund, Sweden*
- 81 *Departamento de Física Teórica C-15, Universidad Autónoma de Madrid, Madrid, Spain*
- 82 *Institut für Physik, Universität Mainz, Mainz, Germany*
- 83 *School of Physics and Astronomy, University of Manchester, Manchester, United Kingdom*
- 84 *CPPM, Aix-Marseille Université and CNRS/IN2P3, Marseille, France*
- 85 *Department of Physics, University of Massachusetts, Amherst MA, U.S.A.*
- 86 *Department of Physics, McGill University, Montreal QC, Canada*
- 87 *School of Physics, University of Melbourne, Victoria, Australia*
- 88 *Department of Physics, The University of Michigan, Ann Arbor MI, U.S.A.*
- 89 *Department of Physics and Astronomy, Michigan State University, East Lansing MI, U.S.A.*
- 90 ^(a) *INFN Sezione di Milano;* ^(b) *Dipartimento di Fisica, Università di Milano, Milano, Italy*
- 91 *B.I. Stepanov Institute of Physics, National Academy of Sciences of Belarus, Minsk, Republic of Belarus*
- 92 *National Scientific and Educational Centre for Particle and High Energy Physics, Minsk, Republic of Belarus*
- 93 *Department of Physics, Massachusetts Institute of Technology, Cambridge MA, U.S.A.*
- 94 *Group of Particle Physics, University of Montreal, Montreal QC, Canada*
- 95 *P.N. Lebedev Institute of Physics, Academy of Sciences, Moscow, Russia*
- 96 *Institute for Theoretical and Experimental Physics (ITEP), Moscow, Russia*
- 97 *Moscow Engineering and Physics Institute (MEPhI), Moscow, Russia*
- 98 *D.V.Skobeltzyn Institute of Nuclear Physics, M.V.Lomonosov Moscow State University, Moscow, Russia*

- 99 *Fakultät für Physik, Ludwig-Maximilians-Universität München, München, Germany*
- 100 *Max-Planck-Institut für Physik (Werner-Heisenberg-Institut), München, Germany*
- 101 *Nagasaki Institute of Applied Science, Nagasaki, Japan*
- 102 *Graduate School of Science and Kobayashi-Maskawa Institute, Nagoya University, Nagoya, Japan*
- 103 ^(a) *INFN Sezione di Napoli;* ^(b) *Dipartimento di Scienze Fisiche, Università di Napoli, Napoli, Italy*
- 104 *Department of Physics and Astronomy, University of New Mexico, Albuquerque NM, U.S.A.*
- 105 *Institute for Mathematics, Astrophysics and Particle Physics, Radboud University Nijmegen/Nikhef, Nijmegen, Netherlands*
- 106 *Nikhef National Institute for Subatomic Physics and University of Amsterdam, Amsterdam, Netherlands*
- 107 *Department of Physics, Northern Illinois University, DeKalb IL, U.S.A.*
- 108 *Budker Institute of Nuclear Physics, SB RAS, Novosibirsk, Russia*
- 109 *Department of Physics, New York University, New York NY, U.S.A.*
- 110 *Ohio State University, Columbus OH, U.S.A.*
- 111 *Faculty of Science, Okayama University, Okayama, Japan*
- 112 *Homer L. Dodge Department of Physics and Astronomy, University of Oklahoma, Norman OK, U.S.A.*
- 113 *Department of Physics, Oklahoma State University, Stillwater OK, U.S.A.*
- 114 *Palacký University, RCPTM, Olomouc, Czech Republic*
- 115 *Center for High Energy Physics, University of Oregon, Eugene OR, U.S.A.*
- 116 *LAL, Université Paris-Sud and CNRS/IN2P3, Orsay, France*
- 117 *Graduate School of Science, Osaka University, Osaka, Japan*
- 118 *Department of Physics, University of Oslo, Oslo, Norway*
- 119 *Department of Physics, Oxford University, Oxford, United Kingdom*
- 120 ^(a) *INFN Sezione di Pavia;* ^(b) *Dipartimento di Fisica, Università di Pavia, Pavia, Italy*
- 121 *Department of Physics, University of Pennsylvania, Philadelphia PA, U.S.A.*
- 122 *Petersburg Nuclear Physics Institute, Gatchina, Russia*
- 123 ^(a) *INFN Sezione di Pisa;* ^(b) *Dipartimento di Fisica E. Fermi, Università di Pisa, Pisa, Italy*
- 124 *Department of Physics and Astronomy, University of Pittsburgh, Pittsburgh PA, U.S.A.*
- 125 ^(a) *Laboratorio de Instrumentacao e Fisica Experimental de Particulas - LIP, Lisboa, Portugal;*
^(b) *Departamento de Fisica Teorica y del Cosmos and CAFPE, Universidad de Granada, Granada, Spain*
- 126 *Institute of Physics, Academy of Sciences of the Czech Republic, Praha, Czech Republic*
- 127 *Czech Technical University in Prague, Praha, Czech Republic*
- 128 *Faculty of Mathematics and Physics, Charles University in Prague, Praha, Czech Republic*
- 129 *State Research Center Institute for High Energy Physics, Protvino, Russia*
- 130 *Particle Physics Department, Rutherford Appleton Laboratory, Didcot, United Kingdom*
- 131 *Physics Department, University of Regina, Regina SK, Canada*
- 132 *Ritsumeikan University, Kusatsu, Shiga, Japan*
- 133 ^(a) *INFN Sezione di Roma I;* ^(b) *Dipartimento di Fisica, Università La Sapienza, Roma, Italy*
- 134 ^(a) *INFN Sezione di Roma Tor Vergata;* ^(b) *Dipartimento di Fisica, Università di Roma Tor Vergata, Roma, Italy*
- 135 ^(a) *INFN Sezione di Roma Tre;* ^(b) *Dipartimento di Matematica e Fisica, Università Roma Tre, Roma, Italy*
- 136 ^(a) *Faculté des Sciences Ain Chock, Réseau Universitaire de Physique des Hautes Energies - Université Hassan II, Casablanca;* ^(b) *Centre National de l'Energie des Sciences Techniques Nucleaires, Rabat;* ^(c) *Faculté des Sciences Semlalia, Université Cadi Ayyad, LPHEA-Marrakech;*
^(d) *Faculté des Sciences, Université Mohamed Premier and LPTPM, Oujda;* ^(e) *Faculté des sciences, Université Mohammed V-Agdal, Rabat, Morocco*
- 137 *DSM/IRFU (Institut de Recherches sur les Lois Fondamentales de l'Univers), CEA Saclay (Commissariat à l'Energie Atomique et aux Energies Alternatives), Gif-sur-Yvette, France*

- 138 *Santa Cruz Institute for Particle Physics, University of California Santa Cruz, Santa Cruz CA, U.S.A.*
- 139 *Department of Physics, University of Washington, Seattle WA, U.S.A.*
- 140 *Department of Physics and Astronomy, University of Sheffield, Sheffield, United Kingdom*
- 141 *Department of Physics, Shinshu University, Nagano, Japan*
- 142 *Fachbereich Physik, Universität Siegen, Siegen, Germany*
- 143 *Department of Physics, Simon Fraser University, Burnaby BC, Canada*
- 144 *SLAC National Accelerator Laboratory, Stanford CA, U.S.A.*
- 145 ^(a) *Faculty of Mathematics, Physics & Informatics, Comenius University, Bratislava;* ^(b) *Department of Subnuclear Physics, Institute of Experimental Physics of the Slovak Academy of Sciences, Kosice, Slovak Republic*
- 146 ^(a) *Department of Physics, University of Cape Town, Cape Town;* ^(b) *Department of Physics, University of Johannesburg, Johannesburg;* ^(c) *School of Physics, University of the Witwatersrand, Johannesburg, South Africa*
- 147 ^(a) *Department of Physics, Stockholm University;* ^(b) *The Oskar Klein Centre, Stockholm, Sweden*
- 148 *Physics Department, Royal Institute of Technology, Stockholm, Sweden*
- 149 *Departments of Physics & Astronomy and Chemistry, Stony Brook University, Stony Brook NY, U.S.A.*
- 150 *Department of Physics and Astronomy, University of Sussex, Brighton, United Kingdom*
- 151 *School of Physics, University of Sydney, Sydney, Australia*
- 152 *Institute of Physics, Academia Sinica, Taipei, Taiwan*
- 153 *Department of Physics, Technion: Israel Institute of Technology, Haifa, Israel*
- 154 *Raymond and Beverly Sackler School of Physics and Astronomy, Tel Aviv University, Tel Aviv, Israel*
- 155 *Department of Physics, Aristotle University of Thessaloniki, Thessaloniki, Greece*
- 156 *International Center for Elementary Particle Physics and Department of Physics, The University of Tokyo, Tokyo, Japan*
- 157 *Graduate School of Science and Technology, Tokyo Metropolitan University, Tokyo, Japan*
- 158 *Department of Physics, Tokyo Institute of Technology, Tokyo, Japan*
- 159 *Department of Physics, University of Toronto, Toronto ON, Canada*
- 160 ^(a) *TRIUMF, Vancouver BC;* ^(b) *Department of Physics and Astronomy, York University, Toronto ON, Canada*
- 161 *Faculty of Pure and Applied Sciences, University of Tsukuba, Tsukuba, Japan*
- 162 *Department of Physics and Astronomy, Tufts University, Medford MA, U.S.A.*
- 163 *Centro de Investigaciones, Universidad Antonio Narino, Bogota, Colombia*
- 164 *Department of Physics and Astronomy, University of California Irvine, Irvine CA, U.S.A.*
- 165 ^(a) *INFN Gruppo Collegato di Udine;* ^(b) *ICTP, Trieste;* ^(c) *Dipartimento di Chimica, Fisica e Ambiente, Università di Udine, Udine, Italy*
- 166 *Department of Physics, University of Illinois, Urbana IL, U.S.A.*
- 167 *Department of Physics and Astronomy, University of Uppsala, Uppsala, Sweden*
- 168 *Instituto de Física Corpuscular (IFIC) and Departamento de Física Atómica, Molecular y Nuclear and Departamento de Ingeniería Electrónica and Instituto de Microelectrónica de Barcelona (IMB-CNM), University of Valencia and CSIC, Valencia, Spain*
- 169 *Department of Physics, University of British Columbia, Vancouver BC, Canada*
- 170 *Department of Physics and Astronomy, University of Victoria, Victoria BC, Canada*
- 171 *Department of Physics, University of Warwick, Coventry, United Kingdom*
- 172 *Waseda University, Tokyo, Japan*
- 173 *Department of Particle Physics, The Weizmann Institute of Science, Rehovot, Israel*
- 174 *Department of Physics, University of Wisconsin, Madison WI, U.S.A.*
- 175 *Fakultät für Physik und Astronomie, Julius-Maximilians-Universität, Würzburg, Germany*
- 176 *Fachbereich C Physik, Bergische Universität Wuppertal, Wuppertal, Germany*
- 177 *Department of Physics, Yale University, New Haven CT, U.S.A.*

- ¹⁷⁸ *Yerevan Physics Institute, Yerevan, Armenia*
- ¹⁷⁹ *Centre de Calcul de l'Institut National de Physique Nucléaire et de Physique des Particules (IN2P3), Villeurbanne, France*
- ^a *Also at Department of Physics, King's College London, London, United Kingdom*
- ^b *Also at Laboratorio de Instrumentacao e Fisica Experimental de Particulas - LIP, Lisboa, Portugal*
- ^c *Also at Faculdade de Ciencias and CFNUL, Universidade de Lisboa, Lisboa, Portugal*
- ^d *Also at Particle Physics Department, Rutherford Appleton Laboratory, Didcot, United Kingdom*
- ^e *Also at TRIUMF, Vancouver BC, Canada*
- ^f *Also at Department of Physics, California State University, Fresno CA, U.S.A.*
- ^g *Also at Novosibirsk State University, Novosibirsk, Russia*
- ^h *Also at Department of Physics, University of Coimbra, Coimbra, Portugal*
- ⁱ *Also at Università di Napoli Parthenope, Napoli, Italy*
- ^j *Also at Institute of Particle Physics (IPP), Canada*
- ^k *Also at Department of Physics, Middle East Technical University, Ankara, Turkey*
- ^l *Also at Louisiana Tech University, Ruston LA, U.S.A.*
- ^m *Also at Dep Fisica and CEFITEC of Faculdade de Ciencias e Tecnologia, Universidade Nova de Lisboa, Caparica, Portugal*
- ⁿ *Also at Department of Physics and Astronomy, Michigan State University, East Lansing MI, U.S.A.*
- ^o *Also at Department of Financial and Management Engineering, University of the Aegean, Chios, Greece*
- ^p *Also at Department of Physics, University of Cape Town, Cape Town, South Africa*
- ^q *Also at Institute of Physics, Azerbaijan Academy of Sciences, Baku, Azerbaijan*
- ^r *Also at Institut für Experimentalphysik, Universität Hamburg, Hamburg, Germany*
- ^s *Also at Manhattan College, New York NY, U.S.A.*
- ^t *Also at CPPM, Aix-Marseille Université and CNRS/IN2P3, Marseille, France*
- ^u *Also at School of Physics and Engineering, Sun Yat-sen University, Guanzhou, China*
- ^v *Also at Academia Sinica Grid Computing, Institute of Physics, Academia Sinica, Taipei, Taiwan*
- ^w *Also at Laboratoire de Physique Nucléaire et de Hautes Energies, UPMC and Université Paris-Diderot and CNRS/IN2P3, Paris, France*
- ^x *Also at School of Physical Sciences, National Institute of Science Education and Research, Bhubaneswar, India*
- ^y *Also at Dipartimento di Fisica, Università La Sapienza, Roma, Italy*
- ^z *Also at DSM/IRFU (Institut de Recherches sur les Lois Fondamentales de l'Univers), CEA Saclay (Commissariat à l'Énergie Atomique et aux Énergies Alternatives), Gif-sur-Yvette, France*
- ^{aa} *Also at Moscow Institute of Physics and Technology State University, Dolgoprudny, Russia*
- ^{ab} *Also at Section de Physique, Université de Genève, Geneva, Switzerland*
- ^{ac} *Also at Departamento de Fisica, Universidade de Minho, Braga, Portugal*
- ^{ad} *Also at Department of Physics, The University of Texas at Austin, Austin TX, U.S.A.*
- ^{ae} *Also at Department of Physics and Astronomy, University of South Carolina, Columbia SC, U.S.A.*
- ^{af} *Also at Institute for Particle and Nuclear Physics, Wigner Research Centre for Physics, Budapest, Hungary*
- ^{ag} *Also at DESY, Hamburg and Zeuthen, Germany*
- ^{ah} *Also at International School for Advanced Studies (SISSA), Trieste, Italy*
- ^{ai} *Also at LAL, Université Paris-Sud and CNRS/IN2P3, Orsay, France*
- ^{aj} *Also at Faculty of Physics, M.V.Lomonosov Moscow State University, Moscow, Russia*
- ^{ak} *Also at Nevis Laboratory, Columbia University, Irvington NY, U.S.A.*
- ^{al} *Also at Physics Department, Brookhaven National Laboratory, Upton NY, U.S.A.*
- ^{am} *Also at Department of Physics, Oxford University, Oxford, United Kingdom*
- ^{an} *Also at Discipline of Physics, University of KwaZulu-Natal, Durban, South Africa*
- ^{*} *Deceased*